THE EARTH TIDE EFFECTS ON PETROLEUM RESERVOIRS

Preliminary Study

A THESIS

SUBMITTED TO THE DEPARTMENT OF

PETROLEUM ENGINEERING

AND THE COMMITTEE ON GRADUATE STUDIES

OF STANFORD UNIVERSITY

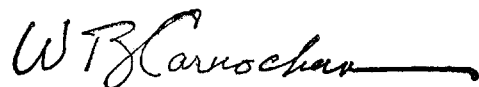IN PARTIAL FULFILLMENT OF THE REQUIREMENTS

FOR THE DEGREE OF

ENGINEER

by

Patricia C. Arditty
May 1978

Approved for the Department:

Henry J Ramsey

Approved for the University Committee
on Graduate Studies:

W B Carnochan
Dean of Graduate Studies

To my husband

iii

ACKNOWLEDGEMENT

TABLE OF CONTENTS

LIST OF TABLES

LIST OF FIGURES

ABSTRACT

The gravitational attraction between the sun, moon, and the earth gives birth to oceanic tides which are visible and sometimes large, and to earth tides whose amplitudes are very small due to the low compressibility of the earth compared to that of water.

Tidal effects are observed quite often in open pits. Bredehoeft (1967), Bodvarsson (1970), and Robinson and Bell (1971) have shown the existence of a relation between rock characteristics and the amplitude of the response of an open well aquifer system. Johnson (1973) described the behavior of such a system in detail.

It was observed that tidal phenomena also exist in closed well reservoir systems. (Khurana, 1976; Strobel et al., 1976). The purpose of this study was:

(1) to develop a theory which describes the pressure variations in closed well reservoir systems caused by the earth tides,

(2) to be able to recognize the important parameters which determine the amplitude of the response, and

(3) to inspect different cases of real field data for gas and oil reservoir systems for which accurate pressure information is available.

The four principal results of this research are:

(1) A new expression for the pressure induced at the borehole by a periodic tidal stress was derived. This work shows that the important parameters for the amplitude response of a closed well reservoir system are the permeability, the porosity, and the rock and fluid compressibilities. The amplitude of the pressure response varies between zero and unity for frequencies varying between zero and infinity.

(2) The frequency at which the response starts to die is the critical frequency, ω_c. When the critical frequency increases, the system becomes frequency independent, and the amplitude response to the diurnal component is equal to that of the semidiurnal component.

(3) For a given rock formation, the largest response is obtained for the more compressible saturating fluid, and for a given saturating fluid, the largest response is obtained for the less compressible formation.

(4) The amplitude of the pressure response increases with an increasing value of bulk system compressibility when the system is frequency dependent. The pressure amplitude increases with increasing values of the difference in fluid and solid compressibility if the system is frequency independent.

1. INTRODUCTION

Petroleum reservoirs are complex systems. A lot of data, such as pressure, rock, and fluid characteristics, geologic configuration, etc., are needed to make a valid and precise physical determination and economic evaluation of a hydrocarbon field. All the conclusions on the shape, size, and possible field production of the reservoir are based on the calculated values of the different parameters used in material balance equations. Erroneous values for these variables can lead to misinterpretation of the field test experiment results.

Two of the most difficult unknowns to be obtained are the porosity and the compressibility of the reservoir, because they imply a precise knowledge of the field structure and fluid composition at reservoir pressure and temperature conditions.

Buildup, drawdown, and pulse tests are used to determine reservoir size and shape, and different parameters, such as (k h) which represents the product of the productive thickness (h) of the reservoir and the permeability (k) of the formation, (ϕC_t) which represents the product of the porosity (ϕ) of the formation and the total compressibility of the system (C_t). This information is so important that much research is devoted to finding new tests to detect this information. Tidal effects may contain important information about reservoirs.

It has been shown that the sinusoidal water level variations observed in open wells are directly related to earth tide phenomena (Sterling and Smith, 1967). Furthermore, it is believed that the magnitude

3

of tidal effects is related to the characteristics of the formation and to the fluid contained in the formation. Many technical papers describe this kind of dependence for open well-aquifer systems wherein the well is relatively shallow (less than 1000 ft deep), while little has been said about closed well-reservoir systems at depths between two to ten thousand feet or more. In this case, a sinusoidal pressure variation is observed, rather than a sinusoidal liquid level variation. The solution which describes pressure in a closed well-reservoir system is based on a modification of Bodvarsson's theory, which explains the mechanism for the open well-reservoir case.

In this study, we will develop the solution for the new closed well-reservoir problem, and verify the validity of the theory using different rock and fluid formation types in numerical applications. Then real field data will be analyzed to test the theory and determine whether a correlation between rock and fluid properties and pressure amplitude response can be found.

2. SOME BACKGROUND ON THE STRESS-STRAIN THEORY AND THE EARTH TIDE MECHANISM

The lunar-solar attraction of the earth generates a state of stress on the earth's surface which induces a radial deformation of the earth. The maximum value of this strain or deformation is around 36 cm (14 in) (Melchior, 1966). To understand the mechanism of the earth's deformation, let us review some of the basic principles of stress-strain theory.

2.1 Stress-Strain Theory

Rock mechanics is the study of the behavior and properties of rock masses under stress or change of conditions. A stress, σ, is a force applied to a surface area. It is defined as:

4

$$\sigma = \frac{\Delta F}{\Delta A} \qquad (2.1)$$

This stress causes a deformation of the surface, called strain, ε.

In the following, we will consider the surface to be the earth surface. The earth is assumed to be a porous elastic and isotropic medium, which reacts linearly to a stress.

This stress is considered positive when compressive, and negative when tensile. In a Cartesian coordinate system, the stress tensor has components in the x, y, and z directions, and these components can be written as:

$$\begin{bmatrix} \sigma_{xx} & \sigma_{xy} & \sigma_{xz} \\ \sigma_{yx} & \sigma_{yy} & \sigma_{yz} \\ \sigma_{zx} & \sigma_{zy} & \sigma_{zz} \end{bmatrix} \quad \text{with} \quad \begin{cases} \sigma_{xy} = \sigma_{yx} \\ \sigma_{yz} = \sigma_{zy} \\ \sigma_{xz} = \sigma_{zx} \end{cases} \qquad (2.2)$$

where σ_{xx}, σ_{yy}, and σ_{zz} are called normal stresses because the surface, ΔA, upon which they are applied, is perpendicular to the x, y, and z axis, respectively. The six other stress components are called shear stresses, because they represent forces tending to slide or shear the material in the plane of ΔA. Figure 2.1 shows some of these stress components applied on a cube in a Cartesian coordinate system. The hydrostatic stress is an invariant and is defined by (Jaeger and Cook, 1969):

$$\sigma_{\alpha\alpha} = \frac{1}{3} (\sigma_{xx} + \sigma_{yy} + \sigma_{zz}) \qquad (2.3)$$

The deviatoric stress components are defined by:

$$S_{xx} = \sigma_{xx} - \sigma_{\alpha\alpha}, \quad s_{yy} = \sigma_{yy} - \sigma_{\alpha\alpha}, \quad s_{zz} = \sigma_{zz} - \sigma_{\alpha\alpha}$$

$$s_{xy} = \sigma_{xy}, \qquad s_{xz} = \sigma_{xz}, \quad \text{and} \quad s_{yz} = \sigma_{yz}$$
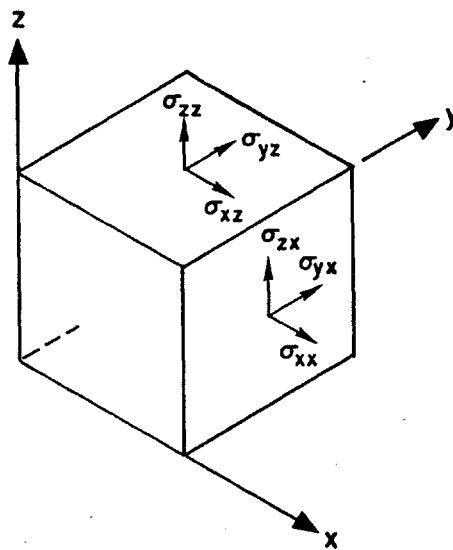
FIG. 2.1: STRESS DEFINITION IN A CARTESIAN COORDINATE SYSTEM

6

The displacement and strain will be considered positive when responding to a positive stress, and negative when responding to a negative stress. In a cartesian coordinate system, the displacement vector can be written as:

$$\vec{U} = \begin{cases} U_x \\ U_y \\ U_z \end{cases}$$

For such displacement, the associated strain is defined by:

$$\varepsilon_{xx} = \frac{\partial U_x}{\partial x}$$

$$\varepsilon_{yy} = \frac{\partial U_y}{\partial y} \qquad\qquad (2.4)$$

$$\varepsilon_{zz} = \frac{\partial U_z}{\partial z}$$

where these three components are the normal strain, and by:

$$\varepsilon_{xy} = \frac{1}{2} \left[\frac{\partial U_z}{\partial y} + \frac{\partial U_y}{\partial z} \right] = \varepsilon_{yx}$$

$$\varepsilon_{xz} = \frac{1}{2} \left[\frac{\partial U_x}{\partial z} + \frac{\partial U_z}{\partial z} \right] = \varepsilon_{zx} \qquad\qquad (2.5a)$$

$$\varepsilon_{yz} = \frac{1}{2} \left[\frac{\partial U_y}{\partial x} + \frac{\partial U_x}{\partial y} \right] = \varepsilon_{zy}$$

7

where these three components are called shear strain. The general expression for the strain, ε, can be written using the different stress-strain and elastic moduli equations, Eq. 2.5a:

$$\varepsilon_{ij} = \frac{1}{2}\left(\frac{\partial U_i}{\partial_j} + \frac{\partial U_j}{\partial_i}\right) = \frac{1}{2}\Delta\vec{U}$$

(2.5b)

$$\varepsilon_{ij} = \frac{1}{2G}(\sigma_{ij} - 1/3\ \sigma_{\alpha\alpha}\ \delta_{ij}) + \frac{1}{3K}\sigma_{rr}\ \delta_{ij}$$

The volumetric strain is an invariant and is defined by:

$$\Delta = \varepsilon_{xx} + \varepsilon_{yy} + \varepsilon_{zz}$$

(2.5c)

The strain can be decomposed in mean normal strain (equivalent to the deviatoric stress):

$$e = \frac{1}{3}(\varepsilon_{xz} + \varepsilon_{yy} + \varepsilon_{zz}) = \frac{1}{3}\Delta$$

(2.5d)

and deviatoric strain (equivalent to the deviatoric stress):

$$e_x = \varepsilon_{xx} - e,\ e_y = \varepsilon_{yy} - e,\ e_z = \varepsilon_{zz} - e$$

(2.5e)

$$e_{xy} = \varepsilon_{xy},\ e_{xz} = \varepsilon_{xz},\ e_{yz} = \varepsilon_{yz}$$

In order to solve a problem on the behavior of a solid medium with specified mechanical properties, we have to combine the stress equations of equilibrium with equations specifying the mechanical behavior of a solid. If this solid is linear and elastic, we use the stress-strain linear relationship and the equations of equilibrium. One important

8

condition of the solid is that its behavior is completely reversible: after the stress is eliminated, the solid returns to its original shape.

The linear strain-stress relationships are:

$$\sigma_{xx} = (\lambda+2G)\ \varepsilon_{xx} + \lambda\varepsilon_{yy} + \lambda\varepsilon_{zz}$$

$$\sigma_{yy} = (\lambda+2G)\ \varepsilon_{yy} + \lambda\varepsilon_{xx} + \lambda\varepsilon_{zz} \qquad (2.6)$$

$$\sigma_{zz} = (\lambda+2G)\ \varepsilon_{zz} + \lambda\varepsilon_{xx} + \lambda\varepsilon_{yy}$$

and:

$$\sigma_{xy} = 2G\ \varepsilon_{xy}$$

$$\sigma_{xz} = 2G\ \varepsilon_{xz} \qquad (2.7)$$

$$\sigma_{yz} = 2G\ \varepsilon_{yz}$$

where λ is the Lame constant, and G is the shear modulus, or modulus of rigidity.

We can write a general linear relationship between stress and strain for a linear solid:

$$\sigma_{ij} = \lambda\varepsilon_{\alpha\alpha}\delta_{ij} + 2G\varepsilon_{ij} = \lambda\Delta\delta_{ij} + 2G\varepsilon_{ij};$$

$$\delta_{ij} = 1, \text{ if } i = j$$

$$\delta_{ij} = 0, \text{ if } i \neq j \qquad (2.8)$$

where:

$$i = x, y, z$$

$$j = x, y, z$$

9

A definition of the Lame constant and modulus of rigidity involves other elastic moduli:

$$\lambda = \frac{E\nu}{(1+\nu)(1-2\nu)}$$
(2.9)

where E is Young's modulus, and ν is Poisson's ratio ($\nu \approx 0$ to 0.50).

Young's modulus is defined as the ratio of stress to strain for a uniaxial stress (σ_{xx} is the only stress different from zero):

$$E = \frac{\sigma_{xx}}{\varepsilon_{xx}} = \frac{G(3\lambda+2G)}{\lambda+G}$$
(2.10)

Poisson's ratio is the ratio of the lateral expansion to the longitudinal contraction:

$$\nu = - \frac{\varepsilon_{yy}}{\varepsilon_{xx}} = \frac{\lambda}{2(\lambda+G)}$$
(2.11)

Finally, the shear modulus, G, can be written as:

$$G = \frac{E}{2(1+\nu)}$$
(2.12)

If $\nu \doteq 0.25$ (a typical value often used for elasticity problems), we have $\lambda = G$ from Eq. 2.11.

The last elastic modulus we need to define is called the bulk modulus. It represents the ratio of the hydrostatic pressure, P_c, to the volumetric strain it produces, Δ. It is also called the "incompressibility."

10

Assuming that the hydrostatic pressure is equal to the hydrostatic stress given by Eq. 2.3, and using Eqs. 2.6 and 2.8 for the expression of the different stress components, we have:

$$\sigma_{\alpha\alpha} = \frac{1}{3}(\sigma_{xx} + \sigma_{yy} + \sigma_{zz}) = P_c = (\lambda + \frac{2}{3}G)\,\Delta \qquad (2.13)$$

We can write:

$$K = \frac{P_c}{\Delta} = \lambda + \frac{2}{3}G \qquad (2.14)$$

We see why this modulus is called the "incompressibility": it represents the resistance of the material to stress. Another definition of K is:

$$K = \frac{1}{C} \qquad (2.15)$$

where C is the compressibility of the solid.

To solve a problem of the behavior of a linear solid, equilibrium equations are needed. The equilibrium equations are partial differential equations which describe the stresses and resulting displacements in the interior of a body. To solve these equations, specific conditions of the surface must be given. It is assumed that there are some body forces (gravity, etc.) throughout the interior of the body. The body force is $\vec{X}$ (X_x, X_y, X_z), and ρ_m is the density of the solid. The equations of equilibrium are (Fung, 1970):

$$\frac{\partial \sigma_x}{\partial_x} + \frac{\partial \sigma_{yx}}{\partial_y} + \frac{\partial \sigma_{zx}}{\partial_z} + \rho_m X_x = 0$$

$$\frac{\partial \sigma_{xy}}{\partial_x} + \frac{\partial \sigma_y}{\partial_y} + \frac{\partial \sigma_{zy}}{\partial_z} + \rho_m X_y = 0 \qquad (2.16)$$

$$\frac{\partial \sigma_{xz}}{\partial_x} + \frac{\partial \sigma_{yz}}{\partial_y} + \frac{\partial \sigma_{zz}}{\partial_z} + \rho_m X_z = 0$$

These equations can be expressed in terms of displacements rather than stresses, using the stress-strain relations described previously.

All the concepts reviewed to this point are for nonporous solids. Most of these concepts (definition of elastic moduli, stress, and strain) remain unchanged for a porous body case. They are the bases of rock mechanics theory. However, some equations have to be changed.

The equation of strain (2.5b) becomes (Nur, Byerlee, 1971):

$$\varepsilon_{ij} = \frac{1}{2G} (\sigma_{ij} - \frac{1}{3} \sigma_{\alpha\alpha} \delta_{ij}) + \frac{1}{9K} (\sigma_{rr} \delta_{ij}) - \frac{1}{3H} (P_p \delta_{ij}) \qquad (2.17)$$

where H is a new effective bulk modulus, which takes the pore effect into account (Biot, 1941), and P_p is the pore pressure. When $P_p = 0$ (nonporous medium), Eq. 2.17 is the same as Eq. 2.5b. The new equation for the volumetric strain is:

$$\Delta = \frac{1}{K} P_c - \frac{1}{H} P_p = \frac{1}{K} (P_c - \alpha P_p) \qquad (2.18)$$

P_c is still the hydrostatic pressure:

$$\frac{1}{3} \left(\sigma_{xx} + \sigma_{yy} + \sigma_{zz} \right) \qquad (2.19)$$

and:
$$\alpha = \frac{K}{H}$$

An effective pressure, $<P>$, is defined (Nur and Byerlee, 1971):

$$<P> = P_c - \alpha P_p$$

and thus Eq. 2.18 is:

$$\Delta = \frac{1}{K} <P> \qquad (2.20)$$

Replacing K, we have:

$$\Delta = <P> \cdot C \qquad (2.21)$$

By defining an effective stress, $<\sigma_{ij}>$, such that:

$$<\sigma_{ij}> = \sigma_{ij} - \alpha P_p \, \delta_{ij} \qquad (2.22)$$

it can be shown that any porous body problem can be reduced to a nonporous one as Eq. 2.17 becomes:

$$\varepsilon_{ij} = \frac{1}{2G} \left(<\sigma_{ij}> - \frac{1}{3} <\sigma_{rr}> \delta_{ij} \right) + \frac{1}{9K} <\sigma_{rr}> \delta_{ij} \qquad (2.23)$$

which is the form of a nonporous strain equation (no P_p term appears) similar to Eq. 2.5b.

Equation 2.21 can be written as:

$$\Delta = \left(P_c - \frac{Cf}{C_m} P_p \right) C_m \qquad (2.24)$$

if we consider that K is the bulk modulus of the rock matrix and H that of the pore material. In this case:

$$K = \frac{1}{C_m} \qquad (2.25a)$$

and:

$$H = \frac{1}{C_p}$$

13

using Eq. 2.15.

If the pores are filled with fluid,

$$H = \frac{1}{C_p} = \frac{1}{C_f} \qquad (2.25b)$$

where the pore compressibility is essentially the fluid compressibility. Any problem involving elastic isotropic bodies (porous or nonporous) can be solved using similar equations. Using the different relations between stress and strain, applied pressure, pore pressure, and elastic moduli, we can develop the equations which express the response of a closed well-reservoir system to periodic tidal stresses. First let us review the important properties and effects of the different tidal components.

2.2 General Information on Tides

Oceanic tides are familiar to everyone who visits the ocean beaches. These tides are often large and easily observed visually. Oceanic tides depend on rotation of the earth, gravitational attraction between the earth, sun, and moon, and other effects. On the other hand, earth tides are small compared to oceanic tides and may not be observed directly with ease. This results because the earth is effectively rigid, and water is not. Another significant difference between oceanic and earth tides is that rotation of the earth appears to have little effect on earth tides (Garland, 1971). The major factor appears to be gravitational attraction between the earth and the moon. Solar gravitational effects are quite small.

14
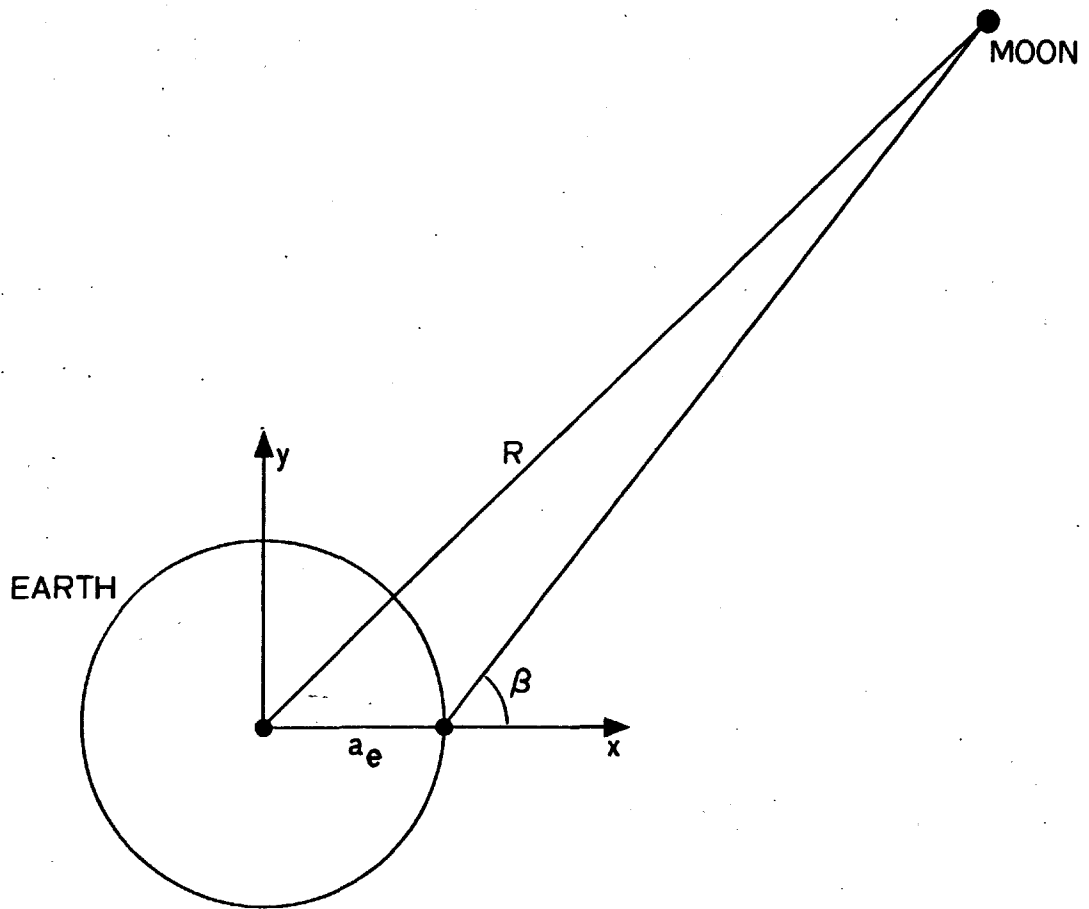
FIG. 2.2: SCHEMATIC REPRESENTATION OF THE EARTH-MOON ATTRACTION

15

As the gravitational force of attraction between two masses is inversely proportional to the square of the distance between these two masses, the potential derived from this force will be inversely proportional to the cube of the distance between the two masses. The tide-generating potential can be defined using a spherical harmonic of the second order, W_2 (Melchior, 1966):

$$W_2 = \frac{1}{2} \frac{\gamma M a_e^2}{R^3} (3 \cos^2 \beta - 1) \tag{2.26}$$

where:

   M = moon mass

   a_e = radius of the earth

   R = distance between the moon and the center of the earth

   β = angle shown in Fig. 2.2

   γ = gravitational constant

Using Eqs. 2.6 and 2.7 in a spherical coordinate system instead of a Cartesian system, the stresses corresponding to the displacements induced by the potential are (Bredehoeft, 1967):

$$\sigma_{rr} = \lambda\theta + 2G_m \varepsilon_{rr} \qquad \text{(a)}$$

$$\sigma_{\theta\theta} = \lambda\theta + 2G_m \varepsilon_{\theta\theta} \qquad \text{(b)} \tag{2.27}$$

$$\sigma_{\psi\psi} = \lambda\theta + 2G_m \varepsilon_{\psi\psi} \qquad \text{(c)}$$

16

At the earth's surface, $\sigma_{rr} = 0$. For the subject well-reservoir problem, we can consider that the reservoir is at the earth's surface. The typical reservoir depths of two to twenty thousand feet are negligible compared to the distance between the moon and earth. Instead of Eq. 2.26 for the tide-generating potential, Melchior found another form which allows one to determine that there are different types of tides. The main difference lies in the tidal periods. The main types of tides are:

Long-period tides (period T = 16 days)

Diurnal tides (period T = 1 day)

Semidiurnal tides (period T = 1/2 day)

Terdiurnal tides (period T = 1/3 day)

The details of the computation and Melchior's development are not given here because it is not necessary for the purposes of this report. A general and complete theory of oceanic and earth tides can be found in Melchior, 1966; Officer, 1974, Ch. 5; and Garland, 1971, Ch. 10. However, for the purpose of this study, the total deformation due to an earth tide is:

$$\theta = f(r) \frac{W_2}{g} \tag{2.28}$$

Using Eq. 2.5b, this equation becomes:

$$\theta = f(r) \frac{W_2}{g} = \varepsilon_{\alpha\alpha} \tag{2.29}$$

Because $f(r) = 0.49/a_e$, Eq. 2.28 can also be written as:

$$\theta = \frac{0.49}{a_e} \frac{W_2}{g} \tag{2.30}$$

17

The value of f(r) has been found by Melchior, 1966, and yields the volumetric strain at the surface of the earth. Values of θ are given in Table 2.1 (Melchior, 1966).

The strain, θ, in a petroleum reservoir is:

$$\theta = \sigma_{rr} \cdot C_t = \frac{0.49 \cdot W_e}{a_e g} = P_c \cdot C_t \tag{2.31}$$

where C_t is the total compressibility of the reservoir considered. From this equation, the value of the stress or pressure applied by the earth tide on the reservoir can be computed if the value of C_t is known. But what is more important is that we can compute C_t if the pressure applied by the earth on the reservoir is known. This is usually the case, as wells are frequently monitored for pressure. So, if we measure the amplitude of the pressure variation generated by the earth tide accurately, we may be able to obtain important information about reservoir characteristics.

Tidal effects have been seen clearly in many wells (Miller, 1972; Narashimhan, 1978; Strobel et al., 1976), and their amplitudes range between 2×10^{-3} psi to 5×10^{-1} psi (see Section 5). Even with such small amplitudes, it has been shown that false interpretation of interference tests may result if one is not aware of the existence of the earth tide effect (Khurana, 1976). An example is shown in Fig. 2.3. Erroneous conclusions about the geometry of the reservoir, the existence of a flow barrier, or interferences from other producing wells can be reached. This is likely to happen for long experiments (times greater than 2 hours) because of the period of the disturbing tides.

TABLE 2.1: PRINCIPAL TIDAL WAVES

SYMBOL	NAME	FREQUENCY (DEGREE/HOUR)	ANGULAR FREQUENCY	PERIOD (HR)	$\theta = \frac{2}{a_e g}(0.49)$	TYPE*
Q_1	Lunar Elliptic of O_1	13.398661	6.50×10^{-5}	26.868	3.536×10^{-9}	D
O_1	Lunar Principal	13.943036	6.76×10^{-5}	w5.819	1.847×10^{-8}	D
M_1	Lunar Elliptic of $^mK_1$	14.496694	7.03×10^{-5}	24.833	1.452×10^{-8}	D
S_1	Solar Elliptic	15.000002	7.27×10^{-5}	24.000	2.073×10^{-10}	D
$^mK_1$	Lunar	15.041069	7.29×10^{-5}	23.935	1.780×10^{-8}	D
N_2	Lunar Major Elliptic of M_2	28.4339730	1.38×10^{-4}	12.658	8.520×10^{-9}	SD
M_2	Lunar Principal	28.984104	1.41×10^{-4}	12.421	4.50×10^{-8}	SD
L_2	Lunar Minor Elliptic of M_2	29.528479	1.45×10^{-4}	12.000	2.072×10^{-9}	SD
S_2	Solar Principal	30.000000	1.43×10^{-4}	12.191	1.258×10^{-8}	SD

Ratio $\frac{O_1}{M_2}$ = 0.415 O_1 and M_2 are the most important tidal waves; K_1 is also important sometimes.

*D = Diurnal, SD = Semidiurnal

Inspection of Table 2.1 indicates that the volumetric strain induced
by the semidiurnal component M_2 is larger than that induced by the diurnal
component, O_1. The volumetric strain ratio of the two components is
equal to (values at the equator):

$$\frac{O_1}{M_2} = \frac{1.847 \times 10^{-8}}{4.450 \times 10^{-8}} = 0.415$$

This is the theroetical value of the ratio. If the experimental value of
the amplitude response of the well is also equal to 0.415, it would mean
that the well responds to the O_1 component as well as to the M_2 component
with the same amplitude, and would prove that the response is frequency
independent.

If the ratio (O_1/M_2) is different, the response will be frequency-
dependent. In all of the following, the oceanic tide effects are neglected.

We will now consider the state-of-the art of knowledge of the effect
of earth tides on open well-aquifer systems.
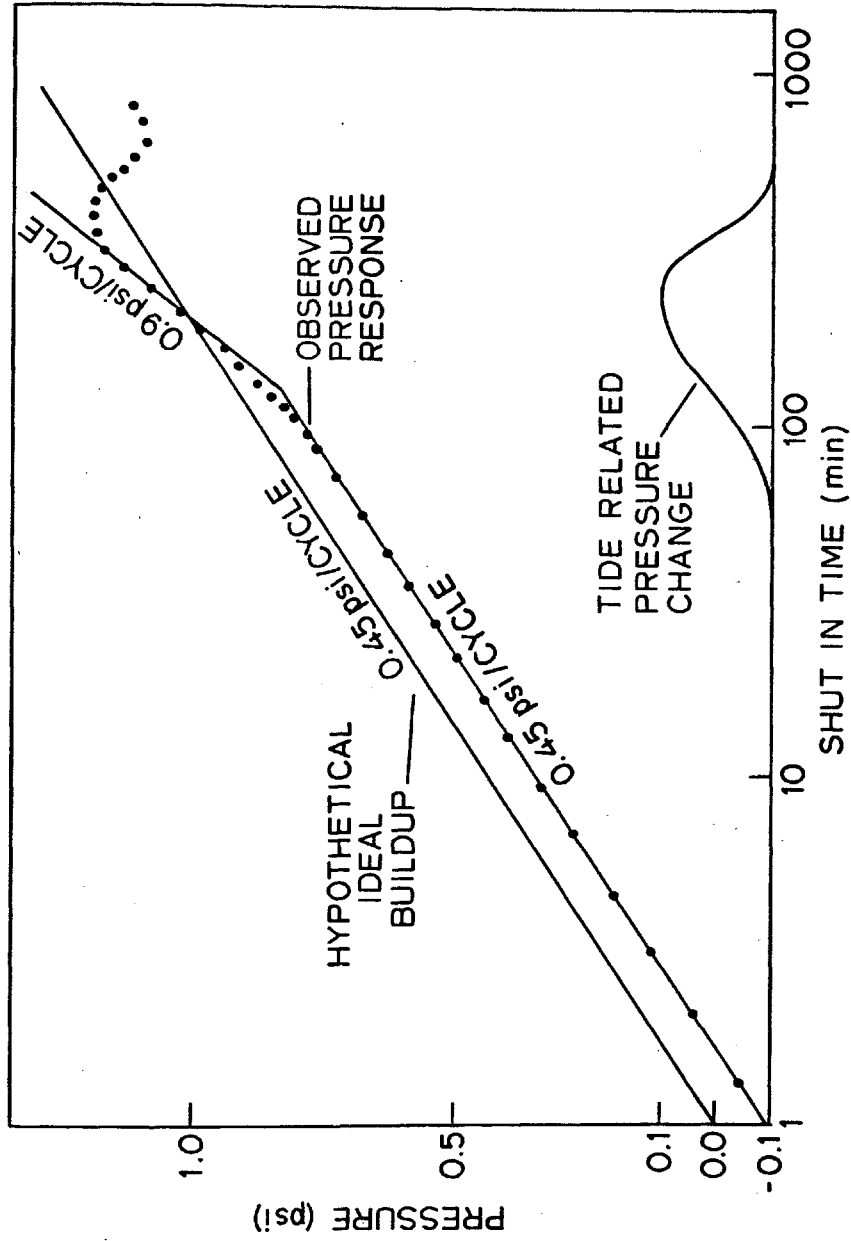
FIG. 2.3: EFFECTS OF SUPERPOSITION OF TIDE-RELATED PRESSURE CHANGE ON
A HYPOTHETICAL PRESSURE BUILDUP (KHURANA, 1976)

3. THE EFFECTS OF EARTH TIDES ON OPEN WELL-AQUIFER SYSTEMS: STATE OF THE ART

Natural phenomena such as tides or earthquakes can lead to a better understanding of the underground, if we can exploit the information they contain. For instance, a recent but powerful tool is the study of seismic wave effects on water level fluctuations in open wells. It has been noticed that prior to and after an earthquake, the water level in a well changes rapidly (Fig. 3.1) (Sterling and Smets, 1970; Witherspoon, 1978). This is due to the stress associated with seismic tremors. This stress generates an increase in pore pressure of the rock mass; this pressure increase pushes the water out of the pore, and causes a water level increase.

In order to study this problem, the following assumptions have been made:

o   The well-aquifer system is far enough from the ocean or sea such that effects of oceanic tides can be neglected.

o   The well-aquifer system is confined, and there is a water level, h, in the borehole.

Two kinds of configurations have been studied: (1) the case where there is no flow into the borehole, and (2) the case where there is flow into the borehole. The solutions for these two models will be called static and dynamic solutions, respectively, as Bodvarsson named them (Bodvardsson, 1970).

After an earthquake, the release of the stress induces the opposite phenomenon, which leads to a decrease in water level (Nur and Booker, 1972; Johnson, 1973; Johnson and Nur, 1977).

22

Sinking of the water-level

Rising of the water-level

5 cm

0   12   0 h   UT

28   29

1964 March 28
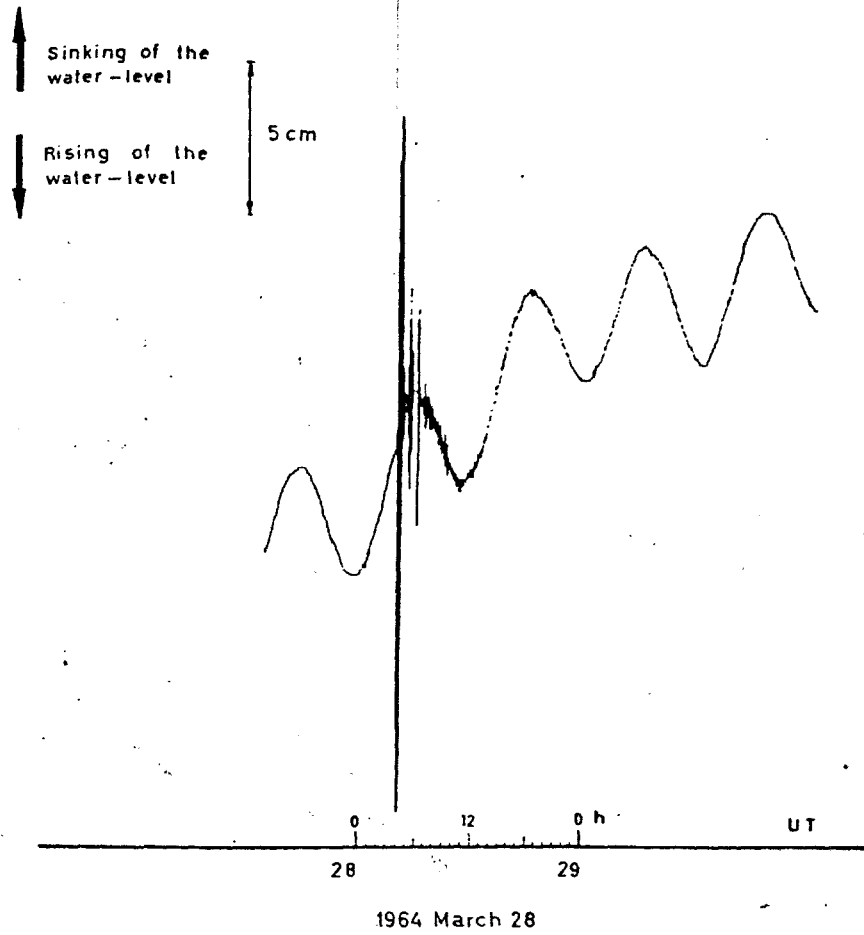
FIG. 3.1: WATER LEVEL VARIATIONS IN AN OPEN WELL DUE TO SEISMIC TREMORS (STERLING ET AL., 1971)

23

While the study of earthquakes is fairly recent, study of the tides is an old endeavor. But a new field of study is to try to get information on the aquifer properties by studying the influence of earth tides on pressure or water level in an open well-aquifer system (Fig. 3.2).

3.1 Static Solution

We consider an aquifer of volume V, of total compressibility, C_t, and of water compressibility, C_w. As shown in Section 2, we can write that the dilitation, θ, due to earth tide-induced pressure, P, is:

$$\theta = P \cdot C_t \qquad (3.1)$$

The increase of confining pressure due to earth tides is:

$$P = dP_c \qquad (3.2)$$

The pore pressure increase associated with dP_c is dP_p. When the equation for dP_p/dP_c is written, strain, θ, can be given in terms of dP_c.

Bredehoeft (1967), Robinson and Bell (1971), and Bodvarsson (1970) proposed different equations to express the response of an open well-reservoir system.

The general form of the equation given by Bredehoeft is that the increase of pressure due to the earth tide is P:

$$P = \rho g dh = \frac{\theta}{C_w \cdot \phi} \qquad (3.3)$$

where ϕ is the porosity of the aquifer. The compressibility of the rock itself was neglected because Bredehoeft assumed that the change in rock matrix volume was small compared to that of the water volume.

24
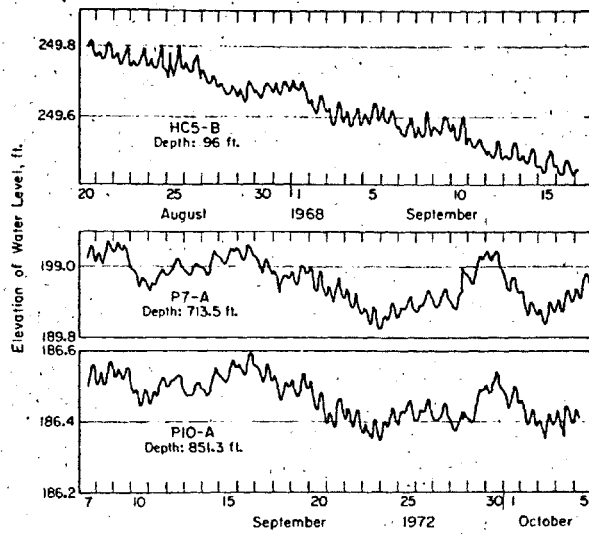
FIGURE 3.2: WATER LEVEL VERSUS TIME RECORDED FOR ONE MONTH IN AN OPEN WELL (MARINE, 1975)

Bodvarsson (1970) and Robinson and Bell (1971) present similar expressions. Bodvarsson called P_S the static pressure:

$$P = -\frac{\varepsilon\theta}{S} = P_S \qquad (3.4)$$

where ε is a factor depending on the aquifer matrix ($\varepsilon \le 1$), and S is defined as:

$$S = \phi C_f + (1-\phi) C_m \qquad (3.5)$$

$\varepsilon\theta$ is called the effective dilatation associated with the earth hole effect. C_f is the fluid compressibility (here $C_f = C_w$) and C_m is the matrix compressibility. Equation 3.5 expresses the average rock-fluid compressibility per unit bulk volume.

A similar equation given by Robinson and Bell is:

$$P = -\frac{\theta}{S} \qquad (3.6)$$

where θ is the dilatation associated with the earth tide effect. No ε factor is considered.

Johnson (1973) found that these three solutions neglected the matrix rock strain. Johnson's theory shows that the increase, dP_c, in confining pressure is accompanied by an increase, dP_p, in pore pressure. Equating the increase in pore volume, V_p, to that of the water volume, V_w, he expressed the response of the system as the ratio of dP_p to dP_c.

$$\frac{dP_p}{dP_c} = \frac{1}{1 + \dfrac{\phi}{C} \left(C_f - C_m + \dfrac{\pi r_o^2}{V\rho g\phi} \right)} \qquad (3.7)$$

where $\bar{C}$ is the effective compressibility of the aquifer as defined by Nur and Byerlee (1971). The term $(\pi r_o{}^2/V\rho g\phi)$ is small compared to the others within the large parenthesis. The response of a well-aquifer system to pressure induced by earth tides is dependent on the rock and fluid characteristics. Thus, information about the aquifer can be found when the amplitude of the response of the well-aquifer system is obtained. Similar information is expected to be given by the dynamic solution of the problem.

These static equations are not valid for the cases when pressure is time dependent. If there is a periodic oscillation of pressure, a dynamic solution is required to solve the frequency-dependent problem. Let us look now at the dynamic solution proposed by Bodvarsson (1970).

3.2 Dynamic Solution

A dynamic solution is necessary to solve the problem related to pressure variation induced by the earth tides. The system should respond to a periodic excitation and should be frequency dependent. The periodic waves are the pressure fluctuations induced by the tides, and these fluctuations are assumed sinusoidal with time. We will review the general development of the theory used by Bodvarsson.

The outer boundary condition is a no-flow boundary because the aquifer is confined. Darcy's law for the well-aquifer system can be written as:

$$q = \frac{-k}{\mu} \nabla p \qquad (3.8)$$

where:

    q = flow rate per unit area

    k = permeability of the aquifer

    μ = viscosity of the fluid (here, μ is the viscosity of the water)

The flow equation is then (Bodvarsson, 1970):

$$d \cdot \nabla^2 P - \frac{\partial P}{\partial t} = - \frac{\partial P_S}{\partial t} \tag{3.9a}$$

$$d = \frac{k}{\mu \rho_S} \tag{3.9b}$$

P_S is defined as the pressure far enough from the well that it does not feel an effect when stress is applied to the aquifer (P_S was defined in the previous section). P_S is a constant for a given well-aquifer system.

Equation 3.9a can be written as:

$$d \cdot \nabla^2 P = - \frac{\partial P_S}{\partial t} + \frac{\partial P}{\partial t} \tag{3.10}$$

Using a change in variables, $D = P - P_S$, Eq. 3.10 becomes:

$$d \cdot \nabla^2 D = \frac{\partial D}{\partial t} \tag{3.11}$$

We consider that the pressure waves are periodic sinusoidal waves, which can be expressed as functions of time such that:

$$P \sim P \exp(-i\omega t)$$

$$\tag{3.12}$$

$$P_S \sim P_S \exp(-i\omega t)$$

Replacing these parameters in Eq. 3.9a, we have:

$$\nabla^2 P - n^2(P - P_S) = 0 \tag{3.13a}$$

with

$$n^2 = \frac{i\omega}{d} \tag{3.13b}$$

28

A general solution of Eq. 3.13a for the pressure, P, due to earth tide at any distance, r, from well, is:

$$P = P_S + \frac{A}{r} e^{-nr}$$

(3.14)

A is a constant and has been found to be equal to:

$$A = \frac{a P_S e^{-na}}{1 + \frac{4kg}{i\omega a\mu} (1+na)}$$

(3.15)

So P is:

$$P = P_S \left(1 - \frac{a}{r} M e^{-n(r-a)} \right)$$

(3.16)

with:

$$M = \frac{1}{1 + \frac{4kg}{i\omega\mu a} (1+na)}$$

(3.17)

Equations 3.14 through 3.17 represent Bodvarsson's dynamic solution.

Let the pressure at the wellbore be pressure, P_a. P_a is given by the following expression:

$$P_a = P_S(1-M)$$

(3.18)

This is a simplification of Eq. 3.16, when r = a. The response is then:

$$\frac{P_a}{P_S} = (1-M)$$

(3.19)

29

When this response is graphed versus the frequency, ω, of the periodic oscillation, the amplitude is larger for small frequencies than for large frequencies.

We now consider modification of this model and theory in order to solve the problem of a closed well-reservoir system. We seek to compute the amplitude of the response of a closed well-reservoir system to earth tides. The solution for this problem may describe a relationship between the amplitude of the response and certain reservoir rock and fluid properties.

4. RESPONSE OF A CLOSED WELL-RESERVOIR SYSTEM TO THE EARTH TIDE STRESS

The preceding section reviewed the theories available to express the response of an <u>open</u> well-reservoir system to a periodic confining pressure. We seek to solve the problem of a <u>closed</u> well-reservoir system. The assumptions we will use are:

(1) The model we choose to use is represented in Fig. 4.1: the well is cased all the way down to the productive zone; this last portion is open and perforated to allow the fluid to enter the borehole.

(2) The flow is always a one-phase flow; either oil or gas is flowing, but never both for the same well.

(3) Water is always present in the petroleum reservoir at its irreducible value, and thus does not flow.

(4) The borehole is completely filled with the formation flowing fluid.

(5) The well is shut in.

4.1 Development of the Solution

In the previous section, the pressure, P_S, or "static" pressure, was considered to be equal to P_∞ where P_∞ is the pressure at a distance r from the well, such that $(r/a) \to \infty$. Bodvarsson did not include the dilatation of the cavity itself.

In our problem, we will consider the dilatation of the well spherical cavity; the static pressure has to consider this effect. The well is considered a single pore in a nonporous formation (Fig. 4.2). The well spherical cavity has a "pore pressure," P_0, induced by the applied tectonic

31
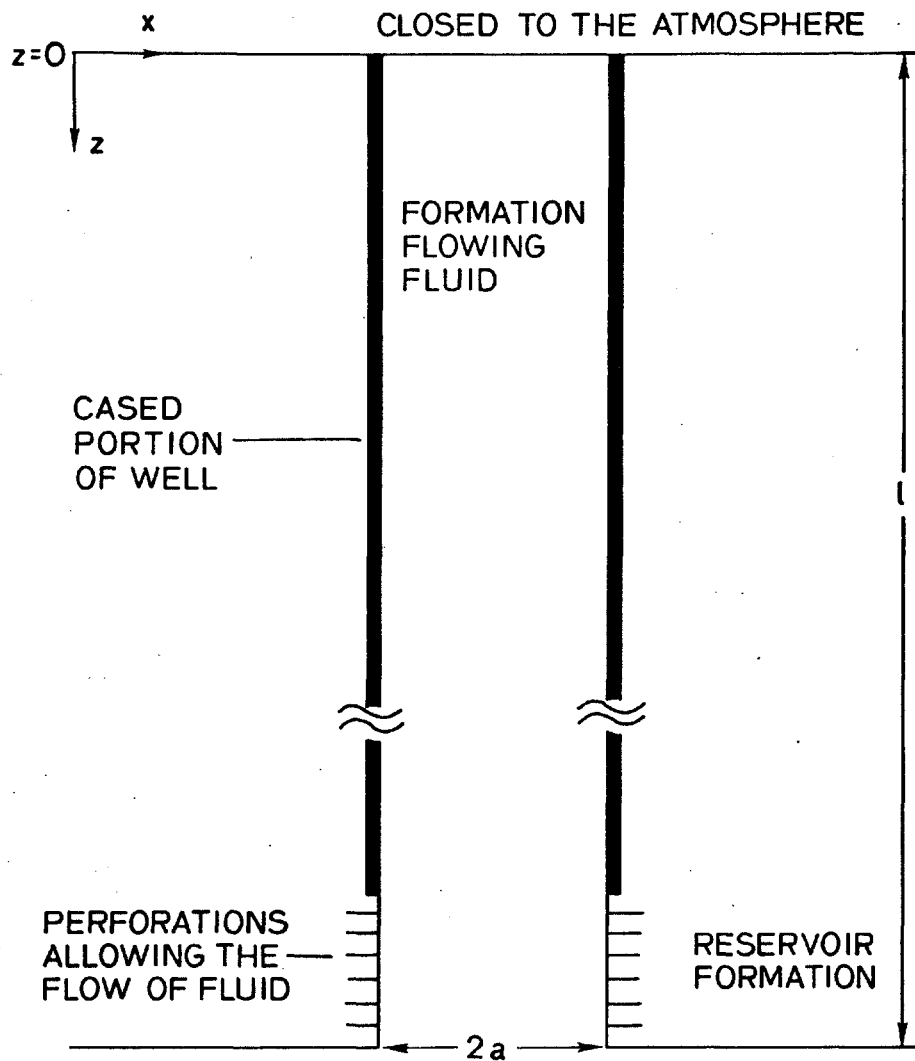
FIG. 4.1: WELL-RESERVOIR MODEL

32

pressure, P_c (Nur and Byerlee, 1971). The expression for P_0 is:

$$P_0 = P_c \ \frac{1 + \dfrac{3}{4G_m C_m}}{1 + \dfrac{3}{4G_m C_m} + \left(\dfrac{C_f}{C_m} - 1 \right) (1-\phi)} \qquad (4.1)$$

where:

G_m = matrix shear modulus

C_m = matrix compressibility

C_f = fluid compressibility

ϕ = porosity

For this equation we assume $\phi = 0$. Equation 4.1 becomes:

$$P_0 = P_c \ \frac{1 + \dfrac{3}{4G_m C_m}}{\dfrac{3}{4} \left(\dfrac{1}{G_m C_m} \right) + \dfrac{C_f}{C_m}} \qquad (4.2)$$

We define an expression for the new static pressure, P_{Sd}, as:

$$P_{Sd} = P_S - P_0 \qquad (4.3)$$

P_S is still equal to P_∞ (or the confining pressure, P_c).

$$P_{Sd} = P_c - P_0 = P_c - P_c \left[\frac{1 + \dfrac{3}{4G_m C_m}}{\dfrac{3}{4G_m C_m} + \dfrac{C_f}{C_m}} \right] \qquad (4.4)$$

or:

$$P_{Sd} = P_c \left(\frac{4G_m [C_f - C_m]}{3 + 4G_m C_f} \right) = P_c \cdot E_o \qquad (4.5)$$

CONFINING PRESSURE P_c

$z=0$ x

z

$P_c \longrightarrow$

WELL SPHERICAL CAVITY

WELL RADIUS

$\longleftarrow P_c$

"NON POROUS"
FORMATION

P_c
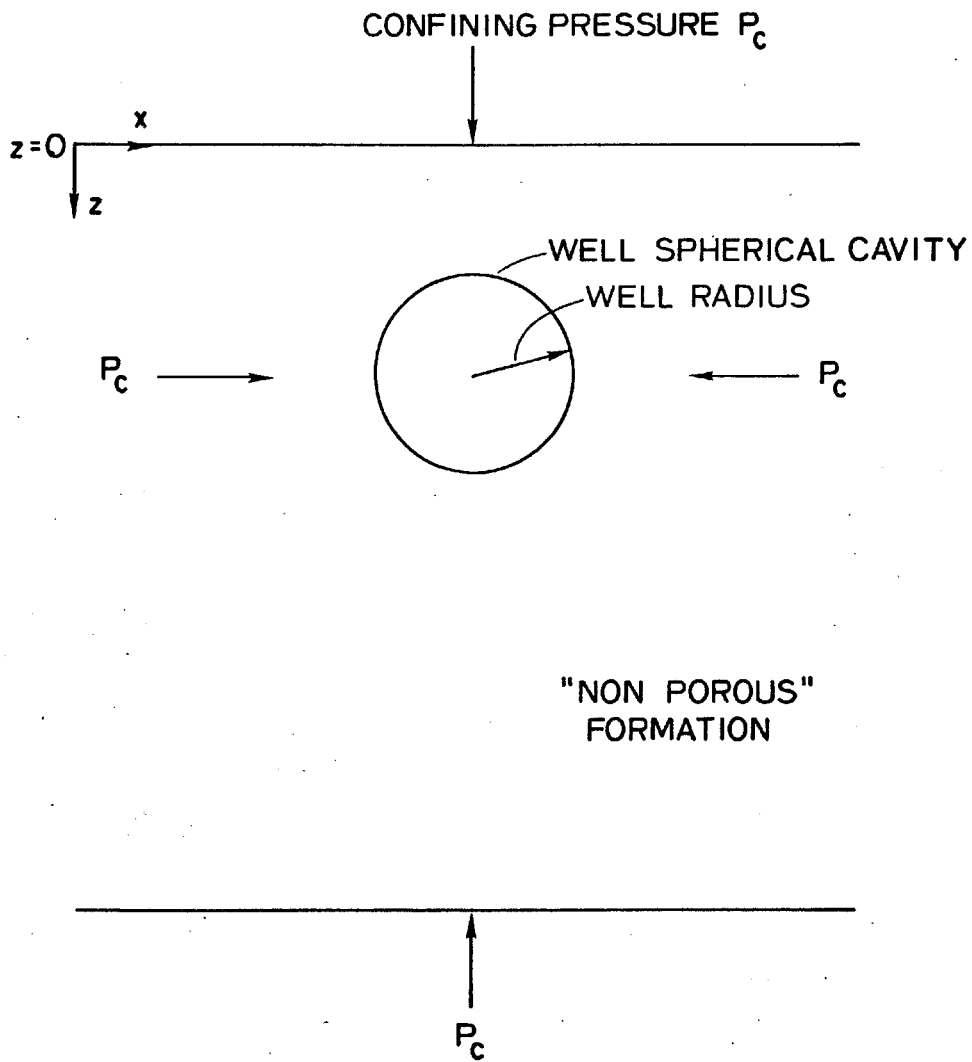
FIG. 4.2: REPRESENTATION OF THE WELL SPHERICAL CAVITY AS A SINGLE PORE
IN A NON-POROUS FORMATION

This equation gives an important difference between the subject problem and Bodvarsson's problem. Using Bodvarsson's definition for the static pressure, we have $P_S = P_c$. For the present problem, for each well-reservoir system, there is a constant E_o which multiplies the value of P_c. The value of the constant, E_o, varies between almost 1.00 and 0.01, and cannot be neglected.

If the fluid in the borehole is very compressible, the term in brackets in Eq. 4.5 becomes essentially unity, because $C_f \gg C_m$, and $4G_m C_f \gg 3$. The expansion of the cavity itself is compensated by the high fluid compressibility.

With the new meaning of the static pressure, Eq. 4.5, we can find a solution which will explain the behavior of a closed well-reservoir system under some periodic stress, such as earth tide stress.

Figure 4.1 defines our system. The volume of the well is:

$$V = \pi a^2 \ell \tag{4.6}$$

The area of the spherical cavity (bottom of the well) is:

$$A = 4\pi a^2 \tag{4.7}$$

The periodic change in volume is equal to the flow rate per unit area times the area through which the flow passes:

$$\frac{dV}{dt} = q \cdot 4\pi a^2 \tag{4.8}$$

Using Darcy's law for the flow of fluid:

$$q = \frac{k}{\mu} \nabla P \tag{4.9}$$

35

where:

q = flow rate per unit area

k = permeability of the formation

μ = flowing fluid viscosity

Using the concept explained in Section 2, we can write that the strain, θ, is proportional to the pressure-compressibility product, and that θ is also equal to $\Delta V/V$, so we can write:

$$\frac{dP}{dt} \simeq \frac{1}{C_f} \frac{d}{dt} \left(\frac{\Delta V}{V}\right) = \frac{1}{C_f V} \frac{dV}{dt} \qquad (4.10)$$

Using Eqs. 4.8 and 4.10:

$$\frac{dP}{dt} = \frac{1}{C_f V} \cdot q \cdot 4\pi a^2$$

and substitution of Eq. 4.9 yields:

$$\frac{dP}{dt} = \frac{1}{C_f V} \frac{k}{\mu} 4\pi a^2 \nabla P$$

and substitution of Eq. 4.6 yields:

$$\frac{dP}{dt} = \frac{4k\pi a^2}{C_f \mu \pi a^2 \ell} \frac{dP}{dr} = \frac{4k}{C_f \mu \ell} \frac{dP}{dr}$$

$$\frac{dP}{dt} = B \frac{dP}{dr} \qquad (4.11a)$$

where $\qquad\qquad\qquad B = \frac{4k}{C_f \mu \ell} \qquad (4.11b)$

36

The differential equation (Eq. 4.11a) is of the same kind as that obtained for an open well-aquifer system. The difference is in the B term.

If P and P_{Sd} are periodic functions of time:

$$P \sim P_e^{-i\omega t}$$

$$P_{Sd} \sim P_{Sd} e^{-i\omega t}$$

Equation 4.11a becomes:

$$i\omega P = B \frac{dP}{dr} \tag{4.12}$$

A general solution to this differential equation is (Bodvarsson, 1970):

$$P = \frac{A'}{r} e^{-nr} + P_{Sd} \tag{4.13}$$

with:

$$n^2 = \frac{i\omega}{d}$$

where $d = \dfrac{k}{\mu[\phi C_f + (1-\phi) C_m]}$

Thus:

$$\frac{dP}{dr} = -\frac{A'}{r^2} e^{-nr} - n \frac{A'}{r} e^{-nr} = -\frac{A'}{r} e^{-nr} \left(\frac{1}{r} + n \right) \tag{4.14a}$$

and:

$$\left. \frac{dP}{dr} \right|_{r=a} = -e^{-na} \left(\frac{A'}{a^2} + \frac{A'}{a} \right) = -\frac{A'}{a} e^{-na} \left(\frac{1}{a} + n \right) \tag{4.14b}$$

In order to obtain the value of A', we write Eq. 4.12 at $r = a$, using Eqs. 4.13 and 4.14c:

$$i\omega \left(\frac{A'}{a} e^{-na} + P_{Sd} \right) = - \frac{BA'}{a^2} e^{-na} (1+na)$$

Solving for A':

$$A' = - \frac{i\omega a P_{Sd} e^{na}}{i\omega+B \left(n + \frac{1}{a} \right)} \qquad (4.15a)$$

We can now give the final expression for the pressure, P_a, at the bottom of the well, induced by an applied tectonic pressure, P_c, when the well is closed to the atmosphere and in communication with an infinite confined reservoir. Using a modified expression for A' such as:

$$A' = \frac{P_{Sd} a e^{na}}{1 + \frac{B}{i\omega} \left(n + \frac{1}{a} \right)} \qquad (4.15b)$$

The pressure, P (anywhere from the well), is:

$$P = P_{Sd} \left[1 - \frac{a e^{n(a-r)}}{r \left(1 + \frac{B}{i\omega} \left(\frac{1}{a} + n \right) \right)} \right] \qquad (4.16)$$

and at the bottom of the well:

$$P_a = P_{Sd} \left[1 - \frac{1}{1 + \frac{B}{i\omega a} (na+1)} \right] \qquad (4.17a)$$

38

Using Eqs. 4.5 and 4.11a, the explicit form for P_a is:

$$P_a = P_c \left(\frac{4G_m(C_f - C_m)}{3+4G_m C_f} \right) \left[1 - \frac{1}{1 + \frac{4k}{ai\omega\mu C_f} \left(\sqrt{\frac{i\omega}{d}} a + 1 \right)} \right]$$
(4.17b)

The "effective response" of the closed well-reservoir system is then:

$$\frac{P_a}{P_c} = \frac{4G_m(C_f - C_m)}{(3+4G_m C_f)} [1-M'] = E_o(1-M')$$
(4.18a)

where:

$$M' = \frac{1}{1 + \frac{4k}{i\omega\mu a \ell C_f} \left(\sqrt{\frac{i\omega}{d}} a+1 \right)}$$
(4.18b)

The difference between this solution and the open well solution lies in the expression of M' compared to that of M and in the constant E_o, which did not exist in the previous solution.

Equation 4.18a may be used to compute the amplitude of the response, P_a/P_c, of the well reservoir system. This response is a function of the frequency ω, because M' is a function of ω, and E_o is independent of ω. To simplify the calculations, and because E_o is a constant for a given well-reservoir system, we will compute the relative response, P_a/P_{Sd}, instead of the effective response, P_a/P_c. The relative response, $P_a/P_{Sd} = (1-M')$ is a complex expression, so the amplitude of P_a/P_{Sd} is equal to:

$$P_a/P_{Sd} = \left[(1-M') \cdot (1-M'*) \right]^{1/2}$$
(4.18c)

where $M'*$ is the complex conjugate of M'. Equation 4.17a can be written:

$$\frac{P_a}{P_{Sd}} = (1 - M') = 1 - \frac{1}{1 + \frac{4k}{i\omega\mu a\ell C_f}\left(\sqrt{\frac{i\omega}{d}}\, a + 1\right)} \qquad (4.19a)$$

Define:

$$\alpha = \frac{4k}{\omega\mu a\ell C_f}, \text{ and } \beta = \frac{a^2\omega}{d} \qquad (4.19b)$$

Equation 4.19a becomes:

$$\frac{P_a}{P_{Sd}} = 1 - \frac{1}{1 + \frac{\alpha}{i}\left(\beta i + 1\right)} \qquad (4.20)$$

We write $\sqrt{i}$ as $\dfrac{\varepsilon}{\sqrt{2}} + \dfrac{i}{\sqrt{2}}$ with $\varepsilon = \pm 1$.

So:

$$\frac{P_a}{P_{Sd}} = 1 - \frac{1}{\left(1 + \varepsilon\alpha\sqrt{\frac{\beta}{2}}\right) - i\left(\alpha - \varepsilon\alpha\sqrt{\frac{\beta}{2}}\right)} \qquad (4.21)$$

Let:

$$F = 1 + \varepsilon\alpha\sqrt{\beta/2}$$

$$\qquad (4.21a)$$

$$I = \alpha - \varepsilon\alpha\sqrt{\beta/2}$$

Then:

$$\frac{P_a}{P_{Sd}} = 1 - \frac{1}{F - iI} = \frac{(F-1) - iI}{F - iI} \qquad (4.22)$$

40

The amplitude of P_a/P_{Sd} becomes:

$$\left| \frac{P_a}{P_{Sd}} \right|^{1/2} = \left[\frac{(F-1)-iI \cdot (F-1)+iI}{F^2+I^2} \right]^{1/2}$$

or:

$$\left| \frac{P_a}{P_{Sd}} \right|^{1/2} = \left[\frac{(F-1)^2+I^2}{F^2+I^2} \right]^{1/2} \tag{4.23a}$$

Using Eqs. 4.21a and 4.18a, the explicit expression for the relative response, P_a/P_{Sd}, of the well-reservoir system is:

$$\left| \frac{P_a}{P_{Sd}} \right|^{1/2} = \left(\frac{\alpha^2\beta/2 + \alpha^2 + \alpha^2\beta/2 + 2\varepsilon\alpha^2 \sqrt{\frac{\beta}{2}}}{1 + \alpha^2\beta/2 + 2\varepsilon\alpha \sqrt{\frac{\beta}{2}} + \alpha^2\beta/2 + 2\varepsilon\alpha^2 \sqrt{\frac{\beta}{2}}} \right)^{1/2} \tag{4.23b}$$

Dividing the numerator and denominator by ^{2} yields:

$$\left| \frac{P_a}{P_{Sd}} \right|^{1/2} = \left(\frac{1 + \beta + \varepsilon \sqrt{2\beta}}{1 + \beta + \varepsilon \sqrt{2\beta} (\frac{1}{\alpha} + 1) + \frac{1}{\alpha^2}} \right)^{1/2} \tag{4.24}$$

This represents the relative amplitude. It is a function of ω and it cannot be larger than unity. Indeed, we always have (for $\varepsilon = \pm 1$):

$$1 + \beta + \varepsilon \sqrt{2\beta} \leq 1 + \beta + \varepsilon \sqrt{2\beta} (\frac{1}{\alpha} + 1) + \frac{1}{\alpha^2}$$

41

Let us inspect the behavior of this function before computing numerical answers:

If $\alpha \to 0$ ($\omega \to \infty$), the response $\to 0$

If $\alpha \to \infty$ ($\omega \to 0$), the response $\to 1$

The amplitude of the response is between 0 and 1, and decreases with increasing values of ω. The important term containing frequency, ω, is (from Eq. 4.19a):

$$\alpha = \frac{4k}{\omega\mu a \ell C_f}$$

This is similar to the open well-aquifer system case, so we can expect to have a similar shape for the curve representing the amplitude of the response versus the frequency. We can expect to see an abrupt decrease of the response starting at a given value of ω, called the critical frequency, ω_c (as in the open well-aquifer system). We will investigate the relationship between this critical frequency value and the closed well-reservoir system characteristics.

Let us assume that instead of Eq. 4.19a, P_a/P_{Sd} can be written as:

$$\frac{P_a}{P_{Sd}} \approx 1 - \frac{1}{1 + \dfrac{4k}{i\omega\mu a \ell C_f}} = \frac{(4k/i\omega\mu a \ell C_f)}{1 + \dfrac{4k}{i\omega\mu a \ell C_f}} \tag{4.25}$$

The critical frequency is the value of ω for which both terms of the denominator have comparable importance, so it is the value of ω for which $0 < P_a/P_{Sd} < 1$.

$$\frac{P_a}{P_{Sd}} = 1, \text{ if } \frac{4k}{\omega\mu a\ell C_f} \gg 1$$

$$\frac{P_a}{P_{Sd}} = 0, \text{ if } \frac{4k}{\omega\mu a\ell C_f} \ll 1$$

So:

$$0 < \frac{P_a}{P_{Sd}} < 1, \text{ if } \frac{4k}{\omega\mu a\ell C_f} \approx 1 \qquad (4.26)$$

and this yields the relationship sought. If:

$$\frac{4k}{\omega\mu a\ell C_f} = 1, \text{ then } \omega = \omega_c = \frac{4k}{\mu a\ell C_f} \qquad (4.27)$$

This is obtained by using the approximation defined in Eq. 4.25.

Let us summarize the equations we have developed which determine the solution for the closed well-reservoir system:

(1)
$$P_{Sd} = P_S - P_0 = P_c \, \frac{4G_m(C_f - C_m)}{3 + 4 \, G_m C_f} = P_c \cdot E_0$$

(2)
$$P_a = (P_c \cdot E_0)(1 - M') = P_{Sd}(1 - M')$$

(3) The effective amplitude response is $\left|\dfrac{P_a}{P_c}\right|^{1/2}$

(4) The relative amplitude response is:

$$\left|\frac{P_a}{P_{Sd}}\right|^{1/2} = \left(\frac{1 + \beta + \varepsilon\sqrt{2\beta}}{1 + \beta + \varepsilon\sqrt{2\beta}(\frac{1}{\alpha} + 1) + \frac{1}{\alpha^2}}\right)^{1/2}$$

43

where:

$$\alpha = \frac{4k}{\omega\mu a \ell C_f} \text{ and } \beta = \frac{a^2 \omega}{d}$$

The approximate critical frequency value is:

$$\omega_c = \frac{4k}{a\ell\mu C_f}$$

(5) The phase of the system response, P_a/P_c, is:

$$\Phi = \tan^{-1} \frac{[I_m(P_a/P_c)]}{[R_e(P_a/P_c)]} = \tan^{-1} \frac{I_m(P_a/P_{Sd})}{R_e(P_a/P_{Sd})}$$

In order to verify the validity of these equations and the theory behind them, we will do some numerical calculations for different reservoir cases.

4.2   Numerical Computations: Selection of Data

We wish to analyze the amplitude response of a system using the results from Section 4.1. In order to do that, we have to select different reservoir models: different in rock characteristics as well as fluid content. We seek the response of these various cases as a function of ω (or the period T, which is $2\pi/\omega$).

It would be expected that the fluid compressibility and the matrix compressibility are important factors. By choosing five different types of rock formation and three different saturating fluids, we will cover a large range of values for these parameters. We will consider the following rock formations:

44

consolidated sandstones (CS_1, CS_2)

consolidated limestones (CL_1, CL_2)

carbonate (CB_1)

and the following types of reservoirs:

dry-gas reservoir (Fluid No. 1)

gas-free oil reservoir (Fluid No. 2)

gas-saturated oil reservoir (Fluid No. 3)

The values of ϕ, k, C_m, and G_m are either calculated or taken from typical values for each formation type. The values of C_f, μ, C_t, ... are also computed or taken from typical values for each fluid case. Table 4.1 presents the values for all parameters, and the method used to obtain the is described in Appendix A. These parameters are expressed in engineering units (lb/in^2, ft^3/lb, ft, md, cp, ...). In order to use them in the equation for the amplitude, we require some unit conversion factors. Permeability, k, which is computed in md, will be used in in^2, so $k(in^2) = 1.55 \times 10^{12} \cdot k(md)$. Viscosity, μ, is computed in cp, and will be used in $lb-sec/in^2$, so $\mu(lb-sec/in^2) = 1.45 \times 10^{-7} \cdot \mu(cp)$. The well diameter and depth expressed in feet will be used in the equation in inches. The shear modulus and compressibility values remain expressed in lb/in^2 and in^2/lb, respectively.

To compute the relative response, P_a/P_{Sd}, and the factor E_o for each fluid and rock type case, we prepared a computer program which would compute the amplitude of the relative response frequency for ω, varying between 9×10^{-6} to 9×10^{-3} sec^{-1}. (T varying between 192 hours and 0.19 hours.) The computer program plots the amplitude of the response versus the period of the oscillation, so it is easy to see the response of the system to diurnal and semidiurnal tidal stresses.

45

TABLE 4.1: ROCK AND FLUID PROPERTIES USED IN THE NUMERICAL APPLICATION OF THE THEORY

PROPERTIES/ROCK	CS_1 Sandstone No. 1	CS_2 Sandstone No. 2	CL_1 Limestone No. 1	CL_2 Limestone No. 2	CB_1 Carbonate No. 1
NO. 1, GAS					
$\mu=\mu_g$ (cp)	0.03	→	→	→	→
$C_f=C_g$ (psi^{-1})x10^{-6}	124.7	→	→	→	→
$\rho=\rho_g$ (lb/ft^3)	20.0	→	→	→	→
NO. 2, OIL					
$\mu=\mu_o$ (cp)	1.80	→	→	→	→
$C_f=C_o$ (psi^{-1})x10^{-1}	7.50	→	→	→	→
$\rho=\rho_o$ (lb/ft^3)	42.50	→	→	→	→
NO. 3, OIL & GAS					
$\mu=\mu_{mix}$ (cp)	0.38	→	→	→	→
$C_f=C_{mix}$ (psi^{-1})x10^{-6}	33.90	→	→	→	→
$\rho=\rho_{mix}$ (lb/ft^3)	40.00	→	→	→	→
ROCK					
k (md)	10.0	900.0	4.0	500.0	1100.0
ϕ (trachon)	0.15	0.30	0.05	0.25	0.10
C_m (psi^{-1})x10^{-6}	3.70	0.95	6.50	3.30	7.00
G_m (psi)x10^{-6}	6.40	6.40	3.60	3.60	4.40

Details of the computations are given in Appendix A.

46

For each of the fifteen different cases, a graph represents the relative response, P_a/P_{Sd}, and the factor E_o is computed and included in the computed P_a/P_c values. The program is listed in Appendix B.

4.3 Results and Discussion

Figures 4.3 through 4.7 present the relative amplitude response, P_a/P_{Sd}, for each rock formation. Figures a are for fluids case No. 1, figures b are for fluid case No. 2, and figures c are for fluid case No. 3.

All the graphs have the same general shape. The amplitude is constant to a certain value of ω, then declines to zero for higher ω values. The response is always higher for long periods than for short periods. The frequency at which the response starts to decline sharply is called the critical frequency, ω_c. Looking at the graphs, we see that when ω_c is much larger than ω_D and ω_{SD}, the amplitude of the response is the same for these two dital components (ω_D is the frequency of the diurnal tide, ω_{SD} is the frequency of the semidiurnal tides; they are 6.68×10^{-5} sec^{-1} and 1.41×10^{-4} sec^{-1}, respectively). When ω_c is very close to ω_D or ω_{SD}, the ratio of their amplitude is between 1.25 and 2.0. When ω_c is smaller than ω_D, their ratio is larger than 2.

We call A_D and A_{SD} the amplitude response to the diurnal tide and to the semidiurnal tide, respectively.

(1) If $\omega_c \gg \omega_{SD} > \omega_D$, then $\dfrac{A_D}{A_{SD}} = 1.0$

(2) If $\omega_D \approx \omega_c$, or $\omega_{SD} \approx \omega_c$, then $\dfrac{A_D}{A_{SD}} = 1.25$ to 2

(3) If $\omega_D \ll {}_D$, then $\dfrac{A_D}{A_{SD}} > 2$

47

FIGURE 4.3: RESPONSE (P_a/P_{Sd}) OF A CLOSED-WELL RESERVOIR SYSTEM FOR ROCK
FORMATION CS_1: (a) FLUID CONTENT NO. 1, (b) FLUID CONTENT
NO. 2, (c) FLUID CONTENT NO. 3
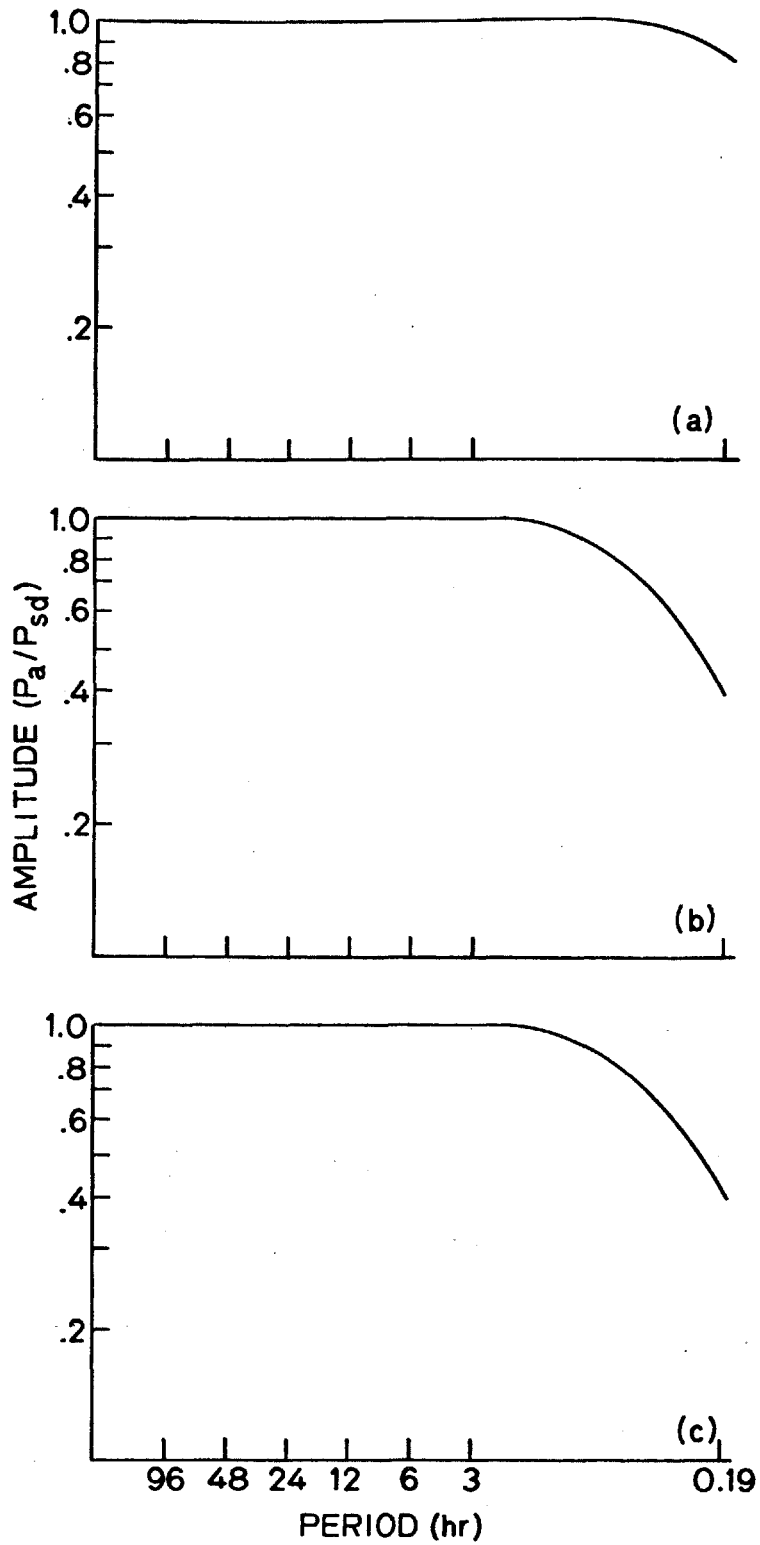
FIGURE 4.4: RESPONSE (p_a/P_{Sd}) OF A CLOSED-WELL RESERVOIR SYSTEM FOR ROCK FORMATION CS_2: (a) FLUID CONTENT NO. 1, (b) FLUID CONTENT NO. 2, (c) FLUID CONTENT NO. 3
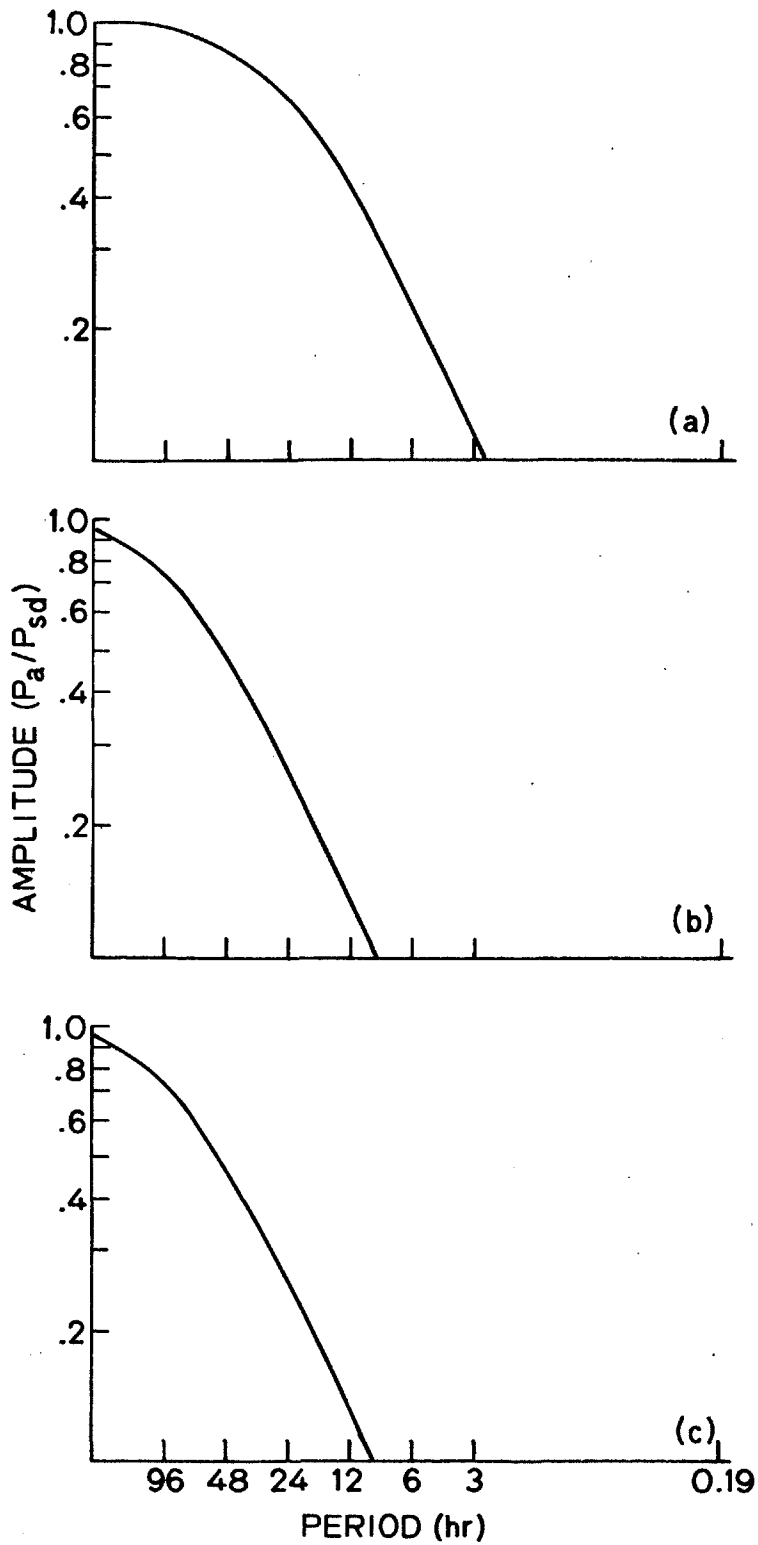
FIGURE 4.5: RESPONSE (p_a/P_{Sd}) OF A CLOSED WELL RESERVOIR SYSTEM FOR ROCK
FORMATION CL_1: (a) FLUID CONTENT NO. 1, (b) FLUID CONTENT Nθ.
2, (c) FLUID CONTENT NO. 3
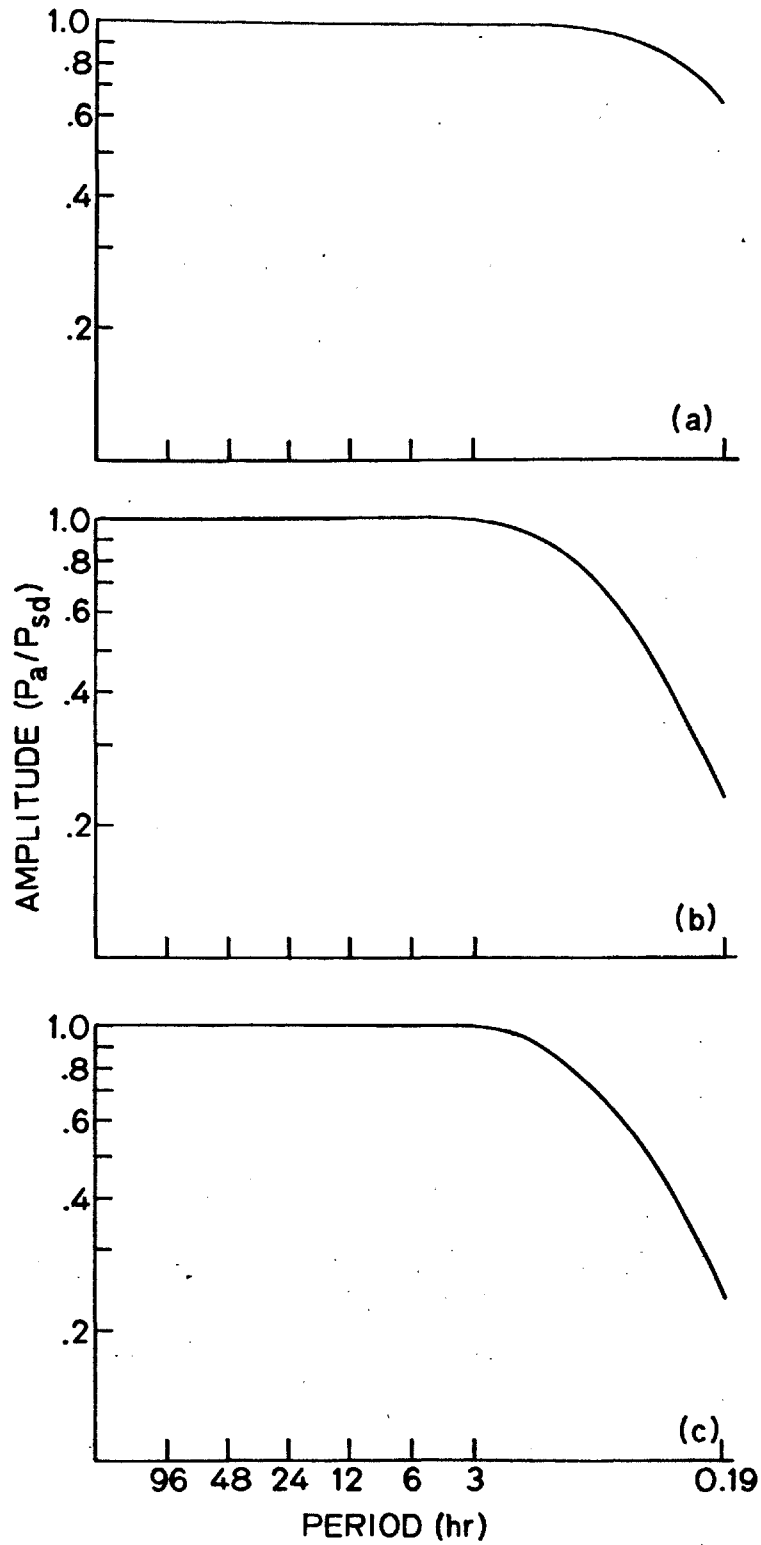
FIGURE 4.6: RESPONSE (P_a/P_{Sd}) OF A CLOSED WELL-RESERVOIR SYSTEM FOR ROCK FORMATION CL_2: (a) FLUID CONTENT NO. 1, (b) FLUID CONTENT NO. 2, (c) FLUID CONTENT NO. 3
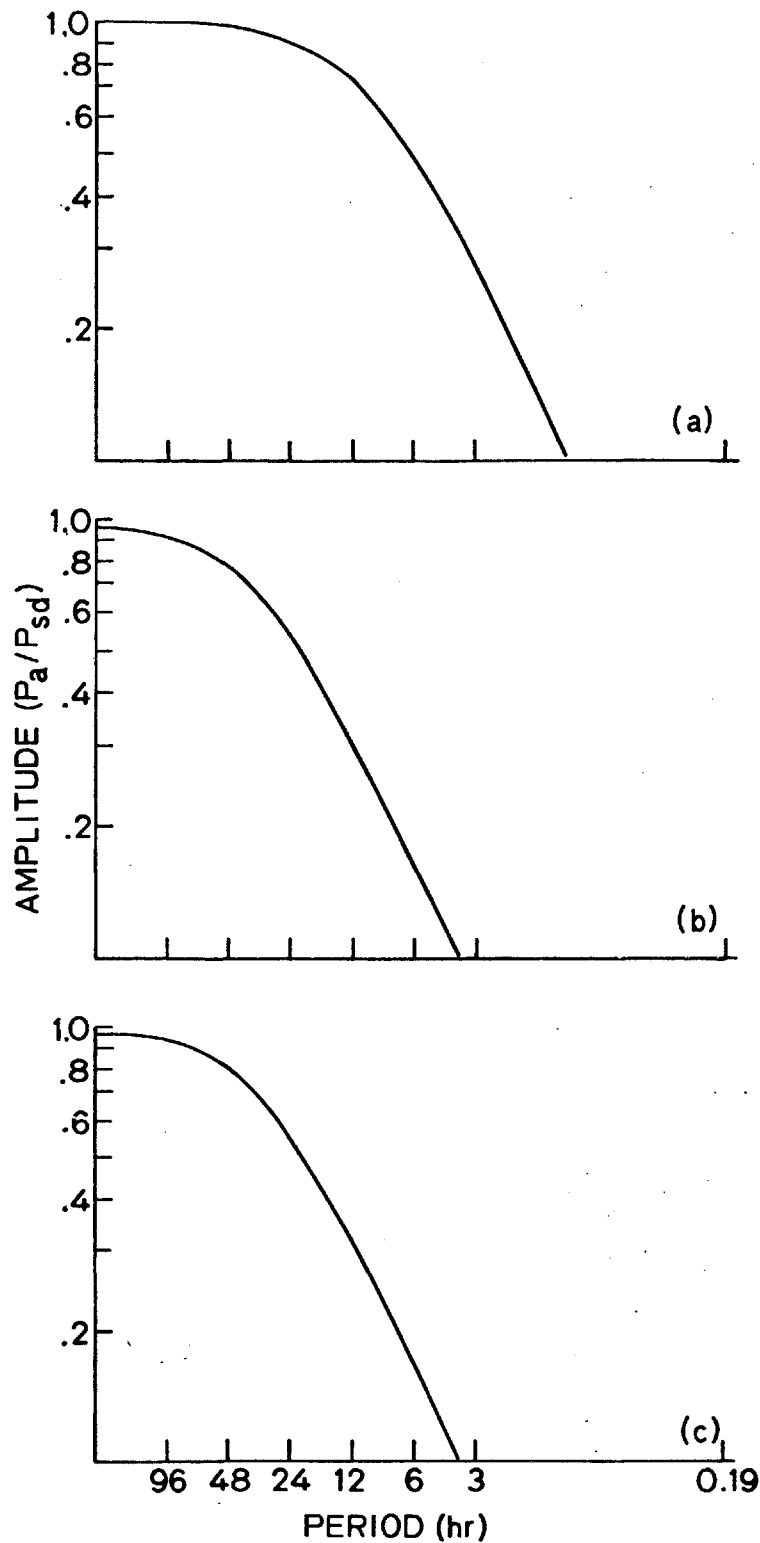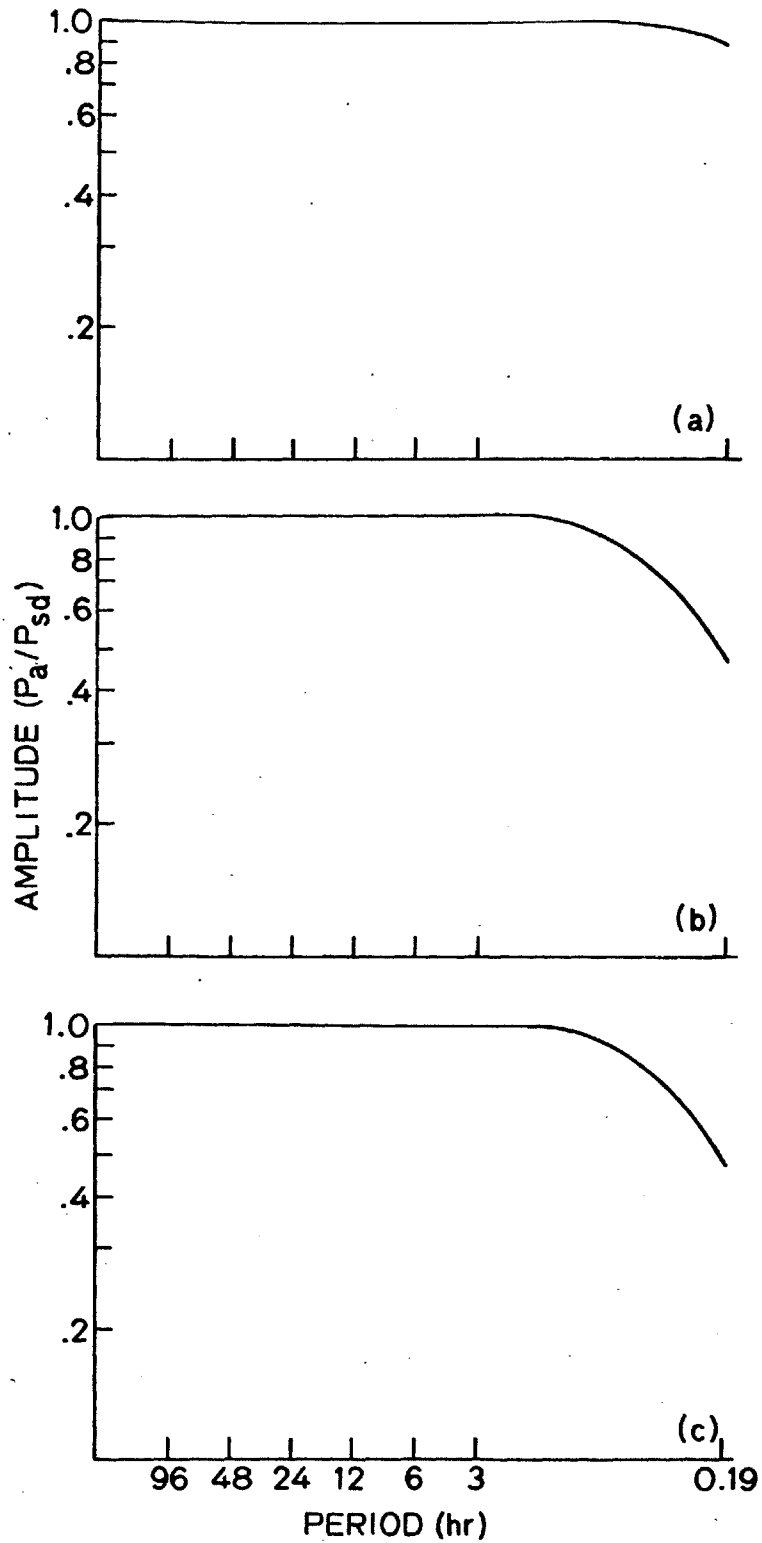
FIGURE 4.7: RESPONSE (P_a/P_{sd}) OF A CLOSED WELL RESERVOIR SYSTEM FOR ROCK FORMATION CB_1: (a) FLUID CONTENT NO. 1, (b) FLUID CONTENT NO. 2, (c) FLUID CONTENT NO. 3

We believe that in the last case, this ratio can reach a value much larger than two, but we do not have an example to cite. The maximum value we witnessed in this numerical application was around three. Not only is the ratio important, but the value of each tidal amplitude response is also important. If ω_c is very small compared to ω_D, it is possible to see the diurnal component amplitude response while the semidiurnal component amplitude response is too weak to be detected. Thus, the variation of values for ω_c may explain why the diurnal component effect is sometimes seen, and the semidiurnal one is not, knowing that pressure fluctuations smaller than 10^{-3} psi cannot be observed.

For rock formations CS_2, CL_2, and CB_1, the ω_c values were the highest, and the amplitude of the relative response, P_a/P_{Sd}, was maximum, constant, and equal to 1 for the frequency range studied. For these three cases we can write:

$$\frac{P_a}{P_{Sd}} = 1, \quad P_a = P_c \cdot E_o = P_c \; \frac{4G_m(C_f - C_m)}{3 + 4G_m C_f} \qquad (4.28)$$

This provides a simple relationship between the pressure, P_a, and the system characteristics for a frequency independent system. In this case, we can get the rock compressibility easily, if the pressure is recorded continuously. Usually wells are monitored for pressure. Fluid compressibility can be obtained without too much difficulty, but C_m is impossible to compute with certainty at this time. Thus this technique allows us to find C_m assuming that the pressure is recorded with a high-precision pressure gage.

The values of ω_c for the five rock cases remain almost the same for gas-free, or gas-saturated, oil reservoir cases, but they are 4 to 6 times

greater for dry-gas reservoirs. This indicates that the fluid composition is an important factor. Furthermore, for a given formation fluid, the value of ω_c increases with increasing values of the formation permeability. Using these different fluid-rock formation cases, we found that the value of the critical frequency, ω_c, increased with increasing values of $(k/\mu C_f)$. When this expression was large, the response remained frequency-independent for a long period of time, and the response of the diurnal and semidiurnal components were equal.

Tables 4.2 and 4.3 present these results. In these tables, the formations CS_1, CS_2, CL_1, CL_2, and CB_1, are called formations No. 1, No. 2, No. 3, No. 4, and No. 5, respectively.

In Section 4.1 we found that if we can assume that:

$$\frac{P_a}{P_{Sd}} = 1 - \frac{1}{1 + \frac{4k}{1\omega\mu a\ell C_f}}$$

The critical frequency, ω_c, can be found easily by using Eq. 4.27:

$$\omega = \omega_c = \frac{4k}{a\ell\mu C_f}$$

In this numerical application, we used the exact equation for P_a/P_{Sd}, which is given by Eq. 4.19a.

The results shown in Figs. 4.3 through 4.7 provide the computed values of ω_c for each case. They are obtained using the exact equation for P_a/P_{Sd}. Equation 4.26 can be used to calculate the theoretical values of ω_c, and the computed value of $(k/\mu C_f)$ for each case.

TABLE 4.2: SUMMARY OF THE RESULTS OF THE NUMERICAL APPLICATION

	CS_1 (NO. 1)	CS_2 (NO. 2)	CL_1 (NO. 3)	CL_2 (NO. 4)	CB_1 (NO. 5)
No. 1 ω-dep	Yes, from ~ 10^{-5} sec^{-1}	No in the interesting ω range	Yes, very important	No in the interesting ω range	No in the interesting ω range
ω_c sec^{-1}	1.58 to 1.99x10^{-4}	0.0125 to 0.0158	6.309 to 7.943x10^{-5}	6.309 to 7.943x10^{-3}	0.0158 to 0.0199
A diurnal	0.928 to 0.894	.999... ≈ 1.0	0.710 to 0.625	0.999... ≈ 1.0	.999... ≈ 1.0
A semidiurnal	0.783 to 0.707	.999... ≈ 1.0	0.452 to 0.373	0.999... ≈ 1.0	.999... ≈ 1.0
Rem	ω_c is very close to ω_D	ω-dependence starts at ω = 5.01 x10^{-4} sec^{-1}	ω_c is almost equal to ω_D	ω-dependence starts at ω semidiurnal	ω-dependence starts at ω = 1.58x10^{-3} sec^{-1}
No. 2 ω-dep	Yes	No in the interesting ω range	Yes, very important	No, in the ω range we are interested	No in the interesting ω range
ω_c sec^{-1}	3.98 to 5.01x10^{-5}	3.162 to 3.98x10^{-3}	1.58 to 1.99x10^{-5}	1.99 to 2.51x10^{-3}	3.98 to 5.01x10^{-3}
A diurnal	0.660 to 0.573	.999... ≈ 1.0	0.272 to 0.218	.999... ≈ 1.0	.999... ≈ 1.0
A semidiurnal	0.322 to 0.270	.999... ≈ 1.0	0.141 to 0.114	.997 to .996	.999... ≈ 1.0
Rem	ω_c is smaller than ω_D and ω_{SD}	The response is maximum as before	ω_c is smaller than the 2 interesting frequencies		ω-dependence starts at ω = 3.98 x10^{-4} sec^{-1}

CONTINUED

TABLE 4.2: CONTINUED

No. 3	CS_1 (NO. 1)	CS_2 N(. 2)	CL_1 (NO. 3)	CL_2 (NO. 4)	CB_1 (NO. 5)
ω-dep	Yes	No in the interesting ω range	Yes, very important	No, in the interesting ω range	No, in the interesting ω range
ω_c sec^{-1}	3.98 to 5.01x10^{-5}	3.98 to 5.01x10^{-3}	1.99 to 2.51x10^{-5}	1.99 to 2.51x10^{-3}	5.01 to 1.03x10^{-3}
A diurnal	0.590 to 0.502	.9997 to 0.9996≈1.0	0.283 to 0.228	.999... ≈ 1.0	.999... ≈ 1.0
A semi-diurnal	0.345 to 0.281	0.9961 to 0.994	0.145 to 0.118	.997 to .995	.999... ≈ 1.0
Rem		ssentially no difference between A_D and A_{SD}		ω-dependence starts at ω_1 = 2.51 x10^{-4} sec	ω-dependence starts at ω_1 = 5.01 x10^{-4} sec

At the beginning of Section 4.1, we defined the model (Fig. 4.1) such that $a = 0.5$ ft, and $\ell = 10,000$ ft; thus:

$$\frac{4}{a\ell} = 5.55 \times 10^{-6} \text{ in}^{-2}$$

Values of $k/\mu C_f$ given in Table 4.3 should be multiplied by:

$$1.07 \times 10^{-5} \; \frac{\frac{\omega^2}{\text{lb-sec}}}{\omega^2} \; / \; \frac{\text{md}}{\text{cp}}$$

in order to have a consistent system of units (see Section 4.2).

Table 4.4 shows the approximate and theoretical values of ω_c. The similarity is excellent. All the approximate values lie in the narrow range of the theoretical values of ω_c for each rock and fluid case. The approximation we suggested is valid, and we can write that $\omega_c \approx 4k/a\ell\mu C_f$.

Values given in Table 4.2 for the amplitude response do not take into account the term E_o. The value of E_o is given with each graph, and one can compute the amplitude of the effective responses, P_a/P_c, from the response P_a/P_{Sd} using:

$$E_o = \frac{4G_m(C_f - C_m)}{3 + 4G_m C_f} \;, \text{ and } \frac{P_a}{P_c} = E_o \cdot \frac{P_a}{P_{Sd}} \tag{4.29}$$

We see that for a given type of rock formation, the highest response is for the gas-filled reservoir; next comes the response of the gas-saturated oil reservoir; and finally, the response of the gas-free oil reservoir is last. This is true for the five formation cases. This proves the importance of the fluid compressibility in the determination of the amplitude

57

TABLE 4.3: RELATION BETWEEN THE VALUES OF $(k/\mu C_f)$, ω_c, AND THE AMPLITUDE OF THE RESPONSE, P_a/P_{Sd}

FORMATION NUMBER	FLUID NUMBER	$(k/\mu C_f) \times 10^{+6} \dfrac{md}{cp-psi}$	REMARKS
5 (CB_1)	1 Gas	294.12	
2 (CS_2)	1 Gas	240.64	
4 (CL_2)	1 Gas	133.69	
5 (CB_1)	3 Oil & Gas	85.40	
5 (CB_1)	2 Oil	81.48	
2 (CS_2)	3 Oil & Gas	69.88	
2 (CS_2)	2 Oil	66.67	
4 (CL_2)	3 Oil & Gas	38.82	
4 (CL_2)	2 Oil	37.04	
1 (CS_1)	1 Gas	2.67	
3 (CL_1)	1 Gas	1.07	
1 (CS_1)	3 Oil & Gas	.78	
1 (CS_1)	2 Oil	.74	
3 (CL_1)	3 Oil & Gas	.31	
3 (CL_1)	2 Oil	.30	

ω_c and amplitude of P_a/P_{Sd} decreases

$\star 6$

TABLE 4.4: COMPARISON OF THE EXACT SOLUTION AND THE APPROXIMATE SOLUTION
FOR THE VALUES OF ω_c

CASE NUMBER	Theoretical ω_c (Eq. 4.19a)	Approximate ω_c (Eq. 4.27)
CS_1 (NO. 1)	1.58 to 1.99×10^{-4}	1.58×10^{-4}
CS_1 (NO. 2)	3.98 to 5.01×10^{-5}	4.39×10^{-5}
CS_1 (NO. 3)	3.98 to 5.01×10^{-5}	4.63×10^{-5}
CS_2 (NO. 1)	1.25 to 1.58×10^{-2}	1.43×10^{-2}
CS_2 (NO. 2)	3.16 to 3.98×10^{-3}	3.96×10^{-3}
CS_2 (NO. 3)	3.98 to 5.01×10^{-3}	4.15×10^{-3}
CL_1 (NO. 1)	6.31 to 7.94×10^{-3}	6.35×10^{-3}
CL_1 (NO. 2)	1.58 to 1.99×10^{-5}	1.78×10^{-5}
CL_1 (NO. 3)	1.99 to 2.51×10^{-5}	1.84×10^{-5}
CL_2 (NO. 1)	6.30 to 7.94×10^{-3}	7.94×10^{-3}
CL_2 (NO. 2)	1.99 to 2.51×10^{-3}	2.20×10^{-3}
CL_2 (NO. 3)	1.99 to 2.51×10^{-3}	2.30×10^{-3}
CB_1 (NO. 1)	1.58 to 1.99×10^{-2}	1.75×10^{-2}
CB_1 (NO. 2)	3.98 to 5.01×10^{-3}	4.84×10^{-3}
CB_1 (NO. 3)	5.01 to 6.03×10^{-3}	3.07×10^{-3}

response. For the fluid cases No. 1 and No. 3, the highest response is obtained for the rock formation CS_2, then CL_2, CB_1, CS_1, and finally CL_1 (Table 4.5).

Considering the gas-free oil reservoir case, we see that the highest response is obtained for rock formation CL_2, then CS_2, CS_1 and CB_1, and finally, CL_1.

When we compare the different rock matrix parameters for fluid cases No. 1 and No. 3, the amplitude of the response decreases with decreasing values of $[\phi C_f + (1-\phi) C_m]$. For fluid case No. 2, this is not true. The amplitude decreases with increasing matrix compressibility values (or increasing $C_f - C_m$ values).

Thus the three important parameters governing the amplitude of the effective response, P_a/P_c, are ϕ, C_f, and C_m. Permeability is important in determining the ω_c values, and thus in determining the frequency dependence of the response. G_m goes not seem to play an important role in the behavior of the system.

From Tables 4.5 and 4.3, we see that the factor E_o is very important, because the response P_a/P_{Sd} for CB_1 was the highest, while P_a/P_c for CB_1 is now one of the two or three lowest.

So, when the system is frequency-independent, the amplitude of the effective response, P_a/P_c, increases with decreasing values of C_m for a given saturating fluid. When the result is frequency-dependent, the amplitude of the response, P_a/P_c, seems to be proportional to $[\phi C_f + (1-\phi) C_m]$.

60

TABLE 4.5: ANALYSIS OF THE EFFECTIVE RESPONSE, P_a/P_c, FOR THE DIFFERENT ROCK AND FLUID CASES

FORMATION	FLUID	$\phi C_f + (1-\phi)C_m$ psi^{-1}	C_m psi^{-1}	$\dfrac{P_a}{P_c}$ S *	$\dfrac{P_a}{P_c}$ SD **	REMARKS
CS_2 (NO. 2)	Gas (NO. 1)	38.08x10^{-6}	.95x10^{-6}	.990	.990	$\phi C_f + (1-\phi)C_m$ decreases. P_a/P_c decreases. ONE INVERSION.
CL_2 (NO. 4)	Gas (NO. 1)	33.58x10^{-6}	3.2x10^{-6}	.972	.972	
CB_1 (NO. 1)	Gas (NO. 1)	21.85x10^{-6}	7x10^{-6}	.943	.943	
CS_1 (NO. 5)	Gas (NO. 1)	18.77x10^{-6}	3.7x10^{-6}	.900	.759	
CL_1 (NO. 3)	Gas (NO. 1)	12.41x10^{-6}	6.5x10^{-6}	.672	.428	
CS_2 (NO. 2)	Oil (NO. 2)	2.92x10^{-6}	.95x10^{-6}	.860	.860	C_m increases with decreasing response. P_a/P_c. ONE INVERSION.
CL_2 (NO. 4)	Oil (NO. 2)	4.27x10^{-6}	3.2x10^{-6}	.587	.557	
CS_1 (NO. 1)	Oil (NO. 2)	4.28x10^{-6}	3.7x10^{-6}	.329	.166	
CB_1 (NO. 3)	Oil (NO. 2)	6.56x10^{-6}	7.0x10^{-6}	.065	.065	
CL_1 (NO. 5)	Oil (NO. 2)	7.05x10^{-6}	6.5x10^{-6}	.035	.018	
CS_2 (NO. 2)	O+G (NO. 3) ***	10.84x10^{-6}	.95x10^{-6}	.968	.965	$\phi C_f + (1-\phi)C_m$ decreases with decreasing P_a/P_c. No inversion. TRUE FOR ALL CASES.
CL_2 (NO. 4)	O+G (NO. 3)	10.83x10^{-6}	3.2x10^{-6}	.900	.900	
CB_1 (NO. 5)	O+G (NO. 3)	9.69x10^{-6}	7x10^{-6}	.789	.789	
CS_1 (NO. 1)	O+G (NO. 3)	8.23x10^{-6}	3.7x10^{-6}	.524	.306	
CL_1 (NO. 3)	O+G (NO. 3)	7.87x10^{-6}	6.5x10^{-6}	.227	.116	

* effective diurnal response
** effective semidiurnal response
*** O+G: oil and gas

At this point, it is not possible to state any general correlation between ϕ, C_f, C_m, and the amplitude of the pressure variations, but we strongly believe that such a correlation does exist.

We have found some interesting conclusions, but we must remember that these conclusions are drawn only from the analysis of the fifteen cases we defined. They would have to be verified on a larger sample of field cases to be considered as general rules. Some of the cases we studied do not behave as expected. These discrepancies have to be explained. The main conclusions are:

1. The critical frequency values are important for determining the existence of earth tide effects and the ratio of the diurnal to the semidiurnal components amplitude.

   a. If ω_c is very large, both the diurnal and semidiurnal tidal components will exist, and have equal amplitudes. If ω_c is very small, neither tide will be seen. If ω_c is of the order of the diurnal component but smaller, we will have a larger diurnal amplitude than the semidiurnal one. It is even possible to see only the diurnal effect, the semidiurnal amplitude being too weak to be detected.

   b. The frequency dependence of the response depends on the value of ω_c. We found a simple relationship between this value and the rock fluid and well-reservoir system characteristics:

$$\omega_c = \frac{4}{a\ell} \frac{k}{\mu C_f}$$

This is an important result. For instance, if ω_c is known, $k/\mu C_f$ can be obtained. If ω_c can be computed, an explanation for the existence or nonexistence of tidal effects can be found.

2. The four principal parameters governing the amplitude of the effective response, P_a/P_c, are ϕ, C_f, C_m, and k.

a. For a given formation, the highest response is obtained when the saturating fluid is gas. This shows the importance of the fluid compressibility, C_f.

b. If the system is frequency independent, the relative amplitude is proportional to (C_f-C_m). For a given fluid reservoir, the relative amplitude decreases with increasing values of C_m. This observation, like others, is based on the nine rock-fluid cases where there was no frequency-dependence.

c. If the system is frequency-dependent, the amplitude is proportional to $[\phi C_f+(1-\phi)C_m]$. This is based on the six different rock-fluid cases, where there was a frequency dependence.

d. The permeability, k, is important in the determination of ω_c. When k increases for a given fluid formation, the critical frequency value increases.

e. The shear modulus is a second-order parameter in the determination of the amplitude response.

This numerical investigation of the results can be misleading due to the choice of the different parameters studies. However, the general ideas obtained from this analysis are expected to be valid for real field cases.

We now consider real field data. The main purpose of this analysis is to:

(1) detect the influence, if any, of the earth tide on reservoir pressure,

63

(2) compare the different tidal component responses, and

(3) check theoretical results and add some new conclusions obtained from field data analysis.

5. ANALYSIS OF FIELD DATA

It is desired to detect pressure variations due to earth tides, using recorded field data. For this purpose we need the following:

(1) A very reliable and sensitive pressuge gage (Section 5.1).

(2) A continuous pressure record for a long period of time. The length and continuity required will be discussed later.

(3) Information on rock and fluid properties in order to be able to analyze the results given by the pressure data.

The pressure recording techniques used, the field data, and the analysis of the field data for each different field will be presented in the following. Then we will discuss the results of these data analyses, and make some suggestions for improving the quality and the meaning of the results obtained.

5.1 Instrumentation

Until recently, the conventional pressure gage used in performing well tests had a resolution of 1 psi at best. Small pressure changes such as those generated by the earth tide stress could not have been detected. Earth tide pressures are on the order of 5×10^{-1} to 10^{-3} psi. With the new Hewlett-Packard 2811B quartz pressure gage, wellbore pressure changes of 0.01 psi can be detected. See Fig. 5.1.

This pressure gage consists of a quartz crystal pressure probe down-hole and a pressure signal processor at the surface. Pressure stress of

Preset Counter

Strip Chart Recorder

Clock and Digital Printer

Pressure Signal Processor

Digital-To-Analog Converter
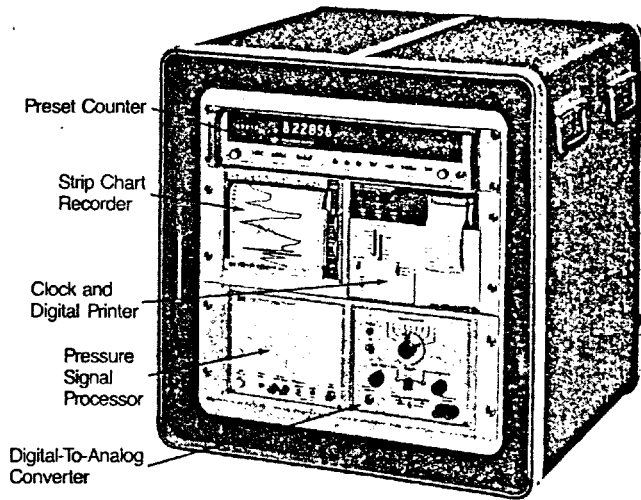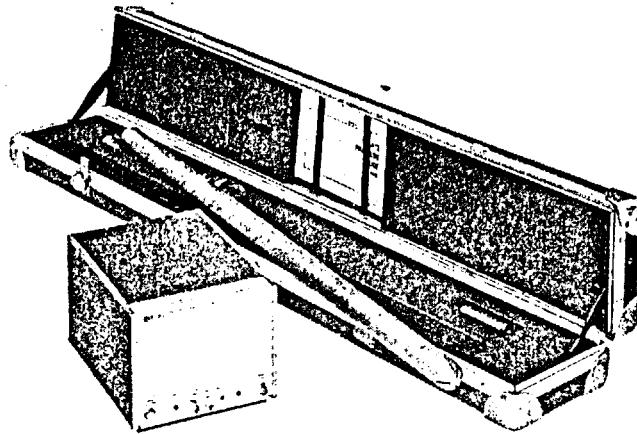
FIGURE 5.1: HP-2811B QUARTZ PRESSURE GAUGE (TOP) AND ANALOG & DIGITAL
RECORDING OPTION (BOTTOM) (HP 1977 ELECTRONIC INSTRUMENT &
SYSTEMS CATALOG)

the crystal causes frequency variations detected by the probe and transmitted to the signal processor by a single conductor, armored electric line. The frequency signal can then be transformed into a pressure-related signal by an analog and digital recording system. Pressure is displayed in psi continuously. If the analog and digital recording system is not used, data are displayed in terms of frequency.

The extremely high resolution of this pressure gage is due to the natural quartz crystal oscillator located in the probe. The quartz crystal is sensitive to a change in pressure of 10^{-2} psi. This kind of pressure gage is now commonly used when high precision is needed, for instance, during interference tests such as buildup, drawdown, or pulse tests. All of the data presented here were recorded with this gage. The details of the gage characteristics are given in Appendix C.

As shown in Appendix C, the maximum temperature the gage can withstand is 302°F. Above this limit, frequent failure of the pressure gage is observed after 40 operating hours or so (Witherspoon et al., 1978). This is a shortcoming when the pressure tests are run in high temperature geothermal wells. Witherspoon reported that while the gage did not work at the East Mesa field where the temperature is 318°F, it worked perfectly at the Raft River field, where the temperature is only 295°F. Indeed, in this case he noticed periodic fluctuations with 0.05 psi amplitude which were definitely associated with tides. So, the precision, accuracy, and feasibility of this gage remains excellent over the entire range of operating pressures and temperatures.

67

5.2 Field Data Exploitation: Original Data, Data Transformation, and the Utilization of the Fast Fourier Transform

We solicited and received data concerning various gas and oil fields. All of these data were recorded with a quartz crystal pressure gage, as described in the previous section. It was assumed that no error existed in the recorded data, and that the data represented the continuous variation of pressure for each tested field.

We want to detect the influence of the tidal stress, if any, for these fields. In order to do that, it is necessary to make a spectrum analysis of the pressure records to identify the different frequency components, and the amplitude of the pressure changes they generate. To obtain a spectrum analysis, it is necessary to perform a Fourier Transform of the data; in fact, a Fast Fourier Transform (FFT) was used. An FFT is simply an algorithm (Brigham, 1974) that can compute the discrete Fourier Transform rapidly. The raw pressure versus time information is transformed into the corresponding amplitude (and phase) versus frequency. The time domain becomes the frequency domain.

In theory, the FFT is done for an infinitely long set of data (FFT is computed from $-\infty$ to $+\infty$). Of course, in real life, all experiments are limited in duration. In order to make an FFT of a periodic functions, we limit the computation to an integer number of the longest period which may exist in the subject function. Here the longest period we are interested in is equal to one day, and the shortest is 1/2 day.

Another requirement for computing an FFT is that the sampling rate of data be equal to or greater than the Nyquist rate. The Nyquist rate sets the minimum number of points needed to reconstruct the initial data from the sampled data (Brigham, 1974).

68

This rate is defined by:

$$\omega_s \ (\text{hrs}^{-1}) = \frac{1}{2} \ T_{\text{min}} \ (\text{shortest period in hours})$$

$$\omega_s = \frac{1}{2\omega_{\text{max}}}$$

where $\omega_{\text{max}} = \dfrac{1}{T_{\text{min}}}$ = the highest frequency encountered in the periodic function

So, for our particular problem, the minimum sampling rate is equal to 1 point every 6 hours. This is the minimum rate; it is not the best one.

We concluded earlier that it is necessary to make the FFT on data for an integer number of days. Furthermore, the first data point and the last data point must be equal. This results from the fact that the FFT is done for sinusoidal functions from $-\infty$ to $+\infty$. Before computing the FFT of a set of data, the set of data must be transformed such that the first and last points are equal (Brigham, 1974). When this is done, we should have 256 data points in the right order so they can be Fourier transformed. Let us explain why we chose to do the FFT on 256 data points. From sampling theory, we have to have at least 2 points per period of the highest frequency. If we consider that the highest frequency is that of the semi-diurnal component, and if we want to be able to use this program for the analysis of a maximum of a 2-month-long experiment, we need (using the Nyquist sampling rate):

4 points per day for (30x2) days = 4 x 60 = 240 points

so we will use 256 points ($256=2^8$) for our analysis. We could do the computation with more data points without a problem, but not with less points, because some of the frequency components eliminated by the restriction of data will create a larger aliasing phenomenon (Brigham, 1974).

69

Aliasing is a phenomenon generated by the fact that the FFT is a digital Fourier Transform, and not a continuous FT. Two parameters influence the amount of aliasing.

One is the nonrespect of the Nyquist sampling law which states that the sampling rate should be higher than twice the frequency of the highest frequency components existing in the original signal. Even so, one may not be interested in the components of high frequencies because such components may be present in the original signal due to noise. The digital FT at a rate too low to encompass this noise will give a spectrum containing peaks which do not really exist, but which are mirror images of noise components of high frequency.

The solution is to filter out the frequency components of frequency higher than one half the Nyquist rate before Fourier transforming the signal.

The other cause of aliasing is that a digital FT of a signal covers the interval from a finite time in the past to a finite time in the future, while a continuous FT covers a time from $-\infty$ to $+\infty$. So, the spectrum obtained is that of a signal which would repeat itself forever by folding the original interval.

At the end of this interval, the phase of the frequency component of interest may not be zero. In this case, the folding effect gives rise to a discontinuity. This discontinuity, which does not exist in the original signal, contains high frequency components which will show in the spectrum as a smearing of the frequency peaks. One way to avoid this effect when the content of the signal is known, and consists of a small number of discrete frequency components, is to choose the time interval carefully such that those frequency components all have a phase equal to zero at the

interval ends. When this is not possible, a better method is to multiply the signal by a "window" function.

A window function is a function which layers down to zero, i.e., is bellshaped, and has a well-behaved FT. This way, the influence of the discontinuity at the interval ends is minimized. In this study, the first method to eliminate the aliasing problem was used.

The method used has some limitations. As the entire experimental length was divided into 256 equally-spaced intervals, a problem may arise if there is a gap in the recorded data longer than (1/256) of the total length of the experiment. In this case, no pressure data are found by the computer for the interval, and the FFT does not work.

One solution for this problem is to take an average value for the empty interval. But if the gap is too big, the average value taken will probably not be representative of reality, and the output of the FFT may be incorrect. Another problem is a phenomenon called "aliasing" (defined earlier) which may be generated by the computation of the FFT. This phenomenon may amplify or mask completely the existence of one or more frequency components by overlapping the real frequency component peak.

The last problem is that if pressure data are recorded for a short period of time, the peaks corresponding to the diurnal components and semidiurnal components will be very close to each other, and some noise or aliasing problem may confuse the spectrum of these two peaks. A minimum of about 16 days should be used to get a clear spectrum analysis. The longer the experiment, the better the spectrum.

In order to enter the field data into different files, to compile all the files corresponding to a same well, and to plot all the data for this well (pressure versus time), two computer programs (Programs No. 1 and No. 2) were prepared. Three other computer programs (Programs No. 3, No. 4, and No. 5) were written to divide the field data into 256 equally-spaced intervals, to modify their relative order so that the first and last points were equal, and to plot the modified data. Finally, we wrote two other computer programs (Programs No. 6 and No. 7) to compute the FFT for the modified data, and to plot the output of the FFT (amplitude and phase versus frequency). These seven programs are listed in detail in Appendix D.

For the modified data plot, the unit of the horizontal axis was chosen arbitrarily to be equal to 1/16 of the length of the experiment. The plots of the output data of the FFT give the amplitude and phase of the pressure variations due to each different component against the frequency of appearance of this component. The smallest division on the frequency axis of the amplitude and phase plots is equal to 16 periods per experiment. It is an arbitrarily chosen number. For the amplitude plots, the height of the peaks corresponding to these components is proportional to the amplitude of the variation induced by these different periodic excitations. The phase plots will not be used in this work. They are presented here to draw the complete FFT calculations, and for possible further work on this subject.

Let us call H_D and H_{SD} the height of the diurnal and semidiurnal peaks, corresponding to the "once per day" and "twice per day" frequency. It is not exactly once per day for the diurnal stress, because the period of the diurnal tidal component (O_1) is 25.82 hours, and not 24 hours. The

72

semidiurnal stress (M_2) does not appear exactly twice a day, because the period is 12.42 hours, and not 12 hours. The 2 peaks will be slightly shifted due to this difference of 1.82 hours and 0.42 hours, respectively. We have the following relationships:

$$\Delta P_{SD} = H_{SD} \cdot \frac{2}{256} \qquad (5.1)$$

$$\Delta P_{D} = H_{D} \cdot \frac{2}{256} \qquad (5.2)$$

where ΔP_{SD} and ΔP_{D} are the pressure variations due to the semidiurnal and diurnal tidal stress. The amplitude of the Fourier Transform of a sinusoidal wave of amplitude 1 is equal to 1/2 (Fig. 5.2). The theory of the FFT says that the amplitude of a Fast Fourier Transformed sinusoidal wave of amplitude 1 is now equal to the number of points used in this FFT computation over 2 (instead of 1 over 2 for the simple FT) (Fig. 5.2). To find the amplitude of the initial sinusoidal wave, the amplitude of output wave is multiplied by 2 over the number of points used (Brigham, 1974). Thus, for our analysis, we multiply by 2 over 256.

Equations 5.1 and 5.2 will be used to interpret the data presented in the next section. We must keep in mind the cited limitations of the method used when we perform the analysis. Let us look now at the different sets of field data available.

5.3 Presentation of the Data

The field data used in this analysis were made available by several different oil companies. Pressure versus time information was available as a series of numbers. This information was entered into a computer and plots of these raw data were prepared. The data were modified as

73
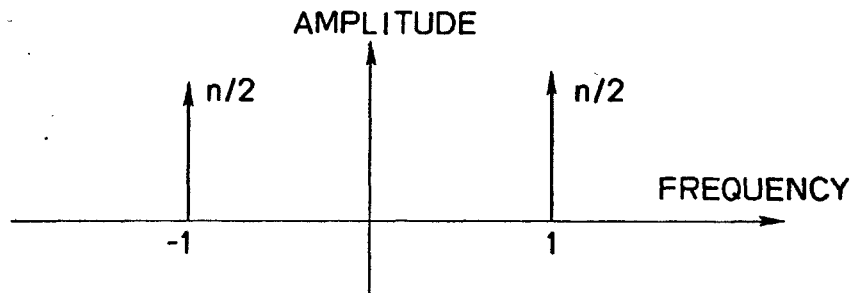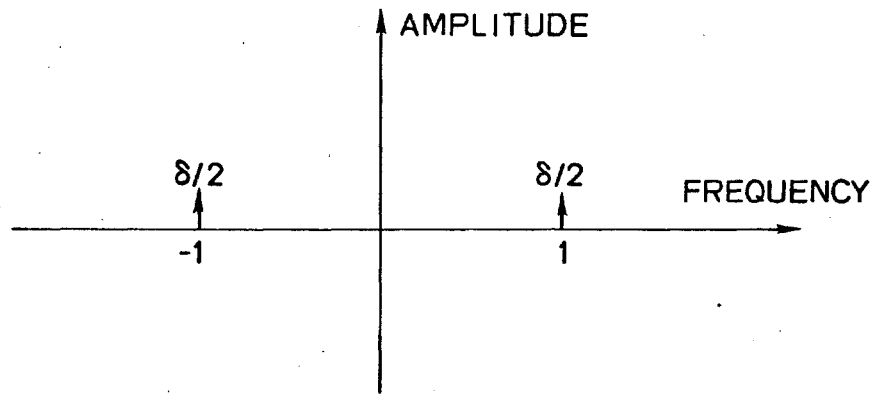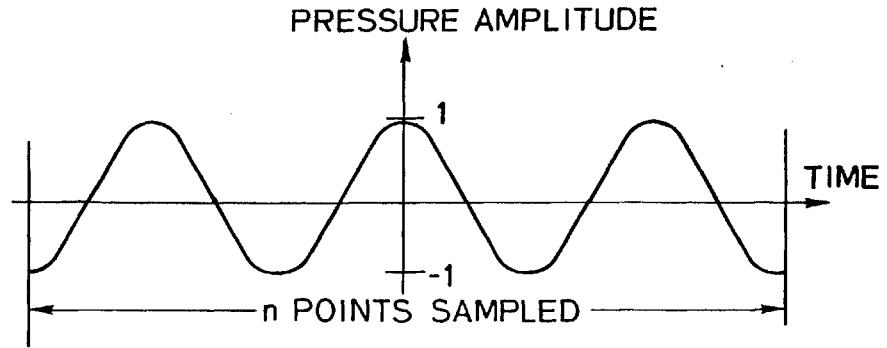
FIG. 5.2: INITIAL DATA (TOP), FOURIER TRANSFORM OF THE INITIAL DATA
(MIDDLE), AND FAST FOURIER TRANSFORM OF THE INITIAL DATA
(BOTTOM)

described in Section 5.2, and a second plot made. This plot represented the data before the FFT was computed. The last step was the computation of the FFT. The results are given in the last graph presented for each set of field data.

Each field contained one or more wells. A file number was assigned to each well to simplify computer work. Depending on the length of the experiment and the sampling rate, the file number might contain from two to ten digits (remember that one file contains 256 data points only). For instance, the data for a certain 17-day-long test could have the file number 12-13-14-15-16. This would correspond to a 17-day-long experiment with a sampling rate of one point every twenty minutes, or 72 points per day; thus, 17x72=1224 data points for this case. This test would require (1224/256) files, which is equal to five data files. The first file containing data is file No. 12.

In this section, we will present the following information for each field:

(1) the details on the length and time of the experiment,

(2) the rock and fluid properties for the well considered,

(3) any additional information on the field (particularly geologic structure or feature, such as fractures, etc.), which may be important for the interpretation of the unit, and

(4) three graphs representing the initial data, the modified data, and the result of the FFT amplitude phase (except for the Big Muddy Field, where only the initial data plots will be shown.

75

Let us consider the different field cases available. The first field case is the "A" field, Australia. The data were taken from a study done by Strobel, Gulati, and Ramey (J. Pet. Tech., 1975). The associated file number is 12-13-14-15-16. The produced fluid was dry gas. Almost all of the gas came from 57 ft of perforations. The productive thickness was less than 85 ft. There were two main formations: a dolomitic section (25 ft) had a matrix porosity less than 1%, and a permeability less than 0.5 md. Below the dolomitic section there was a thinly-bedded clean orthoquartzite which had a porosity of less than 2.1%, and a permeability less than 0.1 md. This productive formation was fractured, and vertical fractures were observed throughout the reservoir thickness.

From pressure buildup and interference tests, a porosity of 0.22% (0.0022 fraction of bulk volume) and a permeability of 48 md were found to be representative of this naturally-fractured reservoir. The formation temperature was 152°F, the recording depth was 5600 ft (KB), and the initial pressure at this depth was 2897.34 psig. The well radius was 0.25 ft. The gas gravity was 0.62, the initial gas viscosity was 0.0186 cp, and the total system compressibility was 274×10^{-6} psi^{-1}.

As stated before, the pressure versus time data were recorded for a 17-day time interval. One point was graphed every 20 minutes for this period of time. This is shown in Fig. 5.3a. The smallest division in the vertical scale is 0.1 psi, and the length of the record is 17 days.

Then the data for the entire 17-day experiment were divided into 256 equally-spaced intervals. An average value for the pressure was computed for each interval. Furthermore, the decreasing level of the pressure was

PRESSURE (psi)

TIME (days)

FILE # 12   13   14   15   16   –

HORIZONTAL SCALE: 0   HOURS TO 432 HOURS IN UNITS OF 24   HOURS
VERTICAL SCALE: 2910.9 PSI TO 2911.9 PSI IN UNITS OF 0.1 PSI
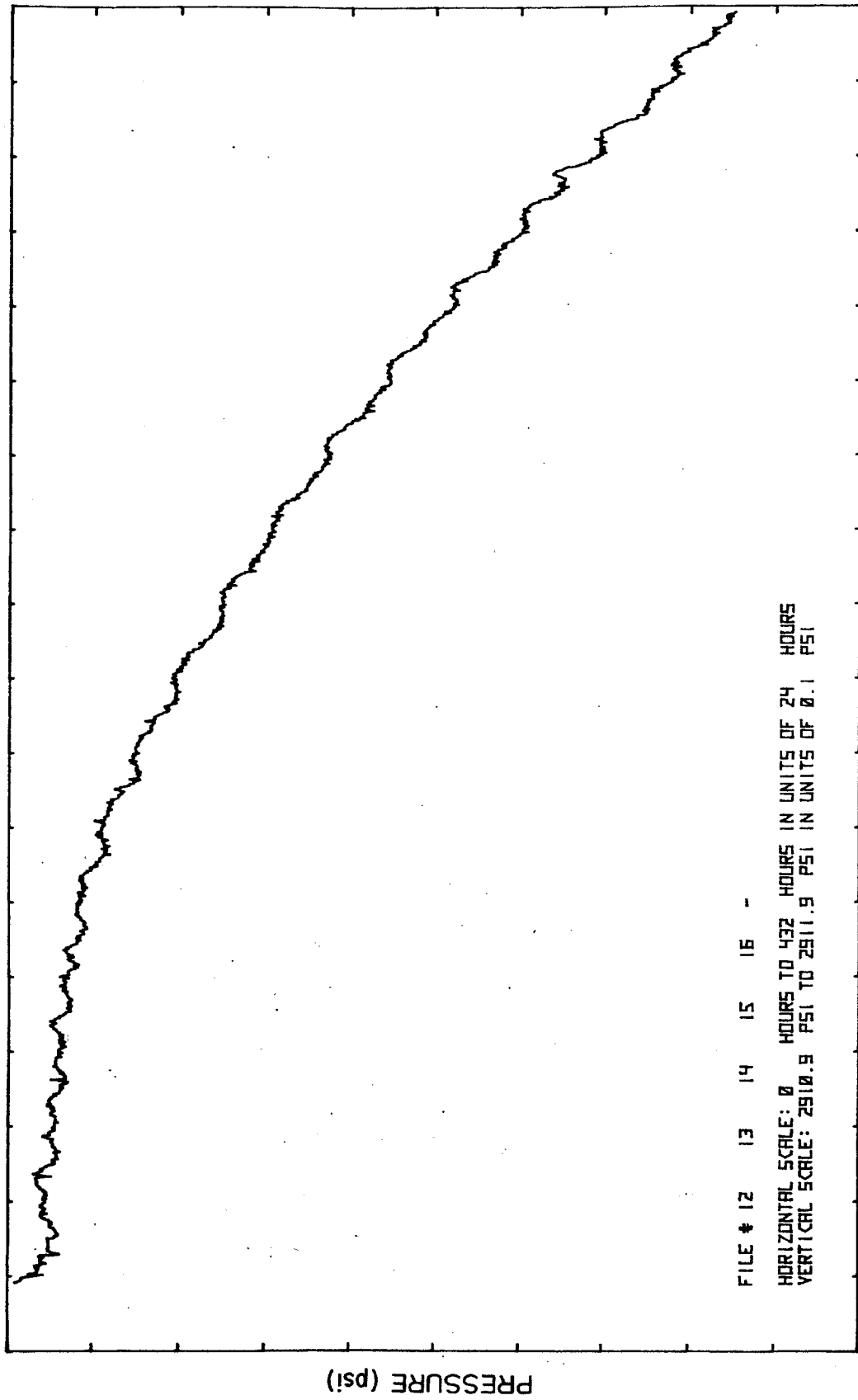
FIG. 5.3a: INITIAL DATA FOR THE "A" FIELD

VERTICAL SCALE:-0.2 PSI TO 0.3 PSI IN UNITS OF 0.1 PSI

TIME (total length = 17 days)
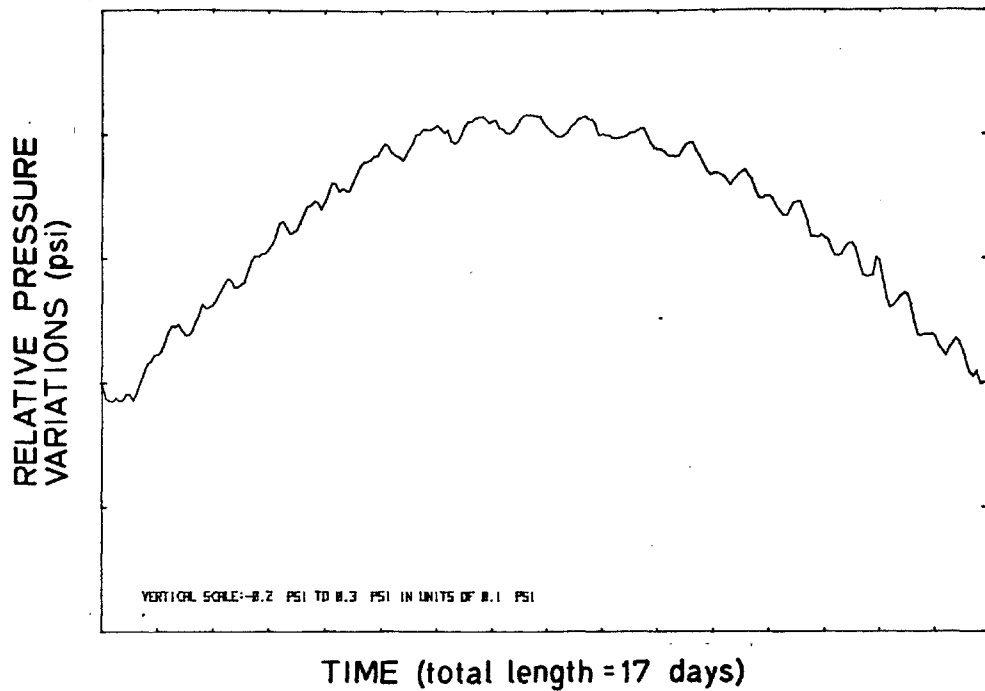
FIG. 5.3b: MODIFIED DATA FOR THE "A" FIELD

VERTICAL SCALE:-1 TO 3 IN UNITS OF 0.5 .

FREQUENCY (unit = 16 periods per experiment)
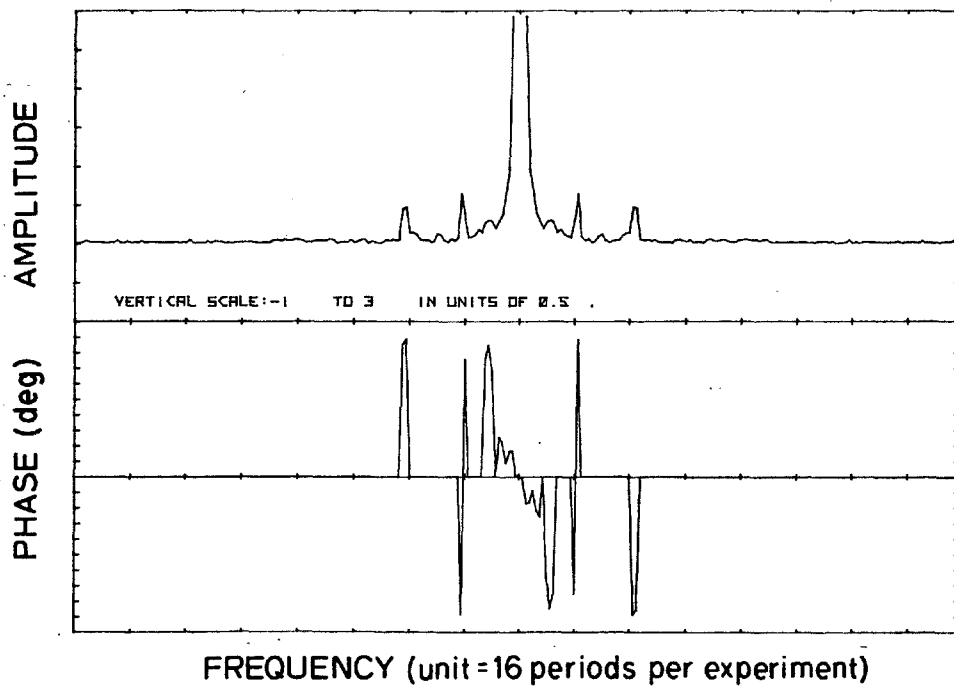
FIG. 5.3c: SPECTRUM ANALYSIS BY FFT FOR "A" FIELD

eliminated and the data were smoothed. This was done by subtracting pressures from a straight line joining the first and last points of the initial plot from the initial data. This modification assures that the first and last point of the revised data are equal. After this transformation, the modified data were plotted. The graphs represent the relative pressure variations (caused mainly by earth tides) versus time. As we said in Section 5.2, the time axis represents the total length of the experiment. Here, it is equal to 17 days (Fig. 5-3b).

Now that the data are in a usable form, it is possible to compute the FFT. The FFT of a periodic function provides the amplitude and the phase of periodic components of the function, Fig. 5-3c. On this figure, the peaks indicate the existence of different frequency components. On the top plot, each peak corresponds to one component with a given amplitude and frequency. The amplitude is given by the height of the peak (Eqs. 5.1 and 5.2), and the frequency of the component is determined by the position of the peak on the frequency axis. On the bottom plot, the height of the peak gives the value of phase of a given frequency component. This information will not be used here, because it has been explained in the previous section.

The next two fields are called "X_{north}" and "X_{south}." Their associated file numbers are 17-18-19 for "X_{north}" and 20-21 and 22-23-24 for "X_{south}." The "X_{south}" experiment has been split into two parts, because a few days of data were missing.

The fluids produced for "X_{north}" and "X_{south}" are gas-saturated oil and water. The perforated interval of the producing well is 12,720 to 12,770 ft for "X_{north}" and 12,636 ft to 12,685 ft for "X_{south}."

79

Interference tests conducted on "X_{north}" and "X_{south}" were done in a similar manner: one well was produced for about five days (producing well) while pressures were recorded in the observation well. Pressures recorded in the observation well, which was shut in, were recorded every hour for a long period of time, including the five days of production of the producing well. The recording depth was 8,500 ft for "X_{north}" and 8,350 ft for X_{south}."

The permeability of "X_{north}" field is about 50 md. The productive formation is a sandstone, with a porosity of 11.8%. The reservoir temperature is 294°F, and the initial pressure is 5,490 psig. The oil, water, and gas viscosities are 0.314 cp, 0.235 cp, and 0.020 cp, respectively. The oil is 35° API, and the gas gravity is 0.875. The connate water saturation is 0.45. The differential gas-oil ratio is 1.025 SCF/bbl, and the gas formation volume factor is 0.00136 bbl/SCF. The oil formation volume factor is 1.41 res bbl/STB, and the water formation volume factor is 1.075 res bbl/STB. The oil, water, and gas compressibilities can be computed from existing correlations.

For the "X_{north}" field, the pressure versus time data were for 30 days. For "X_{south}," the experiment was in two parts: one of 12 days and one of 29 days. Missing data points due to a power generation failure obliged us to separate the record into two experiments for the "X_{south}" field. The pressure was recorded every hour.

Figures 5.4a, 5.5a, and 5.6a represent the pressure versus time data for the "X_{north}" and "X_{south}" fields, rexpectively. The vertical scale is 0.5 psi, 1 psi, and 1 psi for Figs. 5.4a, 5.5a, and 5.6a, respectively. The figures representing the modified data are 5.4b, 5.5b, and 5.6b. Their vertical scales are 0.5, 0.5, and 1 psi, respectively. Figures 5.4c
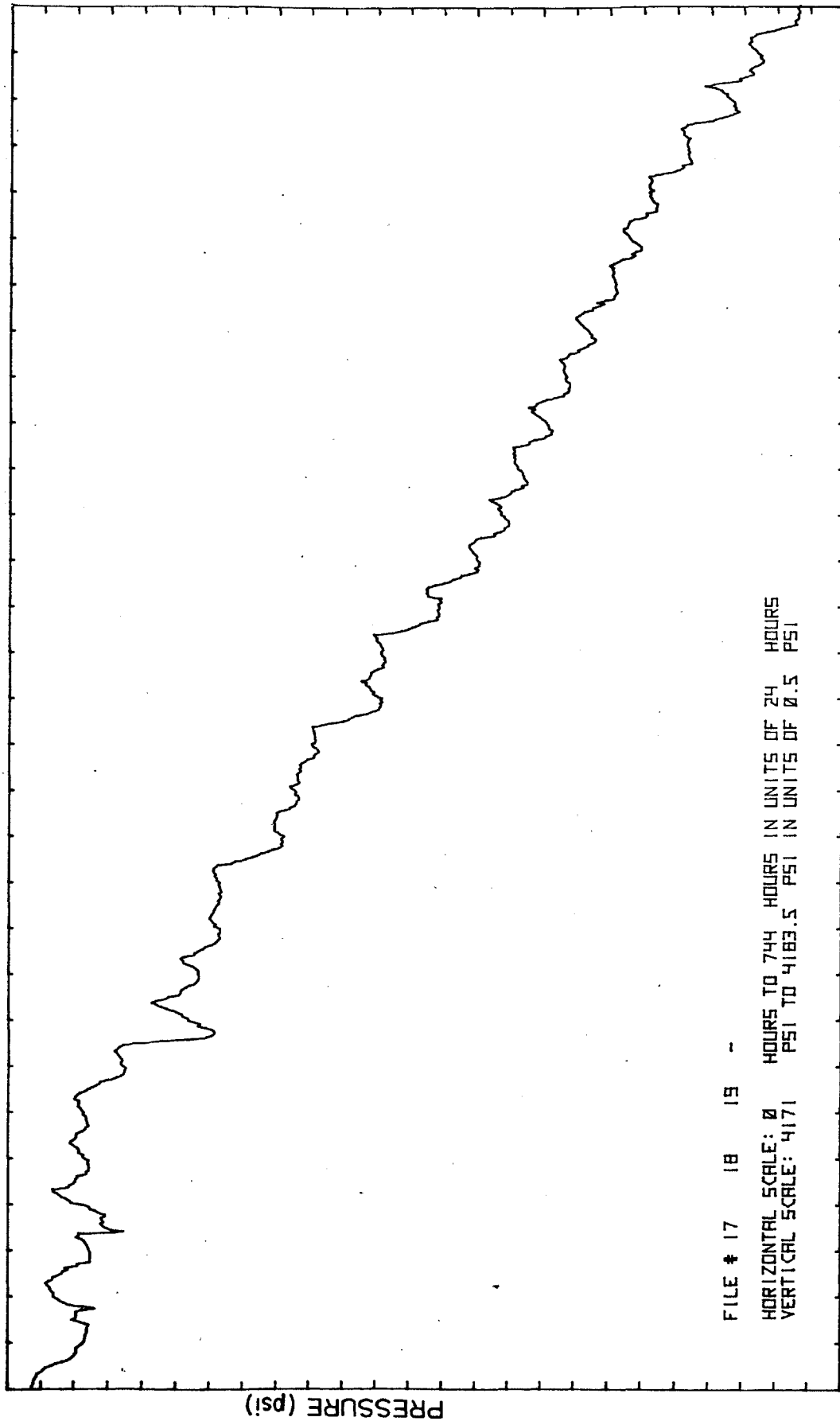
FIG. 5.4a: INITIAL DATA FOR THE "X NORTH" FIELD

FILE # 17   18   19   –

HORIZONTAL SCALE: 0   HOURS TO 744 HOURS IN UNITS OF 24   HOURS
VERTICAL SCALE: 4171   PSI TO 4183.5 PSI IN UNITS OF 0.5   PSI

PRESSURE (psi)

TIME (days)

VERTICAL SCALE:-1   PSI TO 2   PSI IN UNITS OF 0.5 PSI

TIME (total length =30 days)
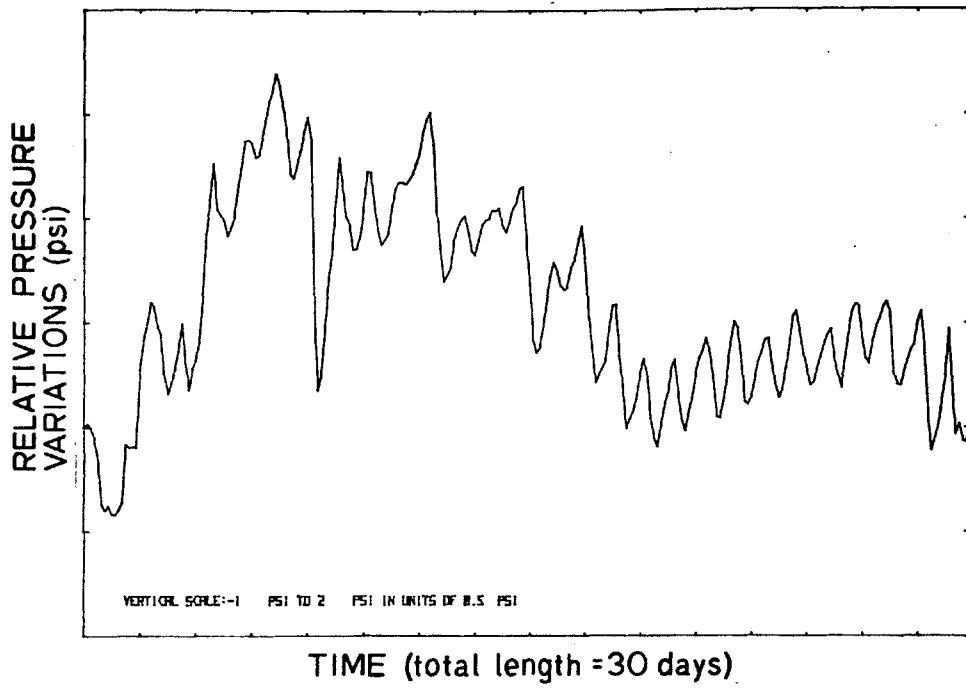
FIG. 5.4b: MODIFIED DATA FOR THE"X NORTH"FIELD

VERTICAL SCALE:-20   TO 30   IN UNITS OF 10

FREQUENCY (unit =16 periods per experiment)
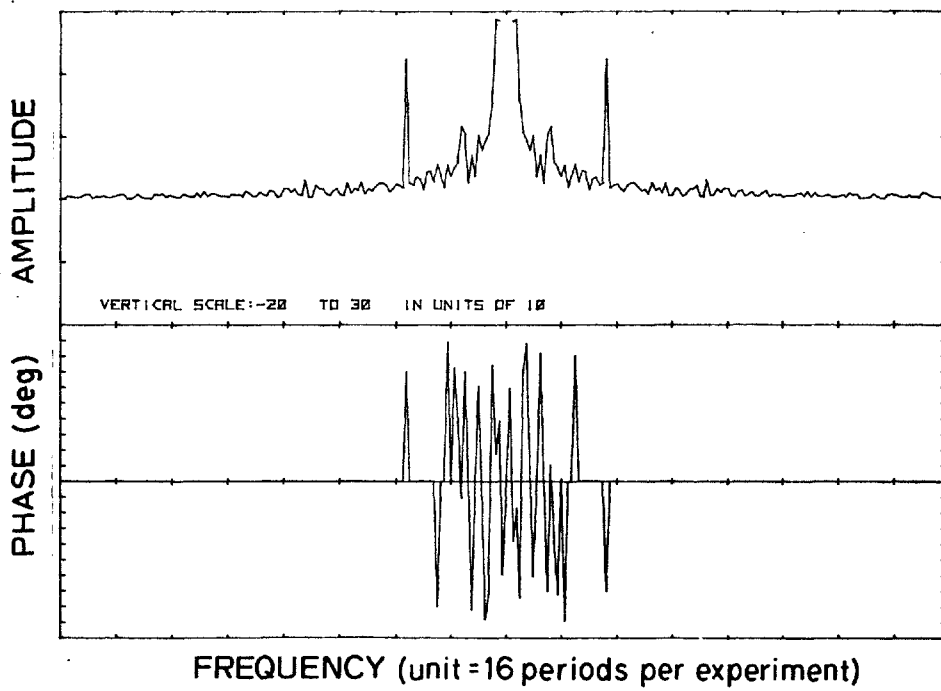
FIG. 5.4a: SPECTRUM ANALYSIS BY FFT FOR THE"X NORTH"FIELD

82

FIG. 5.5a: INITIAL DATA FOR THE "X SOUTH" FIELD, FIRST PART

TIME (days)

PRESSURE (psi)

FILE # 20   21   -

HORIZONTAL SCALE: 0   HOURS TO 360   HOURS IN UNITS OF 24   HOURS
VERTICAL SCALE: 4214   PSI TO 4223   PSI IN UNITS OF 1   PSI

TIME (total length = 12 days)
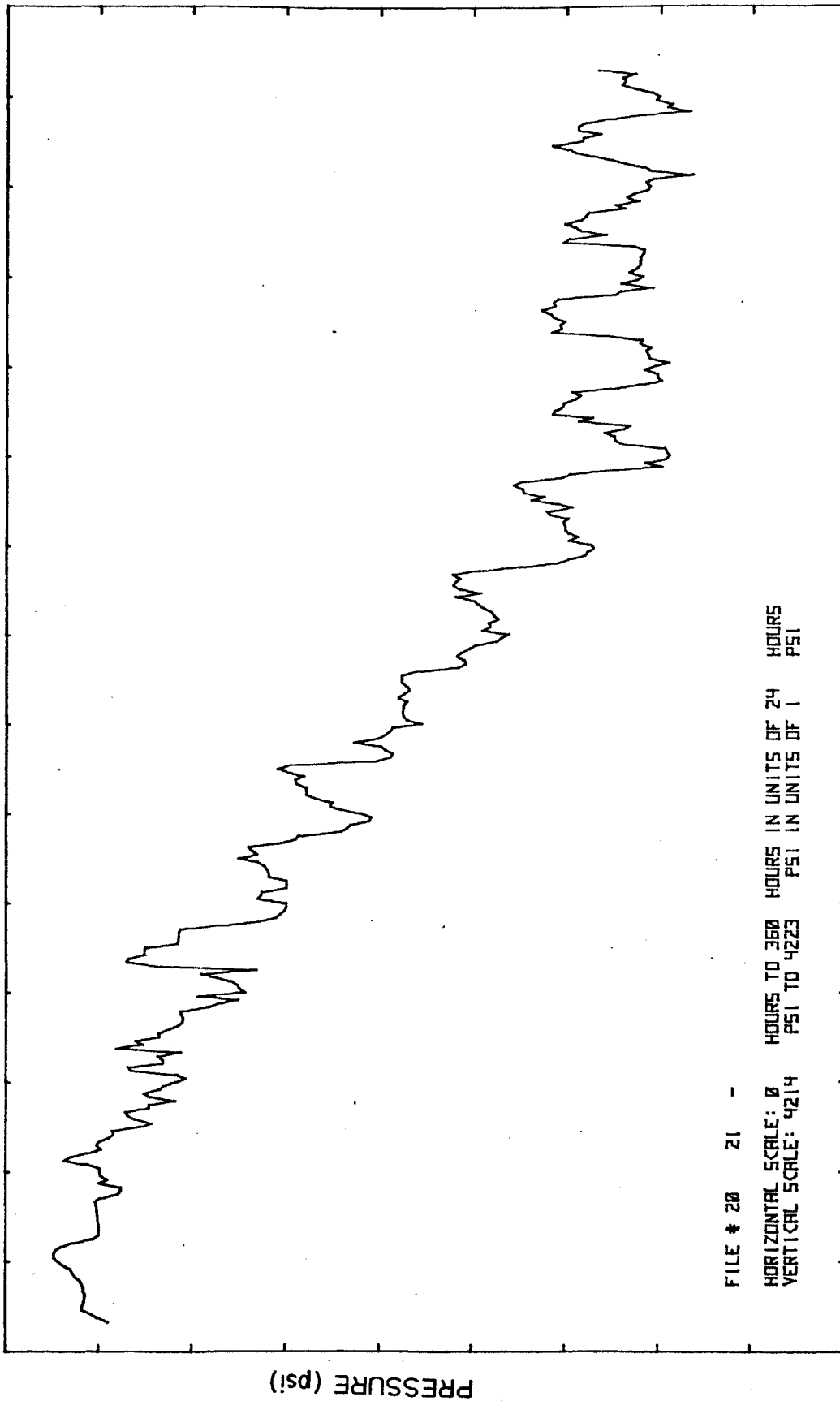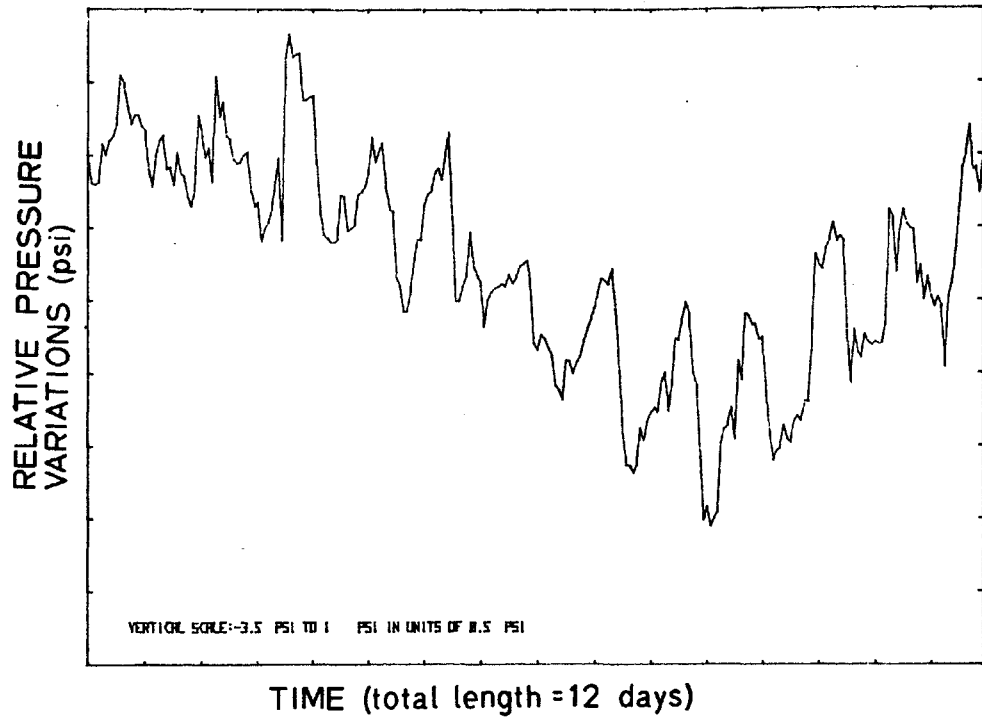
FIG. 5.5b: MODIFIED DATA FOR THE "X SOUTH" FIELD, FIRST PART

FREQUENCY (unit = 16 periods per experiment)

FIG. 5.5c: SPECTRUM ANALYSIS BY FFT FOR THE "X SOUTH" FIELD, FIRST PART
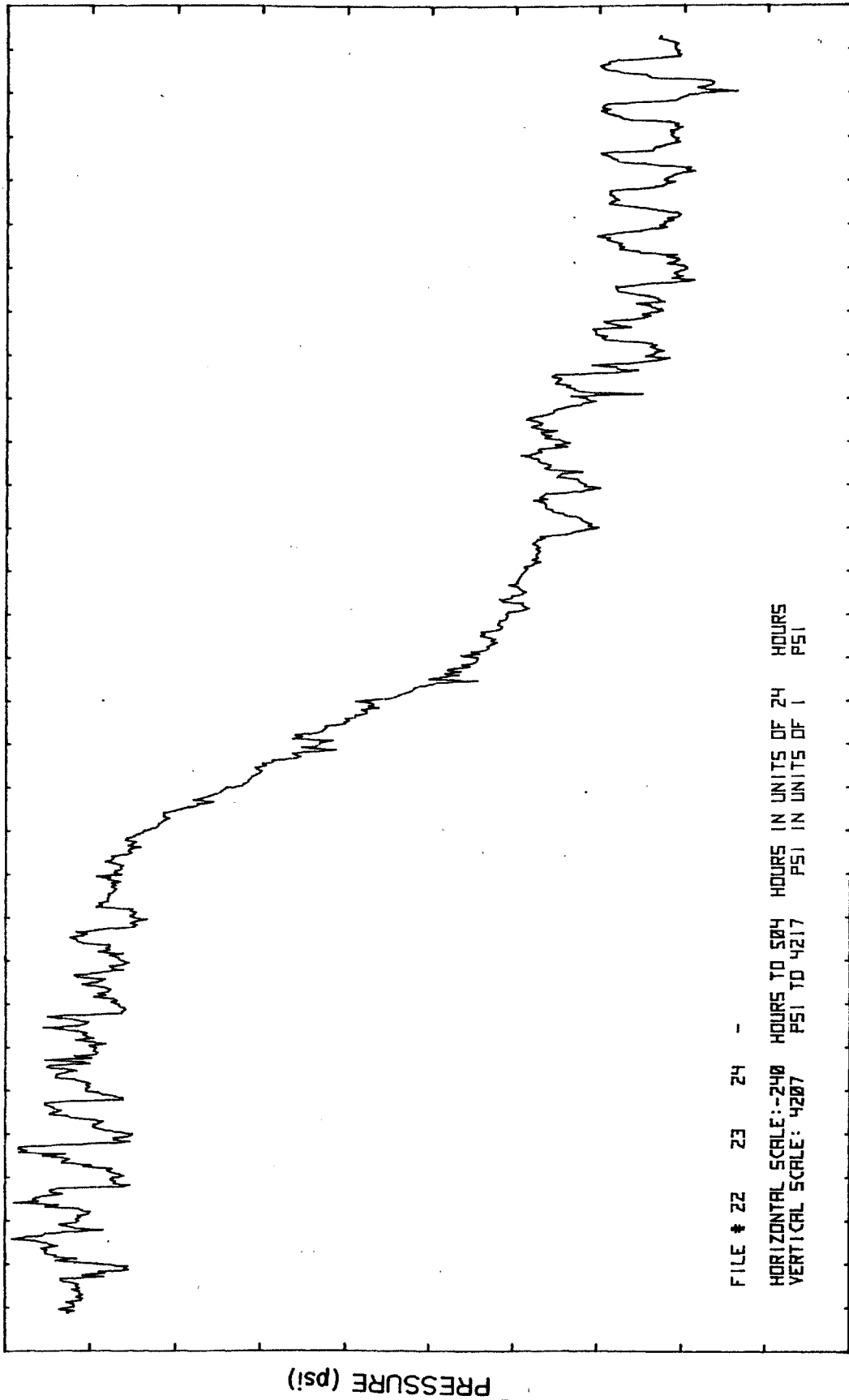
PRESSURE (psi)

TIME (days)

FILE # 22   23   24   -

HORIZONTAL SCALE: -240   HOURS TO 504   HOURS IN UNITS OF 24   HOURS
VERTICAL SCALE: 4207   PSI TO 4217   PSI IN UNITS OF 1   PSI

FIG. 5.6a: INITIAL DATA FOR THE "X SOUTH" FIELD, SECOND PART

85

VERTICAL SCALE:-3 PSI TO 3 PSI IN UNITS OF 1 PSI

TIME (total length = 29 days)

FIG. 5.6b: MODIFIED DATA FOR THE "X SOUTH" FIELD, SECOND PART

VERTICAL SCALE:-20 TO 60 IN UNITS OF 10

FREQUENCY (unit = 16 periods per experiment)

FIG. 5.6c: SPECTRUM ANALYSIS BY FFT FOR THE "X SOUTH" FIELD, SECOND PART

5.5c, and 5.6 c represent the output data of the FFT. The vertical scale is 10 psi for the three figures.

Well No. 609 W, in the Seminole field, Gaines County, Texas, was monitored. These data were provided by Cities Service Company. The corresponding file numbers are 25-26 and 27-28. The produced fluids were oil, water, and gas, but mainly oil. The productive interval was 50 ft thick, and the oil production was 275 BPD. The water production was 10 BPD, and the gas production was 1.54 MMCFD. The well diameter was 5.5 inches and the recording depth 5,050 ft (KB). The pressure was recorded in well No. 609-W at this depth for 69 days, beginning in February 1974, but gaps as long as 90 hours in the record obliged us to choose only part of the data for analysis.

The rock compressibility was $4x15^{-6}$ psi^{-1}, and the porosity was 13.4%. The oil, water, and gas compressibilities were $15x10^{-6}$ psi^{-1}, $3x10^{-6}$ psi^{-1}, $714x10^{-6}$ psi^{-1}. The oil, water, and gas saturations were 73.2%, 16,8%, and 10%, respectively. The oil, water, and gas viscosities were 1.09 cp, 1.00 cp, and $C.0166$ cp, respectively.

Thi: ressure data was for a period of time of 12 days for the first part, anc almost 15 days for the second part. These two parts were separated by an interval of 4 days.

Figures 5.7a and 5.8a present the pressure versus time data for the two data periods. The vertical scale is 0.5 and 0.1 psi, respectively. The figures showing the modified data are 5.7b and 5.8b. The vertical scale is equal to 0.5 psi. The output data of the FFT computation are presented in Figs. 5.7c and 5.8c. The vertical scale is 5 psi.
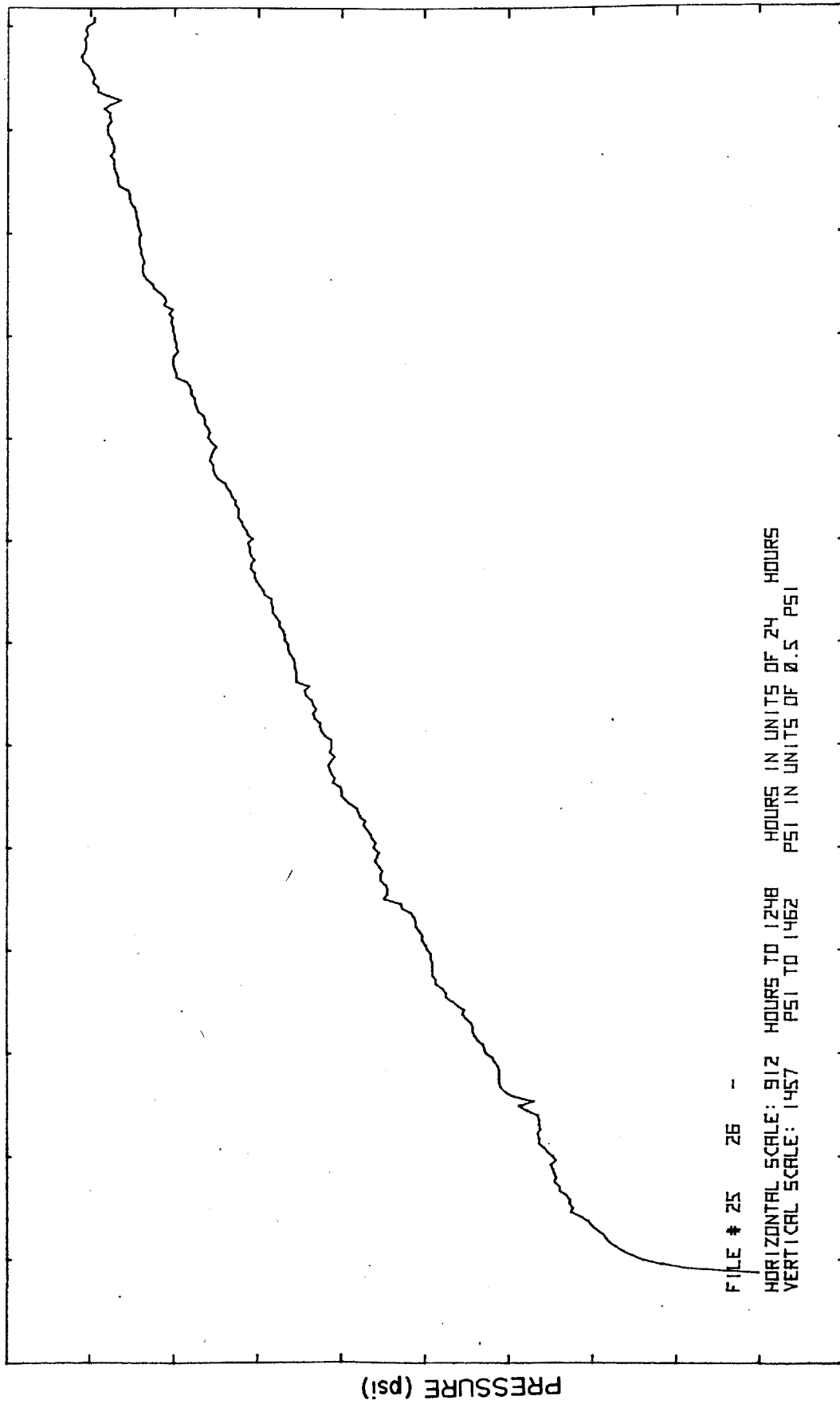
PRESSURE (psi)

TIME (days)

FILE # 25   26   -

HORIZONTAL SCALE: 912   HOURS TO 1248   HOURS IN UNITS OF 24   HOURS
VERTICAL SCALE: 1457   PSI TO 1462   PSI IN UNITS OF 0.5 PSI

FIG. 5.7a: INITIAL DATA FOR THE SEMINOLE FIELD, FIRST PART

88

RELATIVE PRESSURE VARIATIONS (psi)

VERTICAL SCALE:-1 PSI TO 1 PSI IN UNITS OF 0.5 PSI

TIME (total length = 12 days)

FIG. 5.7b: MODIFIED DATA FOR THE SEMINOLE FIELD, FIRST PART

AMPLITUDE

VERTICAL SCALE:-10 TO 15 IN UNITS OF 5

PHASE (deg)
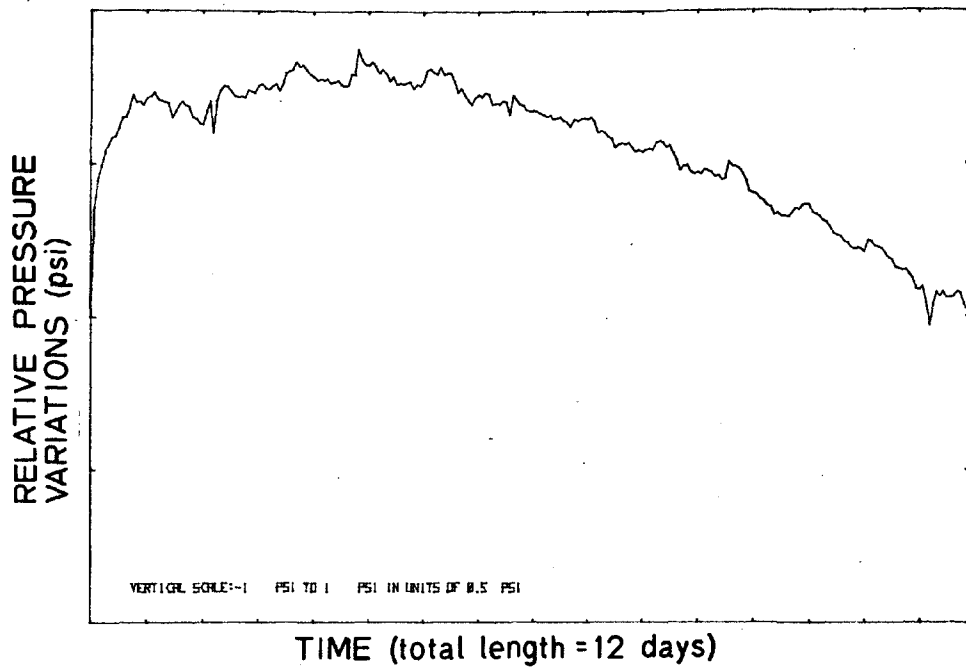
FREQUENCY (unit = 16 periods per experiment)
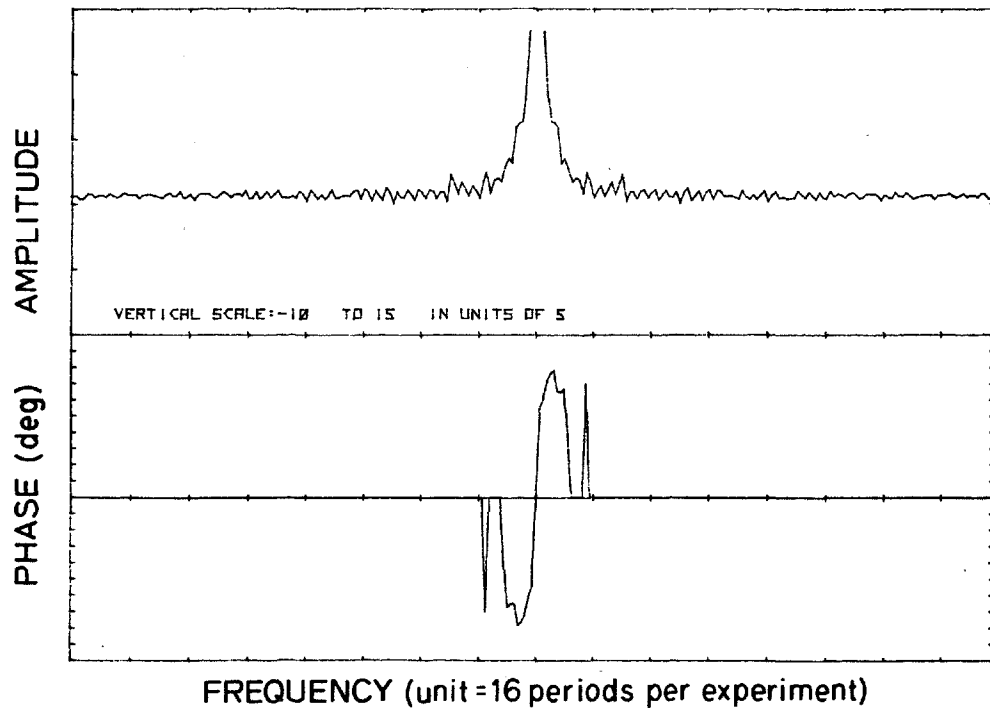
FIG. 5.7c: SPECTRUM ANALYSIS BY FFT FOR THE SEMINOLE FIELD, FIRST PART
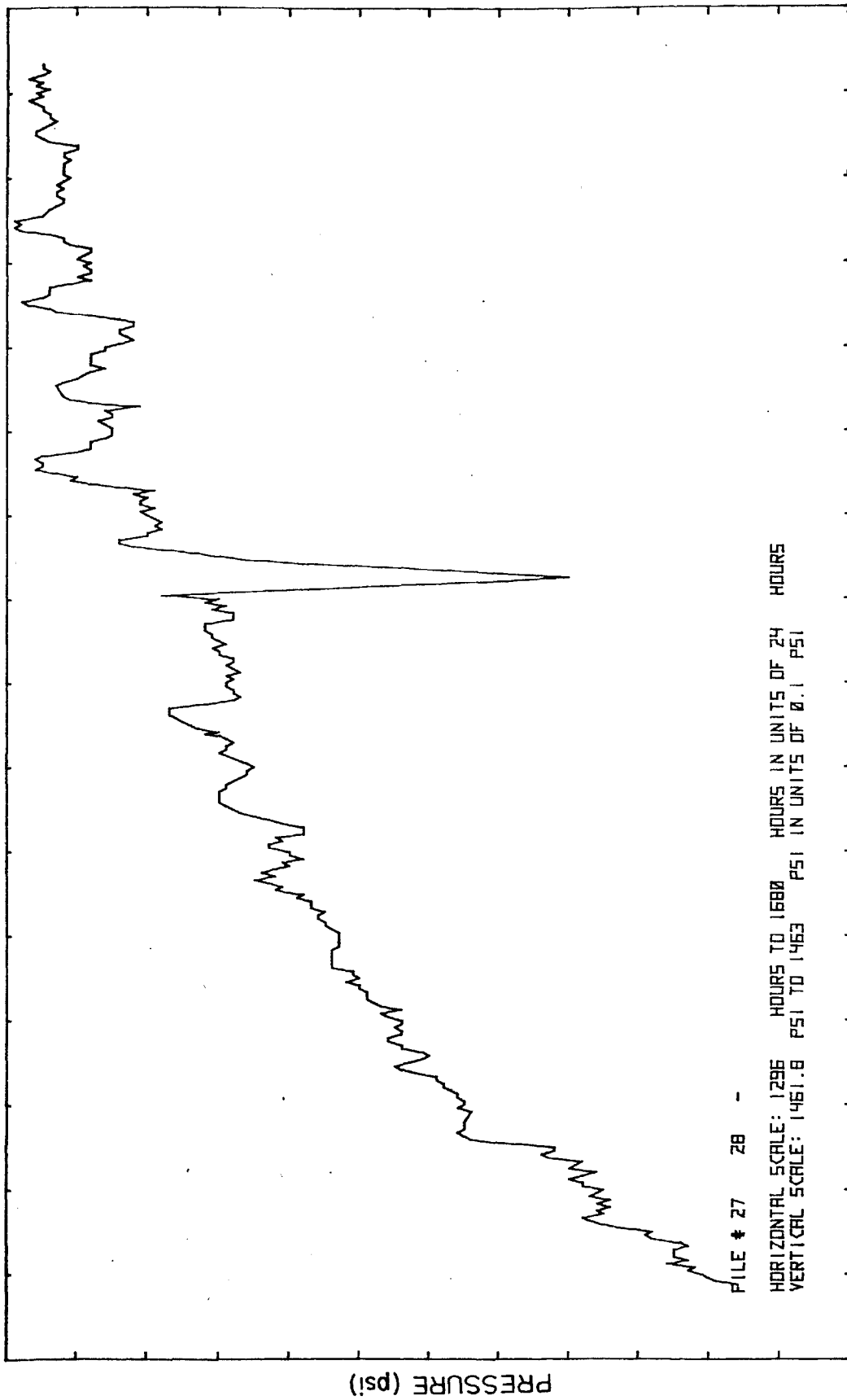
FIG. 5.8a: INITIAL DATA FOR THE SEMINOLE FIELD, SECOND PART

FILE # 27   28   –

HORIZONTAL SCALE: 1296   HOURS TO 1600   HOURS IN UNITS OF 24   HOURS
VERTICAL SCALE: 1461.8   PSI TO 1463   PSI IN UNITS OF 0.1   PSI

TIME (days)

PRESSURE (psi)

90

VERTICAL SCALE:-1   PSI TO 0.5 PSI IN UNITS OF 0.5 PSI

TIME (total length =14 days)

FIG. 5.8b: MODIFIED DATA FOR THE SEMINOLE FIELD, SECOND PART

VERTICAL SCALE:-10   TO 10   IN UNITS OF 5
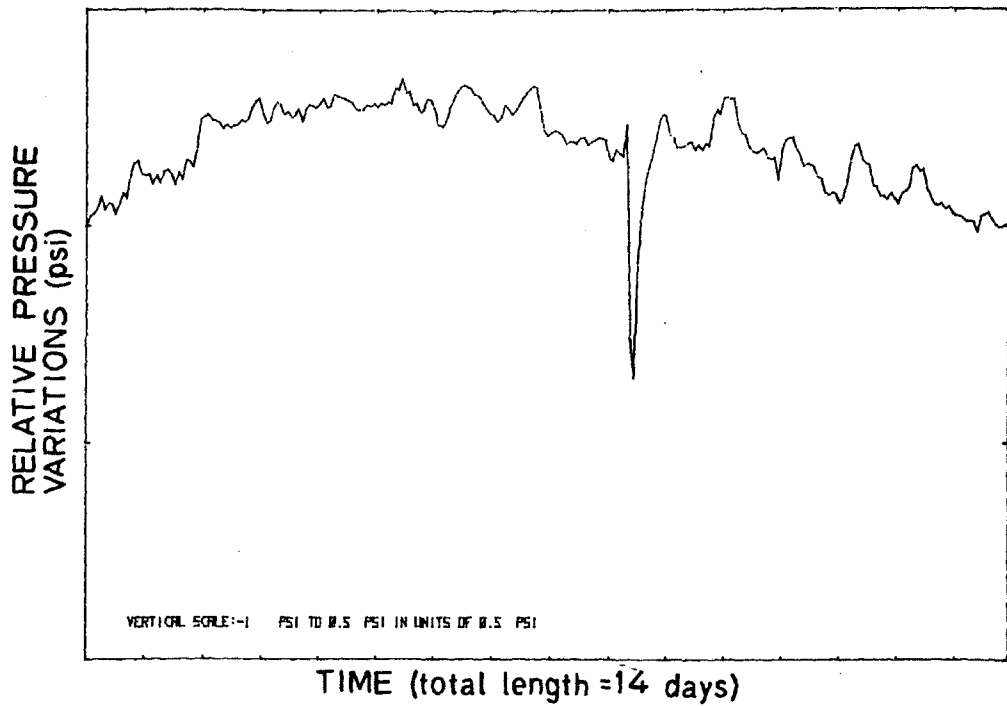
FREQUENCY (unit =16 periods per experiment)
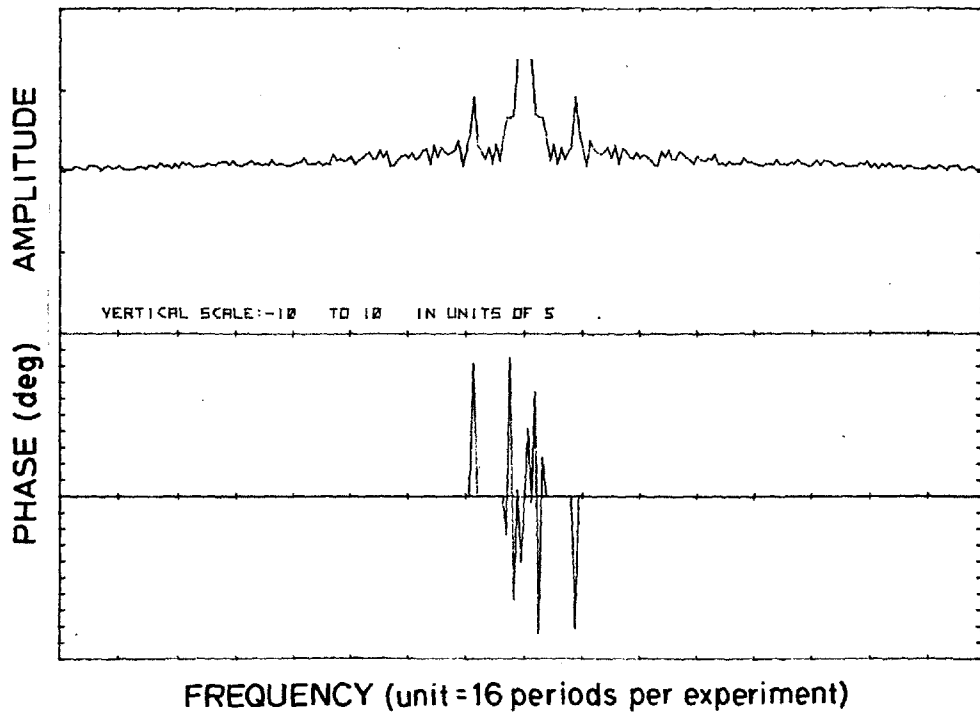
FIG. 5.8c: SPECTRUM ANALYSIS BY FFT FOR THE SEMINOLE FIELD, SECOND PART

91

The next case is an oil field run by Gulf Oil Corporation, located forty miles northeast of Estevan, Saskatchewan, in Canada. We refer to the field as the "Canadian" field. The well which was used for analysis is No. 6-32.

The fluid produced was oil. There was a possibility of some gas saturation, but no proof has been found. The reservoir lies within a carbonate rock. The productive thickness is 60 to 80 ft, the porosity of the productive rock formation is 15 to 30%, and the permeability is 100 to 4,000 md. The average permeability is between 200 and 800 md. The dense rock porosity is between 0 and 10%, with an average value of 3%. The oil viscosity and compressibility at reservoir conditions are 0.48 cp and 15×10^{-6} psi^{-1}. Oil saturation is equal to 73%. The water compressibility at reservoir conditions is 3.1×10^{-6} psi^{-1}. Water saturation is equal to 27%.

Gulf Research Corporation devices isolated the pressure probe from the reservoir, and so eliminated the storage effect of the well. The pressure data used were recorded from June 27, 1977, to July 18, 1977, each hour.

The pressure versus time data for this period are shown in Fig. 5.9a. The vertical scale is 0.5 psi. The modified data shown in Fig. 5.9b have a vertical scale of 0.1 psi, and the output data of the FFT are presented in Fig. 5.9c. The vertical scale is 5 psi.

The last example analyzed was the Big Muddy field, near Casper, Wyoming. Data, in the form of punched cards, were provided by the Continental Oil Company. The experiment was run in January-February 1978.

Only one graph representing the raw pressure versus time data will be given. The format of these graphs is also different. The produced fluids
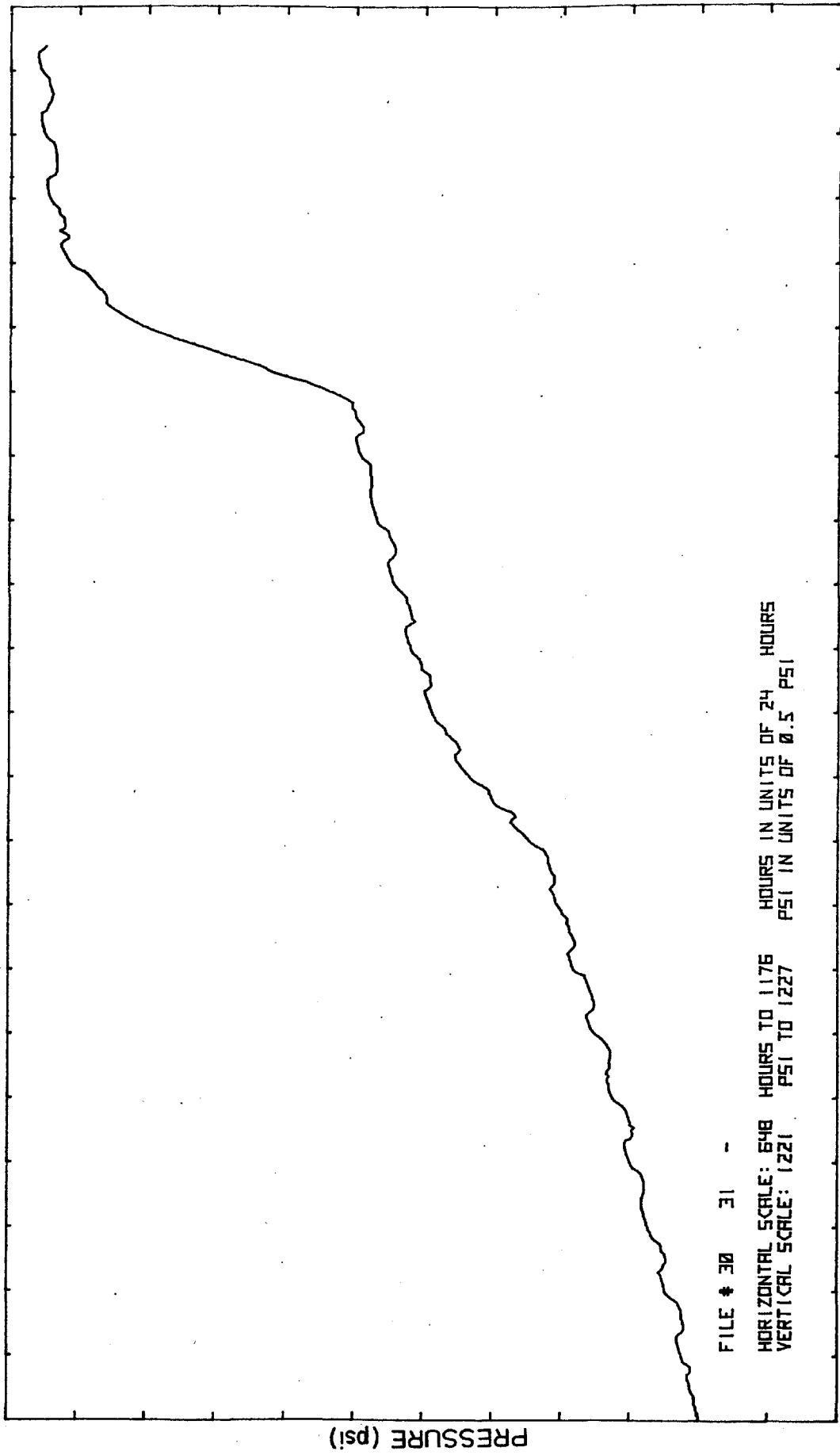
FIG. 5.9a: INITIAL DATA FOR THE CANADIAN FIELD

FILE # 30   31   -

HORIZONTAL SCALE: 648   HOURS TO 1176   HOURS IN UNITS OF 24 HOURS
VERTICAL SCALE: 1221   PSI TO 1227   PSI IN UNITS OF 0.5 PSI

TIME (days)

PRESSURE (psi)

93

VERTICAL SCALE:-1.2 PSI TO 0.5 PSI IN UNITS OF 0.1 PSI

TIME (total length = 21 days)
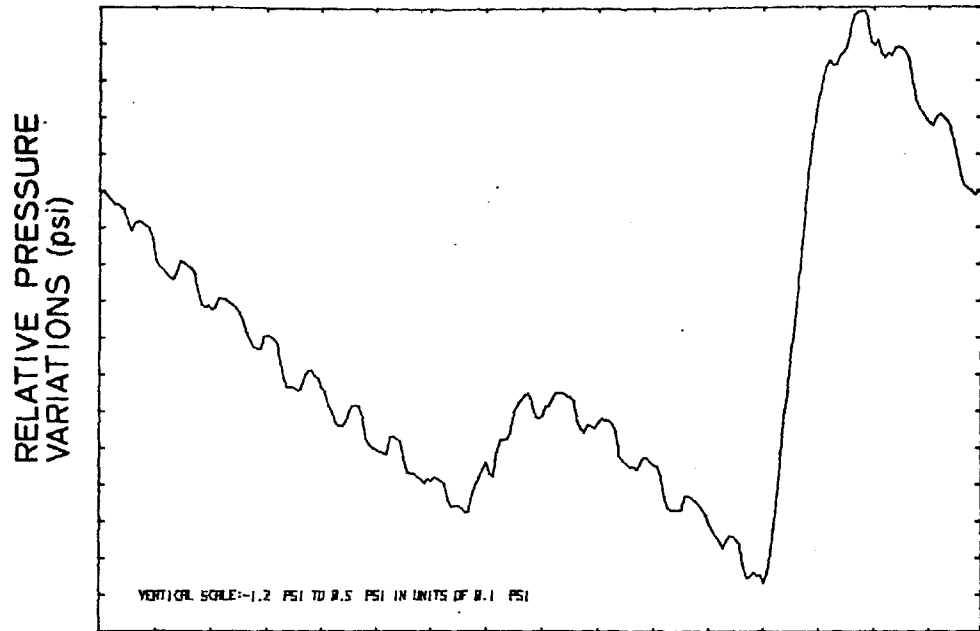
FIG. 5.9b: MODIFIED DATA FOR THE CANADIAN FIELD

VERTICAL SCALE:-10 TO 35 IN UNITS OF 5

FREQUENCY (unit = 16 periods per experiment)
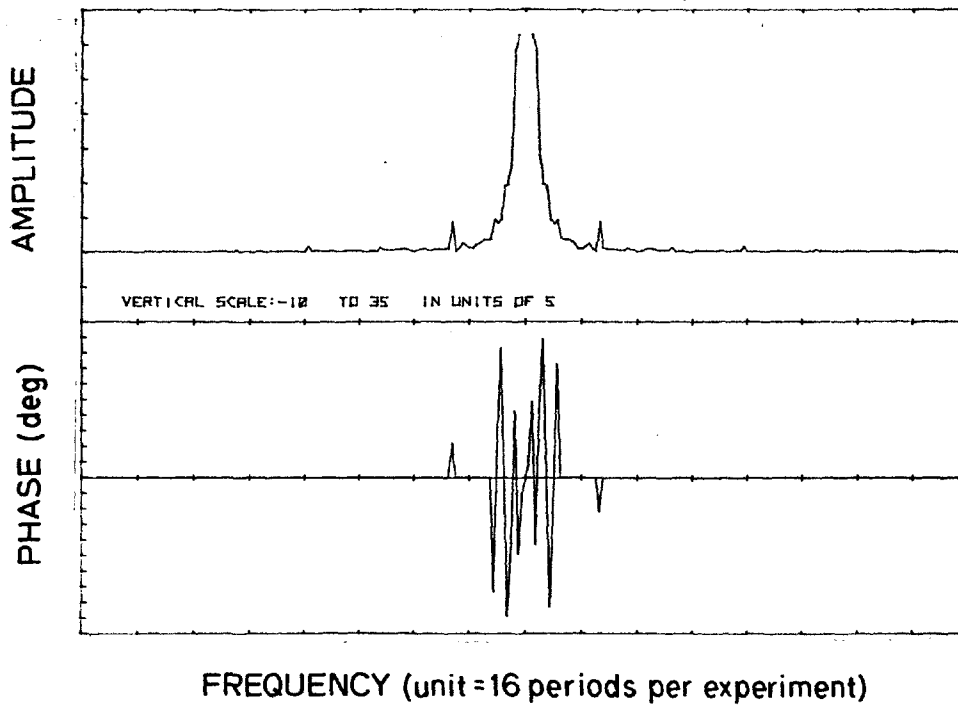
FIG. 5.9c: SPECTRUM ANALYSIS BY FFT FOR THE CANADIAN FIELD

94

are oil and water. The thickness of the productive formation is 65 ft

(gross thickness approximately 73 ft). The productive formation is well-

consolidated sandstone. The depth of the well is 1800 ft subsea. The

reservoir temperature is 130°F. The rock porosity is 17%, and the total

system compressibility is 10×10^{-6} psi^{-1}. The permeability of the forma-

tion is 52 md, the oil gravity is 35° API, and the oil saturation is 70%.

The water saturation is 30%.

The pressure was recorded from January 17, 1978, to February 21, 1978.

Data were recorded each hour. For our analysis, we used the entire 34-day-

long experiment.

Figures 5.10 through 5.13 represent the recorded pressure data. The

time scale is in the original time, t=0 is considered to be on January 1,

1978, at 1:00 A.M. The figures representing the output data of the FFT

are not given for this field; only the numerical results are given. Four

wells were monitored for pressure variation. They have the same rock

formation and fluid properties. These wells are No. 39, No. 53, No. 57,

and No. 68.

We had precise pressure versus time data for these five fields. For

the two following fields, only samples of the records were available, so

we could not perform a complete analysis.

No graphs are presented for the two following fields. We present

them as a matter of interest only. One of these cases is obtained from

the Khurana (1976) study of the Kingfish oil field in Australia. The

reservoir rocks are sands with high permeability—around 1,400 md. The

formation thickness is about 110. The second case concerns the Parentis

Fields, which are located near Bordeaux, in southwest France, near the

Atlantic Ocean. We will consider only two of the wells: Parentis No. 22

and No. 8. They are run by Exxon.
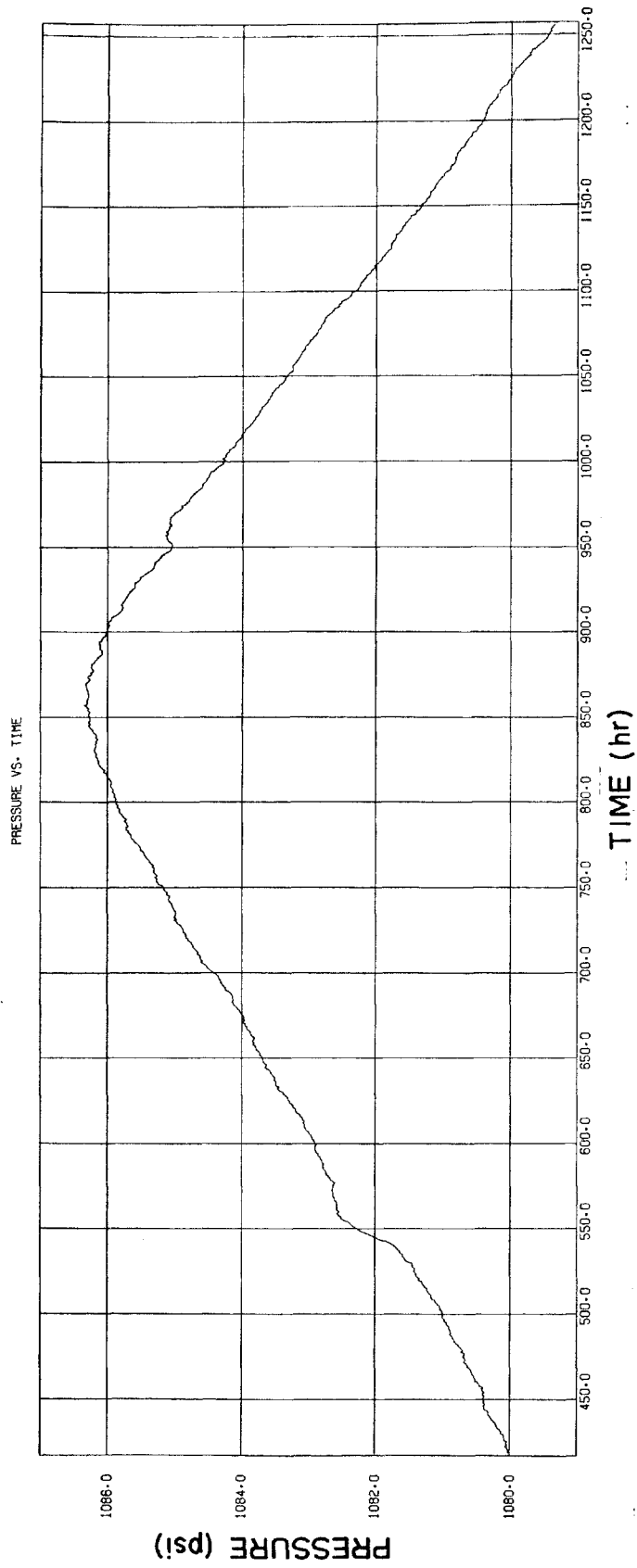
FIGURE 5.10: INITIAL DATA FOR THE BIG MUDDY FIELD, WELL NO. 39

PRESSURE VS. TIME
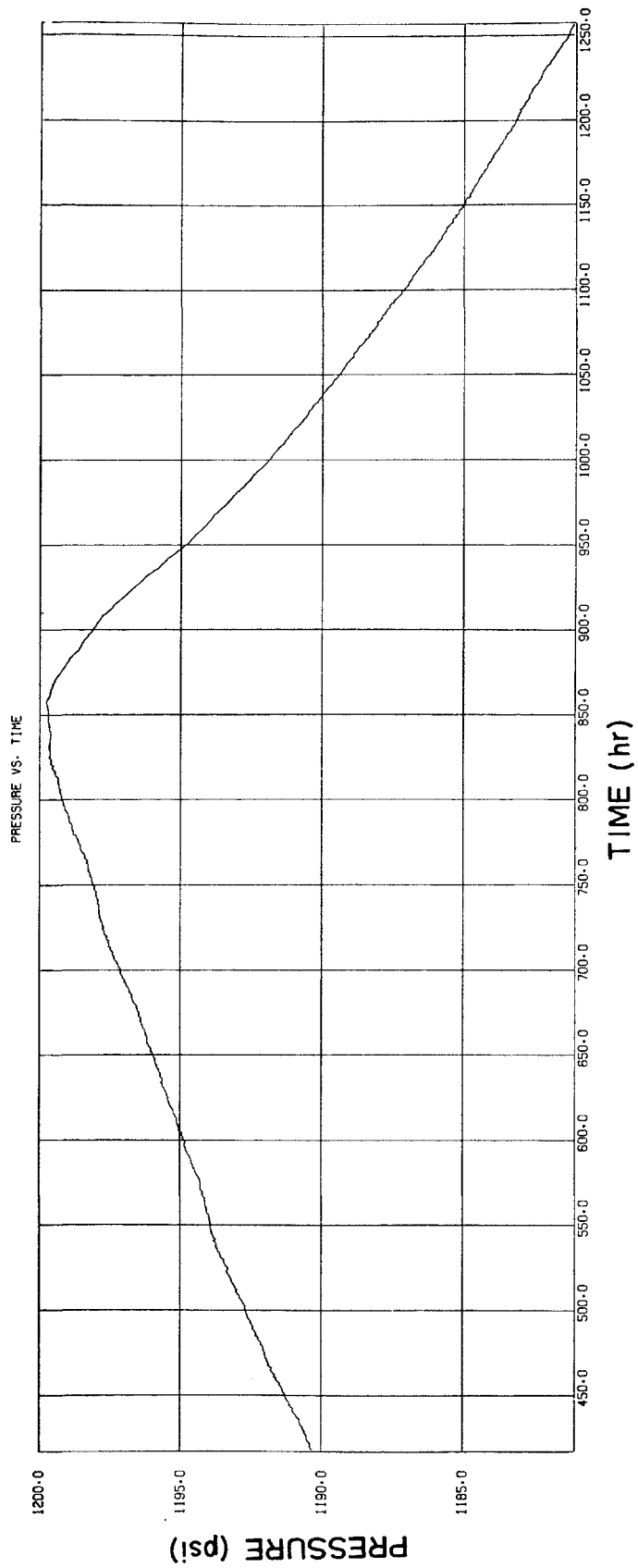
FIGURE 5.11: INITIAL DATA FOR THE BIG MUDDY FIELD, WELL NO. 53

PRESSURE vs. TIM
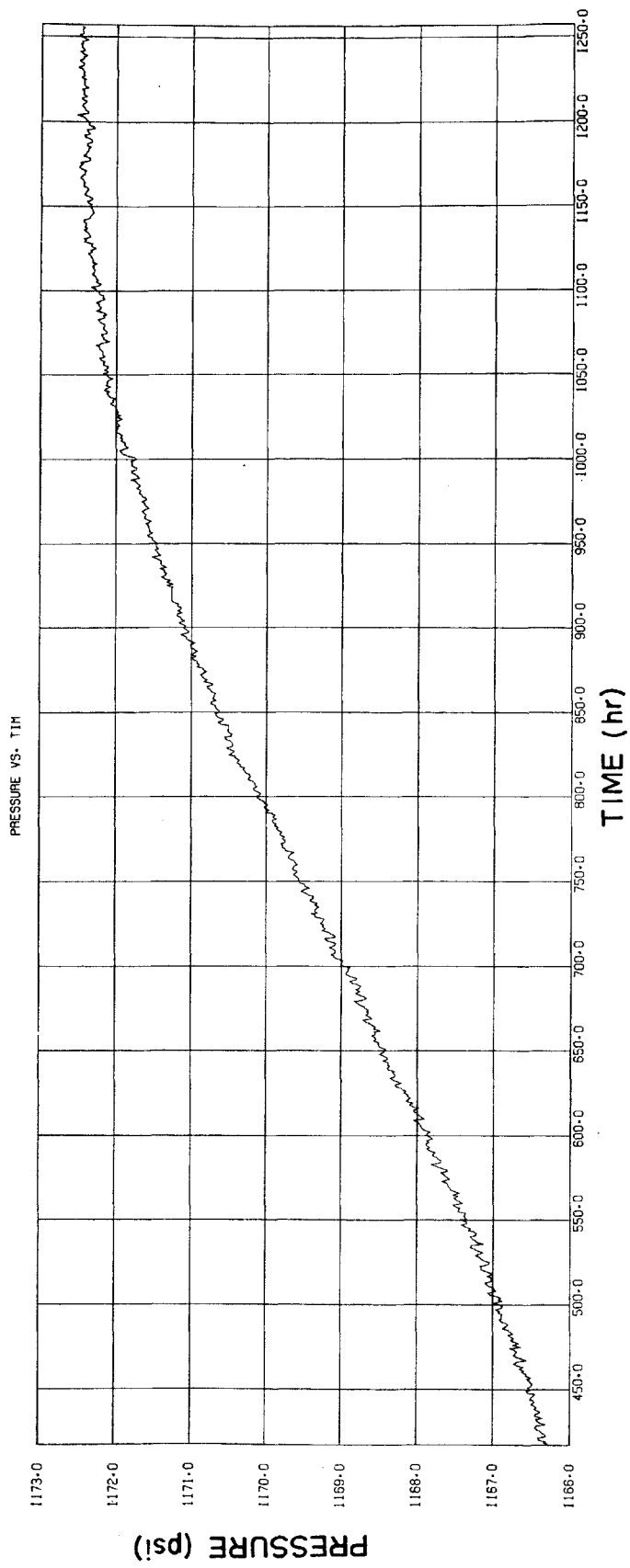
FIGURE 5.12: INITIAL DATA FOR THE BIG MUDDY FIELD, WELL NO. 57

98

PRESSURE VS. TIME
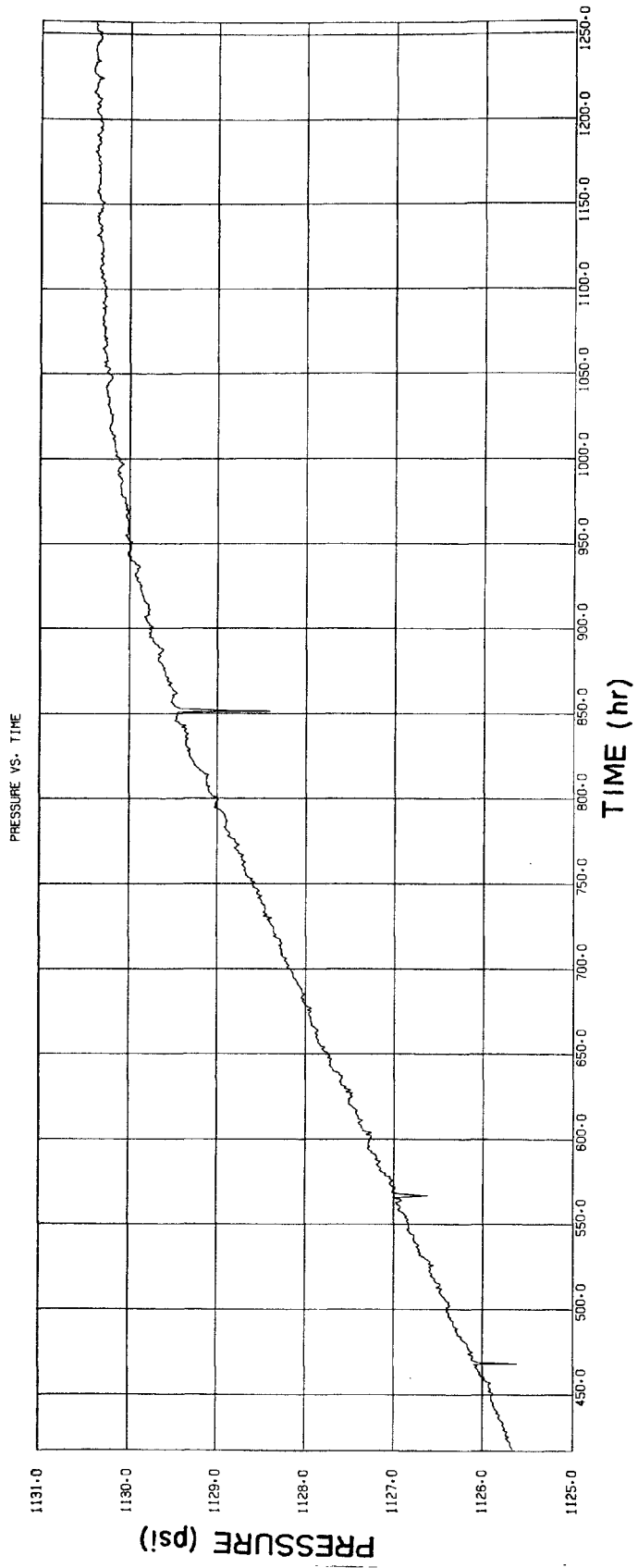
FIGURE 5.13: INITIAL DATA FOR THE BIG MUDDY FIELD, WELL NO. 68

Parentix No. 22 is at 77 ft above sea level; Parentis No. 8 is at 82 ft above sea level. Their distance from the ocean is 7.4 and 9.7 miles, respectively. Their depths are 7,206 and 7,314 ft, and the net thickness of the reservoirs is 73 and 66 ft, respectively. The Parentis No. 22 formation is limestone, and Parentis No. 8 is dolomite. Vertical fractures may be seen throughout the dolomitic formation. The average rock porosity is 9%, permeability is around 5.8 md for Parentis No. 22. It is saturated with oil. Oil viscosity is 2.36 cp, and the total compressibility is 11.2×10^{-6} psi^{-1}. The average rock porosity is 23%. The permeability is around 4,000 md (from the productivity index) for Parentis No. 8. It is saturated with oil and water, and the average fluid viscosity is 1.4 cp.

5.4   Results: Interpretation and Discussion

Diurnal and semidiurnal pressure variations are visible for some cases directly from the initial data plot (Figs. 5.3a through 5.13a). However, if earth tides are not obvious from these graphs, it does not mean that they do not exist. For instance, semidiurnal variations are not visible from Fig. 5.3a, while the output data of the FFT (Fig. 5.3c) shows a semidiurnal tidal component.

We will not discuss the various shapes and features observed on Figs. 5.3a through 5.13a, such as abrupt decreases or increases in the pressure trend. They were caused by different kinds of experiments run while the pressure was recorded (buildup, pulse, or drawdown tests). We will only inspect the periodic pressure variations observed for each well. Looking at Figs. 5.3b through 5.9b, both major tidal effects are easy to detect because the continuous large component existing in the previous set of

figures is eliminated. It is the relative variations with respect to a mean pressure which are represented in these figures; these fluctuations are primarily generated by earth tides (Figs. 5.3b through 5.9b).

The important results are those given by the FFT computation. We will discuss each figure separately; then will try to correlate the results. In all the graphs (Figs. 5.3c through 5.9c), there is a certain amount of noise, probably caused by the pressure gage itself. This will be of no importance if the tidal components have large amplitude, but it also may totally confuse the output data of the FFT. In all these FFT graphs, the peak at the center of the graph represents the continuous component of the pressure. It is of no interest, so the vertical scale was selected to make the important frequency components visible.

For the "A" field, the length of the experiment was 17 days, and there is a peak around one frequency unit and 2 units. Let us recall that 1 unit on the horizontal scale unit is f=16, where f is the number of appearances per experiment. So, for the "A" field, there are both a diurnal variation and a semidiurnal variation. They appear about 17 times and 34 times, respectively, during the experiment (at $f \simeq 17$ and $f \simeq 34$), and correspond to the diurnal and semidiurnal tidal components (Fig. 5.3c).

Using Eqs. 5.1 and 5.2, we can find the respective amplitude of the diurnal and semidiurnal response. If ΔP_D is the diurnal pressure variation, and ΔP_{SD} the semidiurnal pressure variation, we have:

$$\Delta P_D = \frac{2}{256} \times 0.75 = 0.006 \text{ psi (from peak-to-creux)}$$

$$\Delta P_{SD} = \frac{2}{256} \times 0.55 = 0.004 \text{ psi}$$

101

Thus, the amplitude of the variation induced by the O_1 or diurnal component is 1.5 times greater than that induced by that of the semidiurnal tidal component. Both tidal effects are small for a gas reservoir. They would not have been detectable without a very sensitive pressure gage.

For the "X_{north}" field, the semidiurnal component and diurnal components are visible. The length of the experiment was 30 days. In the spectrum analysis there are two peaks (Fig. 5.4c) corresponding to the diurnal and semidiurnal pressure variations ($f \simeq 29$, $f \simeq 58$) (Fig. 5.4c).

$$\Delta P_D = \frac{2}{256} \times 24.706 = 0.193 \text{ psi (0.386 psi peak-to-peak) for the diurnal component}$$

$$\Delta P_{SD} = \frac{2}{256} = 0.022 \text{ psi (peak-to-peak: } \Delta P_{SD} = 0.044 \text{ psi) for the semidiurnal tidal component}$$

For the "X_{south}" field, part No. 1 (file number 20-21), the length of the experiment was only 12 days (less than the length required to get a valid response). The first consequence is that it is very difficult to see the 12-hour period component because of the aliasing and noise. The 24-hour tidal component is clear at $f=12$, Fig. 5.5c. The pressure variation amplitude generated by the diurnal component is:

$$\Delta P_D = \frac{2}{256} \times 45.217 = 0.353 \text{ psi (or peak-to-peak, the amplitude of the pressure variation is 0.706).}$$

This is a very large pressure variation induced by earth tides. We suspect that this value is erroneous.

The second part of the "X_{south}" field (file number 22-23-24) has a length of 29 days. The response is clearer for this part than for the first part (Fig. 5.6c). At $f \simeq 28$, there is a peak of large amplitude, while at $f \simeq 56$ it is difficult, but it is still possible to see the semidiurnal response.

102

f is not equal to 29 and 58, but ~28 and ~56, because of the period
of the tidal component being more than 24 and 12 hours, respectively.
This has been noted previously, and will remain valid throughout the data
analysis.

For the diurnal pressure variation, we find:

$$\Delta P_D = 28.300 \times \frac{2}{256} = 0.221 \text{ psi}$$

The amplitude of the pressure variation induced by the semidiurnal component is:

$$\Delta P_{SD} = \frac{2}{256} \times 5.30 = 0.041 \text{ psi (or peak-to-peak the amplitude is } 0.082 \text{ psi)}$$

So, for the "X_{north}" field, we have:

$$\frac{\Delta P_D}{\Delta P_{SD}} = \frac{0.193}{0.022} \sim 9$$

The pressure variation generated by the diurnal component is about 9 times
larger than that generated by the semidiurnal component.

For the "X_{south}" field, we have:

(Part No. 1)
$$\frac{\Delta P_D}{\Delta P_{SD}} = \text{not defined}$$

(Part No. 2)
$$\frac{\Delta P_D}{\Delta P_{SD}} = \frac{0.221}{0.041} \simeq 5.5$$

The diurnal tidal component is 5.5 times stronger than the semi-
diurnal tidal component.

For the Seminole field in Texas, the length of the experiments was still a problem. It was impossible to see any frequency component in Part No. 1 of this experiment (file number 25-26) (Fig. 5.7c). In the second part of the experiment (file number 27-28), which lasted 14 days, the diurnal components are visible at f=14 and (Fig. 5.8c):

$$\Delta P_D = \frac{2}{256} \times 4.625 = 0.036 \text{ psi (peak-to-peak, the amplitude is } 0.072 \text{ psi)}$$

At f=28, the amplitude of the peak is 1.175 psi; thus, the corresponding variation amplitude appears to be:

$$\Delta P_{SD} = \frac{2}{256} \times 1.175 = 0.009 \text{ psi}$$

The ratio P_D over P_{SD} for part No. 2 of this field is (Fig. 5.8c):

$$\frac{\Delta P_D}{\Delta P_{SD}} = \frac{0.036}{0.009} = 4$$

The response of the field to diurnal stress is 4 times greater than the response to semidiurnal stress.

The next field analyzed is the Canadian field, well No. 6.32 W. The length of this experiment was 21 days. Figure 5.9c shows peaks at f≈21 and f≈42, but also at f≈63 and 84. This is abnormal. We cannot consider that the peaks at f=21 and 42 are representative of the diurnal and semidiurnal component. This is probably a phenomenon caused by the method used.

Hopefully, Figs. 5.9a and 5.9b are proper, and diurnal variations correspond to the diurnal tides. We can evaluate approximately the amplitude of these diurnal variations:

$$\Delta P \sim 0.10 \text{ psi}$$

104

Apparently no semidiurnal variations exist. In this case, it is likely that the 12-hour tidal component is extremely small, because the periodic variations shown in Figs. 5.9a and 5.9b are very regular and do not seem to have any other frequency component. In this case, the effect of the semidiurnal tidal component is so attenuated that we cannot record any induced variation of pressure. Knowing that ΔP_D is approximately 0.1 psi, we can say that the effect of the diurnal tidal component is at least 10 times greater here than the semidiurnal one.

Let us now consider the data from the Big Muddy field. When we look at Figs. 5.10 through 5.13, we see that the diurnal and/or semidiurnal variations are visible for wells No. 51 and 68, while they are not for the two others (No. 39 and No. 53). For the latter, the slope of the pressure versus time curve is much steeper than for the former, so the fairly small pressure fluctuations induced by the tidal stresses are masked by the important continuous pressure variations. In order to detect the tidal effects by sight, the pressure of the well should be maintained as constant as possible (no production). If interference tests are run in the well or in a nearby well, interference effects mask the existing earth tide effects. However, spectrum analysis of the data should permit detection if they exist, so it is important to do spectrum analysis.

When we compute the FFT for these four wells, we obtain values of ΔP_D and ΔP_{SD} for each of the wells. ΔP_D varies between 0.074 and 0.083, and ΔP_{SD} varies between 0.061 and 0.064. The ratio $\Delta P_D / \Delta P_{SD}$ is equal to 1.15 to 1.36.

In the Kharana paper, a 12-hour period wave of 0.040 psi amplitude was detected for the Kingfish sandstone formation. Nothing was said about the 24-hour period wave. The H-P gage was used to record pressure.

105

In the Exxon report on the Parentis field, Lecolazet's method was used to separate the influence of the diurnal wave from that of the semidiurnal wave. Five wells were monitored: Parentis Nos. 8, 13, 21, 22, and 38.

At Parentis No. 22, which is a dolomitic fractured formation, the response to semidiurnal waves was slightly larger than that to the diurnal waves. At Parentis No. 8, which is a limestone non-fractured formation, it was the opposite. This strange response (larger response to the semidiurnal than diurnal wave) could be due essentially to the fact that the oceanic tides cannot be neglected for this field. The oceanic tides at the Bordeaux location are 96% semidiurnal and only 4% diurnal. That is a possible explanation for the response being reversed with respect to what is normally expected. It is the only case studied wherein ΔP_{SD} was larger than ΔP_D.

Now that we have looked at each field separately, we will consider a correlation between the pressure behavior and the reservoir characteristics. Table 5.1 summarizes the fluid characteristics and the results of the analysis.

In all the cases studied here, it appears that the diurnal tidal component has a larger effect than the semidiurnal component (except the case reported by Exxon). This agrees with the results predicted by the theory and the numerical applications shown in Section 4.3. The amplitude of the response of the closed well-reservoir system is larger for smaller frequencies. In Section 4.3, we found that the amplitude of the response of the diurnal waves was one to more than twice greater than that of the semidiurnal waves. We suspected that the upper limit was much larger than two. Here we have observed values between 1.5 and 10

TABLE 5.1: SUMMARY OF THE DATA ANALYSIS RESULTS

	"A" FIELD	"X NORTH" FIELD	"X SOUTH" FIELD	CANADIAN FIELD	SEMINOLE FIELD	BIG MUDDY FIELD
Fluids:	gas	oil & gas	oil & gas	oil	oil & gas	oil
k (md)	48	50	120	200-800	70	52
μ(cp)	0.0168	0.31	0.39	0.48	0.97	4
ϕ(fraction)	0.0022	0.118	0.129	0.200	0.134	0.170
C_f(psi^{-1})x10^{-6}	(?)	32	35	12	83	6.8
C_m(psi^{-1})x10^{-6}	5	4.5	4.3	6	4	3.2
C_t(psi^{-1})x10^{-6}	274				92	10
$\frac{k}{\mu C_f}$ ($\frac{\text{md psi}}{\text{cp}}$) 10^{+6}	10.42	5.04	8.79	37 148	.83	1.3
V_c * (psi^{-1}) 10^{-6}	3.58	7.75	8.28	7.16	14.55	3.81
ΔP_D(psi)	0.006	0.193	0.221	0.110	0.036	0.078
ΔP_{SD}(psi)	0.004	0.022	0.041	(?)	0.009	0.062

$*V_c = \phi C_f + (1-\phi) C_m$

for the ratio of these two tidal components. This is an acceptable result, but there is still a large difference between the theoretical and experimental ratio $\Delta P_D/\Delta P_{SD}$. The variation of this ratio should be related to the expression (Section 4.3):

$$\frac{k}{\mu C_f}$$

From Table 5.1, we see that for the three out of four wells where data are complete ("A" field and fields "X_{north}" and "X_{south}"), the ratio $\Delta P_D/\Delta P_{SD}$ increases with decreasing values of $k/\mu C_f$. This could confirm what we found in Section 4.3 of this work. When $k/\mu C_f$ increases, the response P_a/P_c becomes more and more frequency-independent; thus, the amplitude response of the two tidal components becomes equal.

$$\frac{k}{\mu C_f} \text{ increases} \qquad \lim \frac{\Delta P_D}{\Delta P_{SD}} = 1$$

This does not seem to be true for the case of the Big Muddy field. The reason why it behaves differently is not known.

So, we see that the overall results for this field data analyses are reasonably good and close to the expected result concerning the importance of $\frac{k}{\mu C_f}$, and the $\frac{\Delta P_D}{\Delta P_{SD}}$ variation.

Considering now the relationship between critical frequency, ω_c, and $\Delta P_D/\Delta P_{SD}$ with $\omega_c = \frac{4k}{\mu C_f}$, we see (Table 5.2) that the correspondence between ω_c and the ratio $\Delta P_D/\Delta P_{SD}$ is not clear. In opposition to the theoretical indication, when ω_c increases, there is no evidence of decrease of the ratio $\Delta P_D/\Delta P_{Sd}$.

TABLE 5.2: ω_c AND $\Delta P_D/\Delta P_{SD}$ VALUES FOR THE SIX FIELDS ANALYZED

	"A" FIELD	"X_{NORTH}" FIELD	"X_{SOUTH}" FIELD	CANADIAN FIELD	SEMINOLE FIELD	BIG MUDDY FIELD
a	0.5 ft	0.5 ft	0.5 ft	0.25 ft	0.23 ft	0.5 ft
(sec^{-1}) ω_c	1.106×10^{-3}	3.294×10^{-4}	5.848×10^{-3}	1.078×10^{-2} to 4.31×10^{-2}	2.174×10^{-4}	4.293×10^{-4}
$\dfrac{\Delta P_D}{\Delta P_{SD}}$	1.5	9	5	$\simeq 10$	4	1.19–1.31

It does not mean that we were wrong in the previous section, but that we do need more data to correlate the physical properties of the fields and the pressure variations.

Let us now look at the importance of C_f, C_m, and ϕ. The five non-fractured wells have a larger amplitude response than the fractured gas well. This proves that when C_f is very high, the response can be extremely low due to the existence of fractures. The behavior of fractured wells seems to be very different from other wells. However, the ratio of the amplitude of the diurnal and semidiurnal variations for this fractured well is comparable to the others. We believe that such low response (it is the lowest amplitude response witnessed in this analysis) is caused by the value which is almost zero ($\phi \simeq 0.022\%$).

From Table 5.1, for four out of five non-fractured wells, the amplitude response of diurnal and semidiurnal tidal components increases with an increasing value of the expression $[\phi C_f + (1-\phi)C_m]$. These fields are the Big Muddy, Canadian, "X_{north}," and "X_{south}" fields. The non-fractured field which does not follow this rule is the Seminole field. We do not have any real explanation for this anomaly.

For the Big Muddy field, we used an average C_f value because no data were available. We used Hall's correlation to obtain C_m for the Big Muddy and "X_{north}" and "X_{south}" fields because this information was not available.

All these fields are apparently frequency-dependent, so they all should have responses proportional to the field characteristics ϕ, C_f, C_m, and eventually, k through the expression of ω_c. We do not have enough data to make general statements concerning the relationships between amplitude of pressure variations and these variables. However, we found some interesting conclusions which agree with the theory and with the results of the

numerical applications. Still, questions remain concerning the behavior
of fractured fields, and on the relative importance of the parameters. Also,
some discrepancies exist between the theory and observed data. For instance,
the ratio $\Delta P_D / \Delta P_{SD}$ is larger than expected most of the time. Another problem
is that for all the cases we have studied here, the diurnal pressure varia-
tion is greater than the semidiurnal pressure variation.

If we use the values given by Melchior (1966) for the diurnal and
semidiurnal strains and then compute the pressure variation generated by
the associated stresses, we find that the diurnal pressure variation can
be larger, equal to, or smaller than the semidiurnal pressure variation.
Indeed, Melchior found that $\theta_D = \theta_{01}$, where 0_1 is the diurnal tidal component
which is equal to 1.847×10^{-8}. M_2 is the semidiurnal tidal component.
The semidiurnal stress, θ_{M2}, is equal to 4.45×10^{-8}. For the response
ΔP_D, of diurnal tides and that of semidiurnal tides, P_{SD}, we have:

$$\Delta P_D = P_{c_D} \cdot E_o (1-M')_D$$

(from Section 4.2)

$$\Delta P_{SD} = P_{c_{SD}} \cdot E_o (1-M')_{SD}$$

and

$$P_{c_D} = \frac{\theta_D}{C}$$

$$P_{c_{SD}} = \frac{\theta_{SD}}{C} \quad , \quad \theta_D < \theta_{SD} \rightarrow P_{c_D} < P_{c_{SD}}$$

where:

C = compressibility of the system and thus is equal in the two equations

111

Using these two sets of equations, we can write that $\Delta P_D \geq \Delta P_{SD}$, if the

system is frequency-dependent, and so if $P_{c_D}(1-M')_D > P_{c_{SD}}(1-M')_{SD}(E_o$ is a constan

but $\Delta P_D < \Delta P_{SD}$ if the system is frequency independent because $(1-M')=1$ and so:

$$\Delta P_D = P_{c_D} < \Delta P_{SD} = P_{c_{SD}}$$

ΔP_D can be smaller than ΔP_{SD}, even if it is frequency-dependent, if the

rock and fluid formation are such that the value $(1-M')_D$ is not large

enough compared to $(1-M')_{SD}$ to compensate for the difference in strain

values.

The fact that no semidiurnal pressure variation larger than the

diurnal one is observed is still unexplained. Furthermore, in Section

4.2 we see that we could use an approximation:

$$\frac{P_a}{P_{SD}} \simeq 1 - \frac{1}{1 + \frac{4k}{l\omega\mu a \ell \phi}}$$

In this case, the expression $\phi C_f + (1-\phi)C_m$ does not have an influence on

the amplitude of the response. It appeared in Section 4.3 that this assump-

tion was valid. However, in this last section (5.4), we observed that

four out of five non-fractured reservoirs had larger amplitudes when the

value of $\phi C_f + (1-\phi)C_m$ was larger. So, there is another possible discrep-

ancy between the theory and the field data.

However, the results of this analysis generally are not in contra-

diction with the theory. Except for a few problems, we can say that the

equations developed herein explained the earth tide influence on the pres-

sure variations of a closed well-reservoir system fairly well.

112

6. CONCLUSION AND FUTURE WORK

It is now certain that the earth tides resulting from periodic stresses applied to the earth influence the variations of bottom-hole pressure of a reservoir. These effects are detectable when the well is monitored for pressure with a very sensitive pressure gage. The amplitude of the pressure variations recorded varies between 0.3 and 0.001 psi. Smaller variations cannot be recorded.

The amplitude of the fluctuations may be used to obtain a better knowledge of the well-reservoir system. Two general equations have been developed in this study which show the relationship between the pressure response and the critical frequency of a system and the fluid and rock properties. They are (respectively:

$$P_a = P_c \cdot \frac{4G_m(C_f - C_m)}{3 + 4G_m C_f} \left(1 - \frac{1}{1 + \frac{4k}{\mu C_f a \ell} \left(\sqrt{\frac{i\omega}{d}} \, a + 1 \right)} \right)$$

and:

$$\omega_c = 4k / a \ell \mu C_f$$

We are now certain that a correlation between the important parameters, k, ϕ, C_f, and C_m, and the amplitude of the pressure variation can be found.

113

If rock compressibility, porosity, permeability, and/or fluid compressibility values could be estimated by analyzing the pressure data for the amplitude of the variation due to the tidal components, estimated values obtained from interference tests and/or pulse tests could be checked. Additional information might be obtained on the possible performance of a given field, as well as on important reservoir variables such as C_m, k, and ϕ, which can be difficult to evaluate in a conventional well test analysis under certain conditions.

In order to obtain this kind of correlation and to generate a general method which uses the earth tide data to yield information about petroleum reservoirs, we recomment the following.

(1) Compile a large amount of pressure data for many different kinds of fields.

(2) Make a spectrum analysis of each case.

(3) Classify the output data to find their similarities and differences and the reasons for these.

(4) Correct the earth tide data for the location and the season during which the experiment was performed. The data should then be directly comparable.

We suggest that the experiment for each field should cover at least a period of one month, with a sampling rate of one point every one or two hours in order to reduce the problems generated by the aliasing effect and other disturbances. Information on fluid and rock properties should be as complete as possible, i.e., all compressibilities, viscosity, porosity, and permeability values should be available for the analysis of each field. The phase of the response can be used to study the time lag, if any, between the response and the low or high tides (information on location and season of the experiment are needed).

Hopefully, we should be able to find a direct relationship and correlation between the recorded pressure variation and the system properties. Such a result will be very useful for the study of petroleum reservoirs.

REFERENCES

Beal, C.: "The Viscosity of Air, Water, Natural Gas, Crude Oil, and Its
    Associated Gases at Oil Field Temperature and Pressure," Trans.
    AIME (1946), 165.

Bodvarsson, G.: "Confined Fluid as Strain Meters," J. Geoph. Res. (1970),
    75, No. 14, p. 2711.

Bredehoeft, J.D., Cooper, H.L., Papadopoulos, I.S., and Bennett, R.R.:
    "The Response of Well-Aquifer System to Seismic Waves," J. Geoph.
    Res. (1965), 70, No. 16, p. 3915.

Brigham, E.O.: The Fast Fourier Transform, Englewood Cliffs, N.J.: Pren-
    tice Hall, Inc. (1974), 252 p.

Carr, N.J., Kobayashi, R., and Burrow, D.B.: "Viscosity of Hydrocarbon
    Gases Under Pressure," Trans. AIME (1954), 201.

Chew, J., and Connally, C.A., Jr.: "A Viscosity Correlation for Gas Satur-
    ated Crude Oils," presented at the Annual Meeting of the AIME,
    Houston, 1958.

Cooke, M.M.: "Quartz Gauge Improves Pressure Data," Oil & Gas J. (May 19,
    1975),

Garland, G.D.: Introduction to Geophysics, Phila.: Saunders (1971).

Hall, H.N.: "Compressibility of Reservoir Rocks," Trans. AIME (1953),
    198, p. 309.

Johnson, A.G.: "Pore Pressure Changes Associated with Creep Events on
    the San Andreas Fault," Geophysics Ph.D. Thesis, Stanford Uni-
    versity, 1973.

Johnson, A.G., and Nur, A.: "Coupled Elastic Porous Media Diffusion Solu-
    tion for a Spherical Well-Aquifer System--Tectonic and Barometric
    Responses" (to be published), 1978.

Khurana, A.K.: "Influence of Tidal Phenomena on Interpretation of Pressure
    Buildup and Pulse Test," APE A Jour. (1976), 16, Part 1, p. 99.

Marine, W.I.: Water Level Fluctuations Due to Earth Tides in Well Pumping
    from Slightly Fractured Crystalline Rock," J. of Water Resources
    Research (1975), 11, No. 1, p. 105.

Miller, G.B., Seeds, W.S., and Shira, H.W.: "A New Surface Recording Down-Hole Pressure Gauge," SPE Paper 4125, presented at the Annual Meeting of AIME, New Orleans, 1972.

Nur, A., and Byerlee, J.D.: "An Exact Effective Stress Law for Elastic Deformation of Rock with Fluids," J. Geoph. Res. (1971), 76, No. 26, p. 6414.

Ramey, H.J., Jr.: "Rapid Method for Estimating Reservoir Compressibilities," J. Pet. Tech. (April 1964), p. 417.

Ribout, M.: "High Accuracy BMP Data Improve Reservoir Analysis," World Oil (August 1, 1977), p. 57.

Robinson, E.S., and Bell, R.T.: "Tides in Confined Well-Aquifer Systems," J. Geoph. Res. (1971), 76, No. 8.

Standing, M.B.: "Volumetric Phase Behavior of Oil Field Hydrocarbon Systems" (1951), 122 p.

Standing, M.B., and Katz, D.L.: "Density of Crude Oils Saturated with Natural Gas," Trans. AIME (1942a), 146, p. 159.

Standing, M.B., and Katz, D.L.: "Density of Natural Gases," Trans. AIME (1942b), 146, p. 140.

Sterling, A., and Smets, E.: "Study of Earth Tides, Earthquakes and Terrestrial Spectroscopy by Analysis of Level Fluctuations in a Borehole at Hubaan (Belgium)," Geophys. Jour. Roy. Ast. Soc. (1970), 23, p. 225.

Strobel, C.J., Gulati, M.S., and Ramey, H.J., Jr.: "Reservoir Unit Tests in a Naturally Fractured Reservoir--A Field Case Study Using Type-Curves," J. Pet. Tech. (Sept. 1976), p. 1097.

Trube, A.: "Compressibility of Natural Gases," Trans. AIME (1957), 210, p. 355.

Witherspoon, P.A., Narasimhan, T.N., and McEdwards, D.G.: "Results of Interference Tests from Two Geothermal Reservoirs," J. Pet. Tech. (Jan. 1978), 30.

$a = r_o$ = well radius

a_e = earth radius

A_D = amplitude of the diurnal response in the numerical application

A_{SD} = amplitude of the semidiurnal response in the numerical application

$\bar{C}$ = effective aquifer compressibility (Nur and Byerlee, 1971)

C_f = fluid compressibility

C_m = rock matrix compressibility

C_t = system total compressibility

d = "diffusivity" expression (Bodvarsson, $[d=k/\mu\rho S]$). In this work, $(d=k/\mu S)$

e = normal strain

E = Young's modulus

g = acceleration of gravity

$G = G_m$ = rock matrix shear modulus

h = thickness of the reservoir

H = effective bulk modulus of the porous rock

k = permeability to air of the formation

K = bulk modulus of the rock matrix

ℓ = depth of the well

M = mass of the moon

M_D = height of the peak corresponding to the diurnal frequency component in the spectrum analysis

M_{SD} = height of the peak corresponding to the semidiurnal frequency component in the spectrum analysis

M_2 = principal semidiurnal lunar tidal component

n^2 = $i\omega/d$

O_1 = principal diurnal lunar tidal component

P = reservoir pressure at a distance r from the wellbore

$<P>$ = effective pressure

P_a = bottom-hole pressure induced by the pressure P_c

P_c = tectonic pressure

P_o = well spherical cavity pressure

P_p = pore pressure in a porous formation

P_s = static pressure defined by Bodvarsson

P_{Sd} = new static pressure defined in this work

ΔP_D = diurnal pressure variation induced by the diurnal components

ΔP_{SD} = semidiurnal pressure variation induced by the semidiurnal components

r = distance away from the wellbore in the reservoir

S = storage coefficient

S_g = gas saturation

S_{gc} = critical gas saturation

S_{ij} = component of the deviation stress, in the i direction, perpendicular to the j axis

$S_{i\omega}$ = irreducible water saturation

S_o = oil saturation

U_i = displacement in the ith direction

W_2 = second order harmonic

X_i = body force acting in the i direction

GREEK

ε_{ij} = strain component in the i direction applied on a surface perpendicular to the j direction

σ_{ij} = stress component in the i direction applied on a surface perpendicular to the j direction

$\sigma_{\alpha\alpha}$ = hydrostatic stress

$<\sigma_{ij}>$ = effective stress

λ = Lame's Constant

ν = Poisson's Ratio

ρ = density of the formation fluid

μ = viscosity of the formation fluid

119

ϕ = porosity

γ = gravitational constant

γ_g = gas gravity

Δ = volumetric strain

θ_{01} = strain induced by the 0_1 tidal component

θ_{M2} = strain induced by the M_2 tidal component

ρ_m = density of the rock

ω = frequency of the oscillation

ω_c = critical frequency

ω_D = frequency of the diurnal tidal component, 0_1

ω_{SD} = frequency of the semidiurnal tidal component M_2

APPENDIX A

RESERVOIR PROPERTIES

In order to obtain reservoir fluid properties, we must specify the model of the reservoir. We assume that the temperature of the reservoir is $250^{\circ}F$, and the pressure is 4300 psia for all the cases cited below.

In Case No. 1 (dry gas reservoir), the basic assumptions are:

γ_g = 0.65 (to air)

S_g = 0.75

$S_{i\omega}$ = 0.25

In Case No. 2 (gas-free oil reservoir), the basic assumptions are:

oil $\sim$ 30° API

S_o = 0.75

$S_{i\omega}$ = 0.25

In Case No. 3 (gas-saturated oil reservoir), the basic assumptions are:

oil = 30° API

$\gamma_g \sim$ 0.65 (to air)

S_o = 0.65

$S_{i\omega}$ = 0.20

S_g = .15

$S_g < S_{g_c}$ (no gas flow)

For all these cases, the depth, ℓ, is equal to 10,000 ft, and the well radius is equal to 0.5 ft. Using these values, the density, compressibility, and viscosity of the reservoir fluids can be computed. The values of the permeability, k, and porosity, ϕ, of the rock are chosen arbitrarily in the range of known typical values. Rock compressibility is either obtained from Hall's correlation or chosen arbitrarily from the range of typical values.

Let us look first at the values of k, ϕ, and C_m. Assuming that for sandstones average values are defined by 1 md $\leq$ k $\leq$ 2,000 md, and 0.15 $\leq \phi \leq$ 0.35, for CS_1 we selected a value of k = 10 md and ϕ = 0.15. Using ϕ = 0.15 and the Hall porosity-compressibility chart, we computed the value of C_m (Newman, 1973):

$$C_m = 3.7 \times 10^{-6} \text{ psi}^{-1}$$

For CS_2, we selected.a value of k = 900 md and ϕ = 0.30. By the same method, we found a value of C_m:

$$C_m = 1.00 \times 10^{-6} \text{ psi}^{-1}$$

Knowing that for limestones 0.8 $\leq$ k $\leq$ 1,000 md and 0.04 $\leq \phi \leq$ 0.30, we used k = 4 md and ϕ = 0.05 for CL_1, and k = 500 md and ϕ = 0.25 for CL_2.

Using Hall's correlation, we found that:

$$C_m = 6.5 \times 10^{-6} \text{ psi}^{-1} \text{ for } CL_1$$

122

and: $$C_m = 3.3 \times 10^{-6} \text{ psi}^{-1} \text{ for } CL_2$$

For the carbonate rock, we know that the porosity is relatively low for a high permeability. We used $k = 1,100$ md and $\phi = 0.10$. We estimated the rock compressibility (using field data) to:

$$C_m = 7.0 \times 10^{-6}$$

The values selected provide an interesting range of reservoir conditions suitable for purposes of discussion in this study. Other values may be used in the general solution, of course.

For Case No. 1:

C_g is computed using P-C_g chart for different values of T (Trube, 1957).

ρ_g is computed using Standings correlation (1951) P-V-T chart for different values of γ_g or the Standing et al. correlation (Standing and Katz, 1942b).

μ_g is computed using the Carr et al. chart (1954).

For Case No. 2:

C_o, ρ_o, and μ_o are estimated from typical values encountered in field data.

For Case No. 3:

ρ_{mix} (gas-saturated oil density) is computed from the Standing et al. (1942a) correlation.

C_{mix} (gas-saturated oil compressibility) is computed from Ramey's method, assuming GOR = 850 ft^3/bbl. We calculate B_{ob} and B_g from Standing's California crude correlation (Standing, 1951), and then use Ramey's method (Ramey, 1964). Initial pressure of the reservoir is assumed to be equal to P_{bp}.

μ_{mix} (gas-saturated oil viscosity) is computed from Beal's correlation (1946) and from the Chew and Connaly correlation (1959).

APPENDIX B

HEWLETT-PACKARD QUARTZ CRYSTAL PRESSURE GAUGE

This device has been used since 1972. It contains: (1) a pressure probe in the well, (2) a single conductor electric line, and (3) a signal processor at the surface. It may also contain a digital and analog recording system. The operating pressure range is from 0 to 12,000 psia. The gage requires a power generator to run it. The probe dimensions and weight are 1-7/16 in. OD by 39-3/8 in. long, and it weighs 11 lbs (5.0 Kg).

The signal processor dimensions and weight are 6-1/16 in. high by 7-3/4 in wide by 11 in. deep (15.4 x 19.7 x 27.9 cm), and it weighs 7 lbs (3.2 Kg).

The gage accuracy is 0.025% of the reading for pressures greater than 1,000 psia, and the precision is better than 0.15 psi throughout the entire range. The resolution is 0.01 psia and the repeatability is $\pm$0.4 psi over the entire range. The operating temperature range is from 32°F to 302°F (0°C to 150°C) for the probe, and 32°F to 131°F (0°C to 55°C) for the signal processor. The gage can be run while the well is flowing.

Many field experiments have been run to test this pressure gage since 1972 (Miller, 1972; Cooke, 1975; Riboul, 1977). All of these tests cited results extremely favorable toward this new device; results showed time was saved and accuracy was gained by using this device.

APPENDIX C

PROGRAM FOR THE NUMERICAL APPLICATION OF THE THEORY

The program used for the numerical application of the theory developed is listed here. It is written in basic and can be used for any well-reservoir system which follows the assumptions stated at the beginning of Section 4.

```
10 PRINT
20 PRINT
30 PRINT
40 PRINT"THE SYSTEM OF UNITS USED IN THIS PROGRAM IS :"
50 PRINT"LENGTH-INCH  TIME-SECOND  FORCE-POUNDFORCE"
60 PRINT
70 DIM M5(2,70)
80 READ R1,D1,E1
90 PRINT"WELL RADIUS ";R1;"WELL DEPTH ";D1;"SIGN OF ROOT ";E1
100 PRINT
110 REM FLUID CONTENT
120  FOR I=1 TO 3
130   READ U0(I),C0(I),R0(I)
140   PRINT"FLUID CONTENT #";I;"MU=";U0(I);"CF=";C0(I);"RO=";R0(I)
150   NEXT I
160 PRINT
170 REM ROCK FORMATION
180  FOR J=1 TO 5
190   READ K0(J),F0(J),M0(J),G0(J)
200   PRINT"ROCK FORMATION #";J;"K=";K0(J);"PHI=";F0(J);"CM=";M0(J);"GM=";G0(J)
210   NEXT J
220 DATA 6.0,120000.0,1
230 DATA 4.35E-09,1.247E-04,0.0116,2.61E-07,7.5E-06,0.0246,5.51E-08,3.39E-05,0
.0231
240 DATA 1.55E-11,0.15,3.7E-06,640000.0,1.39E-09,0.3,5.5E-07,640000.0,6.22E-
12,0.05,6.5E-06
250 DATA 360000.0,7.75E-10,0.25,3.2E-06,3600000.0,1.7E-09,0.1,7E-06,4400000.0
260 DATA 500.0,0.25,3.2E-06,3600000.0,1100,6.1,7E-06,4400000.0
270  FOR I=1 TO 3
280   FOR J=1 TO 5
290    PRINT
300    PRINT
310    PRINT
320    PRINT
330    PRINT
340    PRINT
350    A2=4.0*K0(J)/(U0(I)*R1*D1*C0(I))
360    D2=F0(J)/(U0(I)*(F0(J)*C0(I)+(1.0-F0(J))*M0(J)))
370    B2=R1*R1/D2
380    C9=4.0*G0(J)*(C0(I)-M0(J))/(3.0+4.0*(G0(J)*C0(I)))
390    C9=1E-06*INT(1000000.0*C9+0.5)
400    M6=1E-03
410    M7=1
430     FOR M=0 TO 50
440      T=192.0/(2.0^(M/5.0))
450      W=2.0*3.14159/(T*3600.0)
460      A3=A2/W
470      B3=W*B2
480      N4=1.0+B3+E1*SQR(2.0*B3)
490      D4=(1.0/(A3*A3))+B3+E1*(SQR(2.0*B3))*((1.0/A3)+1.0)`
500      D4=D4+1
510      M5(2,M)=SQR(N4/D4)
520      M5(1,M)=W
550      NEXT M
560     PRINT
```

COMPUTER PROGRAM USED FOR THE NUMERICAL APPLICATION

127

```
620    PRINT
630    PRINT
640    PRINT"    FREQUENCY RESPONSE";"ROCK FORMATION ";J;"FLUID CONTENT ";I
650    PRINT
660    PRINT"    WELL RADIUS = ";R1;"        ";"WELL DEPTH = ";D1
670    PRINT"    K = ";K0(J);"PHI = ";P0(J);"CM = ";M0(J);"GM = ";G0(J)
680    PRINT"    MU = ";U0(I);"CF = ";C0(I);"PO = ";R0(I)
690    PRINT"    ABSOLUTE DC RESPONSE = ";C9;"(UNITS: INCH, POUND, SECOND)"
700    PRINT
710    PRINT"    PERIOD (HOURS)          VS          AMPLITUDE (0.1 TO 1.0)"
720    PRINT
730    PRINT"              1 * * * * * * * * * 2 * * * * *3* * * 4 * * 5 * *6* *7*
8  *9* 1"
740    FOR M=0 TO 50
760    T=192.0/(2.0^(M/5.0))
770    T=INT(100.0*T+0.5)/100.0
780    X=LOG(M5(2,M))/LOG(10.0)
790    X=60.0*X
800    X=INT(72.5+X)
810    IF X>12 THEN 840
820    PRINT"    ";T;TAB(12);"*"
830    GOTO 850
840    PRINT"    ";T;TAB(12);"*";TAB(X);"*"
850    NEXT M
870    PRINT"              1 * * * * * * * * * 2 * * * * *3* * * 4 * * 5 * *6* *7*
8  *9* 1"
880    PRINT
890    PRINT
900    PRINT
910    PRINT
920    PRINT
930    PRINT
940    NEXT J
950    NEXT I
960 STOP
970 END
```

CONTINUED

128

APPENDIX D

COMPUTER PROGRAMS USED FOR THE FIELD DATA ANALYSIS

All these programs are written in basic language. They have been run on a Hewlett-Packard 9889 printer computer. In order to compute a Fast Fourier Transform (FFT) from an initial set of data, we have to run Program Nos. 3, 4, and 6 successively, and in this order.

To obtain the Fast Fourier Transform plot, we must run Program No. 6. To obtain the graph of the data in the modified form, which are the input data for the Fast Fourier Transform, we have to run Program No. 5. These seven programs are listed in the following pages.

```
10 DIM A[8,256]
20 PRINT "THIS PROGRAM ALLOWS TO ENTER (TIME-PRESSURE-P.ATM-GRAVITY) DATA"
30 PRINT "IN AN EXISTING OR NEWLY CREATED -A- FILE"
40 PRINT
50 PRINT
60 PRINT "GIVE # OF THE ORIGINAL FILE (0 IF NEW FILE, 10 TO 41 OTHERWISE)"
70 PRINT
80 INPUT B1
90 PRINT B1
100 PRINT "GIVE # OF THE FILE ONCE MODIFIED (10 TO 41)"
110 PRINT
120 INPUT B2
130 PRINT B2
140 IF (((B1=0) OR ((B1>9) AND (B1<42))) AND ((B2>9) AND (B2<42))) THEN 170
150 PRINT "OUT OF RANGE! TRY AGAIN"
160 GOTO 50
170 IF B1#0 THEN 270
180 FOR I=1 TO 8
190 FOR J=1 TO 256
200 A[I,J]=0
210 NEXT J
220 NEXT I
230 PRINT "THE DATA YOU WILL NOW ENTER WILL GO IN A NEW FILE"
240 PRINT "WHICH WILL THEN BE STORED IN FILE",B2
250 PRINT "THE PREVIOUS CONTENT OF FILE",B2,"WILL BE LOST"
260 GOTO 340
270 PRINT "THE DATA YOU WILL NOW ENTER WILL BE ADDED TO THAT OF FILE",B1
280 PRINT "AND THE RESULT STORED IN FILE ",B2
290 IF B1#B2 THEN 320
300 PRINT "THE PREVIOUS CONTENT OF ",B1," WILLHENCE BE LOST"
310 GOTO 340
320 PRINT "THE PREVIOUS CONTENT OF FILE ",B1,"IS CONSEVED"
330 PRINT "BUT THE PREVIOUS CONTENT OF FILE ",B2," WILL BE LOST"
340 PRINT "DO YOU WANT TO MAKE A CHANGE"
350 PRINT
360 INPUT C
370 PRINT C
380 IF C=1 THEN 50
390 IF B1=0 THEN 490
400 PRINT "MAKE SURE THE DISC NOW IN THE DRIVE CONTAINS THE ORIGINAL FILE"
410 PRINT "THEN PRESS     -    0     EXECUTE     -"
420 PRINT
430 INPUT W
440 LOAD   DATA #5,50,Z
450 PRINT " DISC NOW IN DRIVE  IS #",Z[1,1]
460 PRINT
470 LOAD   DATA #5,B1,A
480 PRINT "ORIGINAL FILE LOADED  -   THANKS"
490 PRINT "GIVE # OF THE DISC YOU WILL BE USING TO STORE THIS FILE #",B2
500 PRINT (INT(A[8,1]/100))
510 PRINT
520 INPUT B3
530 PRINT B3
540 PRINT "THE ASOLUTE FILE NUMBER USED TO BE",A[8,1]
550 A[8,1]=(100*B3)+B2
560 PRINT "THE ABSOLUTE FILE NUMBER OF THIS SET OF DATA (A(8,1)) IS",A[8,1]
570 PRINT
580 PRINT "GIVE THE ORIGIN OF TIME IN THE FOLLOWING FORMAT"
590 PRINT "YEAR,MONTH,DAY,HOURS MINUTES TO ZULU TIME (+ FOR WEST,- FOR EAST)"
600 PRINT "    YYYY,MM,DD,+HHMM    "
610 PRINT A[8,33],A[8,34],A[8,35],A[8,36]
620 PRINT
630 INPUT A[8,33],A[8,34],A[8,35],A[8,36]
640 PRINT A[8,33],A[8,34],A[8,35],A[8,36]
650 PRINT "ENTER LATITUDE AND LONGITUDE IN THE FOLLOWING FORM"
660 PRINT "       +DD,MMSS,+DDD,MMSS"
670 PRINT A[8,9],A[8,10],A[8,11],A[8,12]
```

PROGRAM NO. 1: INITIAL DATA PROCESSING INTO DIFFERENT COMPUTER FILES

```
680 PRINT
690 INPUT A[8,9],A[8,10],A[8,11],A[8,12]
700 PRINT A[8,9],A[8,10],A[8,11],A[8,12]
710 PRINT "ENTER ALTITUDE OF THE WELL ABOVE MEAN SEA LEVEL IN FEET"
720 PRINT A[8,13]
730 PRINT
740 INPUT A[8,13]
750 PRINT A[8,13]
760 PRINT "DEPTH OF PRESSURE GAUGE IN WELL IN FEET"
770 PRINT A[8,14]
780 PRINT
790 INPUT A[8,14]
800 PRINT A[8,14]
810 PRINT
820 REM AT THIS POINT THE PROGRAM IS SIMPLIFIED FOR THE TIME BEING
830 PRINT "WE SWITCH TO A SIMPLE PROG"
840 PRINT "AT EACH LINE ENTER DAY, HOURMINUTE, PSI, PSI/1000"
850 PRINT "LINES ARE 1 TO 256"
860 PRINT "ENTER FIRST LINE NUMBER"
870 PRINT
880 INPUT D
890 PRINT D
900 PRINT "TO GET OUT TYPE 0,0,0,0"
910 PRINT "YOU CAN NOW ENTER FIXED CONSTANTS WHICH WILL BE ADDED TO THE DAYS"
920 PRINT "AND TO THE HOURMINUTES, TO DISPLACE THEIR ORIGINS"
930 PRINT "THE ORIGIN IS 00 HOURS 00 MINUTES OF THE DATE RECORDED PREVIOUSLY"
940 PRINT "ENTER DISPLACEMENT IN   -DAYS , HOURMINUTES-"
950 PRINT
960 INPUT F1,F2
970 PRINT F1,F2
980 FOR N=D TO 256
990 PRINT
1000 PRINT
1010 PRINT N
1020 PRINT A[1,N],A[2,N],A[3,N],A[4,N]/10
1030 PRINT "   DAYS , HOURMINUTES , PRESSURE   "
1040 PRINT
1050 INPUT E1,E2,E3
1060 IF E3#0 THEN 1090
1070 N=256
1080 GOTO 1190
1090 PRINT E1,E2,E3
1100 A[4,N]=10000*(E3-INT(E3))
1110 E1=E1+F1
1120 F3=(F2-100*INT(F2/100))+(E2-100*INT(E2/100))
1130 E2=100*INT(E2/100)+100*INT(F3/60)+(F3-60*INT(F3/60))+100*INT(F2/100)
1140 A[1,N]=E1+INT(INT(E2/100)/24)
1150 A[2,N]=E2-2400*INT(INT(E2/100)/24)
1160 A[3,N]=INT(E3)
1170 PRINT E1,E2,E3
1180 PRINT A[1,N],A[2,N],A[3,N],A[4,N]/10
1190 NEXT N
1200 PRINT "DO YOU WISH TO MAKE A CHANGE BEFORE FILE IS STORED AT NEW POSITION"
1210 PRINT
1220 INPUT C
1230 IF C=1 THEN 170
1240 LOAD  DATA #5,50,Z
1250 PRINT "THE DISC NOW IN DRIVE IS",Z[1,1]
1260 PRINT "THE DISC YOU SPECIFIED IS",B3
1270 PRINT "IF YOU WANT TO GO AHEAD PRESS  -0  EXECUTE-"
1280 PRINT "IF YOU WANT TO ABORT PRESS   -STOP-"
1290 PRINT
1300 INPUT W
1310 STORE  DATA #5,B2,A
1320 PRINT "NEW FILE STORED"
1330 FOR N=1 TO 256
1340 WRITE (15,1360)N,A[1,N],A[2,N],A[3,N],A[4,N],A[5,N],A[6,N],A[7,N],A[8,N]
1350 NEXT N
1360 FORMAT 9F6.0
1370 STOP
1380 END
```

PROGRAM NO. 1, CONTINUED

```
10 PRINT "THIS PROGRAM PLOTS ON ONE GRAPH PRESSURE VS TIME"
20 PRINT "FOR ANY NUMBER OF TIME CONSECUTIVE DATA FILES"
30 PRINT
40 PRINT "THE SCALING IS AUTOMATIC WITH MANUAL UNIT SELECTION"
50 PRINT
60 PRINT "NOTE THAT ALL FILES MUST HAVE THE SAME TIME ORIGIN (Y-M-D)"
70 PRINT
80 DIM ZI[8,256],P[50]
90 FOR I=1 TO 50
100 P[I]=0
110 NEXT I
120 FOR I=1 TO 50
130 PRINT "ENTER FILE NUMBER FOR PART #";I;"OF THE GRAPH"
140 PRINT
150 INPUT N
160 IF N=0 THEN 220
170 IF (N<10) OR (N>41) THEN 150
180 P[I]=N
190 PRINT "PART #";I;"FROM FILE #";N
200 PRINT
210 NEXT I
220 PRINT "FILES :";
230 FOR J=1 TO (I-1)
240 PRINT P[J];
250 NEXT J
260 PRINT
270 PRINT
280 Y1=33000
290 Y2=0
300 X1=10000000
310 X2=0
320 FOR J=1 TO (I-1)
330 LOAD  DATA #5,P[J],Z
340 FOR M=1 TO 256
350 IF Z[3,M]=0 THEN 460
360 X=24*60*Z[1,M]-40*INT(Z[2,M]/100)+Z[2,M]
370 Y=Z[3,M]+Z[4,M]/10000
380 IF X>X1 THEN 400
390 X1=X
400 IF X<X2 THEN 420
410 X2=X
420 IF Y>Y1 THEN 440
430 Y1=Y
440 IF Y<Y2 THEN 460
450 Y2=Y
460 NEXT M
470 NEXT J
480 PRINT "THE TIME SPAN PLOTTED IS FROM";X1;"MINUTES FROM TIME ORIGIN "
490 PRINT "TO";X2;"MINUTES FROM TIME ORIGIN"
500 PRINT "ENTER SCALE UNIT FOR THE TIME AXIS IN MINUTES (ONE DAY IS 1440 MIN)"
```

PROGRAM NO. 2: INITIAL DATA PLOTTING

```
510 INPUT T1
520 PRINT "THE PRESSURE RANGE IS FROM";Y1;"PSI TO";Y2;"PSI"
530 PRINT "ENTER SCALE UNIT FOR THE PRESSURE AXIS IN PSI"
540 INPUT T2
550 X3=T1*INT(X1/T1)
560 X4=T1*INT(X2/T1+1)
570 Y3=T2*INT(Y1/T2-1)
580 Y4=T2*INT(Y2/T2+1)
590 PRINT "TIME AXIS FROM";X3;"MIN TO";X4;"MIN IN UNITS OF";T1;"MINUTES"
600 PRINT "PRESSURE AXIS FROM";Y3;"PSI TO ";Y4;"PSI IN UNITS OF";T2;"PSI"
610 PRINT "PREPARE PAPER, PEN AND GRAPH LIMITS THEN PRESS -CONT-EXEC-"
620 STOP
630 SCALE X3,X4,Y3,Y4
640 XAXIS Y3,T1
650 XAXIS Y4,T1
660 YAXIS X3,T2
670 YAXIS X4,T2
680 FOR J=1 TO (I-1)
690 LOAD  DATA #5,P[J],Z
700 FOR M=1 TO 256
710 IF Z[3,M]=0 THEN 750
720 X=24*60*Z[1,M]-40*INT(Z[2,M]/100)+Z[2,M]
730 Y=Z[3,M]+Z[4,M]/10000
740 PLOT X,Y
750 NEXT M
760 NEXT J
770 PEN
780 PLOT (X3+(X4-X3)/20),(Y3+(Y4-Y3)/8),1
790 LABEL (*,1.4,3,0,1)"FILE #";
800 FOR J=1 TO (I-1)
810 LABEL (*)P[J];
820 NEXT J
830 LABEL (*)"-"
840 LABEL (*)" "
850 X5=X3/60
860 X6=X4/60
870 T3=T1/60
880 LABEL (*)"HORIZONTAL SCALE:";X5;"HOURS TO";X6;"HOURS IN UNITS OF";T3;"HOURS"
890 LABEL (*)"VERTICAL SCALE:";Y3;"PSI TO";Y4;"PSI IN UNITS OF";T2;"PSI"
900 PRINT "PLOT  COMPLETED"
910 PRINT
920 END
```

PROGRAM NO. 2: CONTINUED

```
10 PRINT "THIS PROGRAM PREPARES THE INPUT FILE FOR THE FFT"
20 PRINT
30 PRINT "IT EXTRACTS 256 EQUALY SPACED DATA POINTS FROM ANY NUMBER OF TIME"
40 PRINT "CONSECUTIVE STANDARD DATA FILES "
50 PRINT
60 PRINT "AT THIS TIME  THE PROGRAM SIMPLY DIVIDES THE TOTAL TIME SPAN INTO"
70 PRINT "256 EQUAL TIME INTERVALS AND TAKE THE AVERAGE OF THE DATA POINTS"
80 PRINT "CONTAINED IN EACH INTERVAL AS RESULT."
90 PRINT
100 PRINT "TO REDUCE ALIASING AND BECAUSE THE MAJORITY OF THE FREQUENCY LINES"
110 PRINT "OF INTEREST ARE MULTIPLES OF 1-PER-DAY, THE TIME SPAN CONSIDERED"
120 PRINT "IS AN INTEGER NUMBER OF DAYS"
130 PRINT
140 PRINT "TO OBTAIN A USEFUL FFT THE TIME SPAN SHOULD BE NO SHORTER THAN "
150 PRINT "16 OF THE LONGUEST PERIODS (DAYS) (FOR A MINIMUM OF COMPLETE PERIODS"
160 PRINT "IN THE EXPERIMENT TIME SPAN), AND NO LONGER THAN 128 TIMES THE "
170 PRINT "SHORTEST PERIOD (8 OR 12 HOURS) (FOR A MINIMUM OF SAMPLES PER PERIOD)
180 PRINT
190 DIM A[2,256],X[8,256]
200 PRINT "ENTER TIME SPAN IN DAYS (INTEGER)"
210 INPUT S
220 S=INT(S)
230 P=24*60*S/256
240 PRINT S;"DAYS, SAMPLES EVERY";P;"MINUTES"
250 PRINT "ENTER FILE # CONTAINING THE ORIGIN OF THE TIMSPAN"
260 INPUT N
270 LOAD  DATA #5,N,X
280 PRINT "FILE #";N;"LOADED, ABSOLUTE FILE NUMBER:";X[8,1]
290 PRINT "ENTER LINE NUMBER OF ORIGIN"
300 INPUT O
310 PRINT "LINE";O;"X  ";X[1,0];X[2,0];X[3,0];X[4,0];X[5,0];X[6,0];X[7,0];X[8,0]
320 T=24*60*X[1,0]-40*INT(X[2,0]/100)+X[2,0]
330 PRINT "THE ORIGIN OF THE FIRST TIME INTERVAL IS";T;"MINUTES"
340 PRINT "AFTER THE ORIGIN OF THE DATA SET"
350 PRINT
360 PRINT
370 FOR I=1 TO 256
380 M=0
390 Y=0
400 T=T+P
410 IF O>256 THEN 610
420 IF X[3,0]=0 THEN 610
430 T1=24*60*X[1,0]-40*INT(X[2,0]/100)+X[2,0]
440 IF T1 >= T THEN 510
450 M=M+1
460 Y=Y+X[3,0]+X[4,0]/10000
470 O=O+1
480 GOTO 410
490 NEXT I
```

PROGRAM NO. 3: PREPARATION OF THE INPUT FILE FOR THE COMPUTATION OF THE
FAST FOURIER TRANSFORM (FFT)

134

```
 500 GOTO 790
 510 IF M#0 THEN 560
 520 PRINT "I HAVE FOUND AN INTERVAL LARGER THAN";P;"MINUTES"
 530 PRINT "CONTAINING NO DATA. SORRY I HAVE TO ABORT EXECUTION".
 540 PRINT "(THIS IS AROUND LINE #";O;"OF FILE #";N;")."
 550 GOTO 850
 560 A[1,I]=Y/M
 570 A[2,I]=0
 580 M=0
 590 Y=0
 600 GOTO 490
 610 O=O-1
 620 PRINT "LINE";O;"X ";X[1,0];X[2,0];X[3,0];X[4,0];X[5,0];X[6,0];X[7,0];X[8,0]
 630 T8=24*60*X[1,0]-40*INT(X[2,0]/100)+X[2,0]
 640 PRINT "THE TIME OF THE LAST LINE OF THE PRESENT FILE IS";T8;"MINUTES"
 650 PRINT "AFTER THE ORIGIN OF THE DATA SET"
 660 PRINT
 670 PRINT "I NEED AN OTHER FILE: ENTER NEW NUMBER"
 680 INPUT N
 690 O=1
 700 LOAD   DATA #5,N,X
 710 PRINT "FILE #";N;"LOADED, ABSOLUTE FILE NUMBER:";X[8,1]
 720 PRINT "LINE";O;"X  ";X[1,0];X[2,0];X[3,0];X[4,0];X[5,0];X[6,0];X[7,0];X[8,0]
 730 T8=24*60*X[1,0]-40*INT(X[2,0]/100)+X[2,0]
 740 PRINT "THE TIME OF THE LAST LINE OF THE PRESENT FILE IS";T8;"MINUTES"
 750 PRINT "AFTER THE ORIGIN OF THE DATA SET"
 760 PRINT
 770 PRINT
 780 GOTO 430
 790 PRINT "LINE";O;"X ";X[1,0];X[2,0];X[3,0];X[4,0];X[5,0];X[6,0];X[7,0];X[8,0]
 800 T8=24*60*X[1,0]-40*INT(X[2,0]/100)+X[2,0]
 810 PRINT "THE TIME OF THE LAST LINE USED IS";T8;"MINUTES"
 820 PRINT
 830 STORE   DATA #5,45,A
 840 PRINT "FFT INPUT FILE STORED - THANKS"
 850 PRINT
 860 END
```

PROGRAM NO. 3: CONTINUED

```
10 PRINT "THIS PROGRAM SORTS AND SCALES THE DATA FOR THE FFT"
20 PRINT
30 PRINT "THE SORTING PUTS THE CENTER OF THE CURVE IN POSITION 1, THE POINT"
40 PRINT "TO ITS RIGHT IN POSITION 2, ETC, LAST POINT AT RIGHT IN POSITION 128"
50 PRINT "LAST POINT AT LEFT IN POSITION 129, ETC, AND THEFIRST POINT AT LEFT"
60 PRINT "OF CENTER IN POSITION 256."
70 PRINT
80 PRINT "THE SCALING SUPPRESSES THE LINEAR SLOPE IN THE INPUT DATA TO GIVE "
90 PRINT "EQUAL VALUES TO THE FIRST AND LAST POINTS. THIS REDUCES THE SPURIOUS"
100 PRINT "ODD HARMONICS DUE TO THE SAWTOOTH SHAPE OBTAINED BY FOLDING"
110 PRINT
120 DIM X[2,256],Y[2,256],P[256]
130 LOAD  DATA #5,45,X
140 X1=X[1,1]
150 X2=X[1,256]
160 FOR I=1 TO 256
170 P[I]=X[1,I]-X1+(I-1)*(X1-X2)/255
180 I6=I
190 IF I <= 128 THEN 210
200 I6=I6-256
210 I6=I6+128
220 Y[1,I6]=P[I]
230 Y[2,I6]=0
240 NEXT I
250 STORE  DATA #5,46,Y
260 PRINT "SORTING AND SCALING FOR THE FFT COMPLETED"
270 END
```

PROGRAM NO. 4: SORTING AND SCALING OF THE DATA FOR THE FAST FOURIER
TRANSFORM (FFT)

136

```
10 PRINT "THIS PROGRAM PLOTS THE DATA PREPARED FOR INPUT OF FFT"
20 PRINT
30 DIM Z[2,256]
40 PRINT "ENTER 0 IF YOU WANT IT BEFORE SCALING AND SORTING, 1 OTHERWISE"
50 INPUT W
60 IF W=0 THEN 90
70 LOAD  DATA #5,46,Z
80 GOTO 100
90 LOAD  DATA #5,45,Z
100 Y1=33000
110 Y2=0
120 FOR M=1 TO 256
130 Y=Z[1,M]
140 IF Y>Y1 THEN 160
150 Y1=Y
160 IF Y<Y2 THEN 180
170 Y2=Y
180 NEXT M
190 PRINT "THE PRESSURE RANGE IS FROM";Y1;"PSI TO";Y2;"PSI"
200 PRINT "ENTER SCALE UNIT FOR THE PRESSURE AXIS IN PSI"
210 INPUT T2
220 Y3=T2*INT(Y1/T2-1)
230 Y4=T2*INT(Y2/T2+1)
240 PRINT "PRESSURE AXIS FROM";Y3;"PSI TO ";Y4;"PSI IN UNITS OF";T2;"PSI"
250 PRINT "PREPARE PAPER, PEN AND GRAPH LIMITS THEN PRESS -CONT-EXEC-"
260 STOP
270 SCALE 1,256,Y3,Y4
280 XAXIS Y3,16
290 XAXIS Y4,16
300 YAXIS 1,T2
310 YAXIS 256,T2
320 FOR I=1 TO 256
330 I6=I
340 IF I <= 128 THEN 360
350 I6=I6-256
360 I6=I6+128
370 Y=Z[1,I6]
380 X1=I
390 PLOT X1,Y
400 NEXT I
410 PEN
420 PLOT 256/20,(Y3+(Y4-Y3)/20),1
430 LABEL (*,1.4,3,0,1)
440 LABEL (*)"VERTICAL SCALE:";Y3;"PSI TO";Y4;"PSI IN UNITS OF";T2;"PSI"
450 PRINT "PLOT  COMPLETED"
460 PRINT
470 END
```

PROGRAM NO. 5: DATA PLOT FOR RESULTS FROM PROGRAM NO. 4

```
20 PRINT "THIS PROGRAM CACULATES THE FFT OF THE COMPLEX FUNCTION X(2,256)"
30 PRINT "WHERE THE FIRST INDEX IS 1 FOR THE REAL PART AND 2 FOR THE IMAG PART"
40 PRINT "AND THE SECOND INDEX IS THE TIME"
50 PRINT
60 PRINT "TO MODIFY THE TIME SPAN (SET HERE AT 256) CHANGE N AND E IN THE "
70 PRINT "FOLLOWING LINES - N=2↑E - ALSO CHANGE E IN THE FUNCTION FNI"
80 PRINT "DO NOT CHANGE THE DIM STATEMENT"
90 PRINT
100 PRINT "X(2,256) IS HERE SITUATED IN DISC FILE #3"
110 PRINT "THIS FILE SHOULD BE ENTIRELY DEFINED (IE EMPTY SPACES FILLED WITH 0)"
120 PRINT
130 PRINT "THE RESULTING FFT IS STORED IN A (2,256) DISC FILE, HERE #4"
140 PRINT
150 PRINT "THE RUN CONSIST OF : LOADING, 8 STEPS, SORTING, AND STORING"
160 PRINT "TOTAL EXECUTION TIME IS APPROX 16 MINUTES"
170 PRINT
180 PRINT " LOADING"
190 DIM X[2,256]
200 LOAD  DATA #5,46,X
210 N=256
220 E=8
230 N2=N/2
240 N1=E-1
250 K=0
260 FOR L=1 TO E
270 PRINT " ENTERING STEP ";L
280 FOR I=1 TO N2
290 F=INT(K/2↑N1)
300 P=FNIF
310 A=2*PI*P/N
320 C=COS(A)
330 S=SIN(A)
340 K1=K+1
350 K2=K1+N2
360 T1=X[1,K2]*C+X[2,K2]*S
370 T2=X[2,K2]*C-X[1,K2]*S
380 X[1,K2]=X[1,K1]-T1
390 X[2,K2]=X[2,K1]-T2
400 X[1,K1]=X[1,K1]+T1
410 X[2,K1]=X[2,K1]+T2
420 K=K+1
430 NEXT I
```

PROGRAM NO. 6: COMPUTING THE FAST FOURIER TRANSFORM (FFT) OF THE PRE-
PARED INPUT DATA

138

```
440 K=K+N2
450 IF (K<N) THEN 280
460 K=0
470 N1=N1-1
480 N2=N2/2
490 NEXT L
500 PRINT " SORTING"
510 FOR K=1 TO N
520 F=K-1
530 I=FNIF+1
540 IF (I <= K) THEN 610
550 T1=X[1,K]
560 T2=X[2,K]
570 X[1,K]=X[1,I]
580 X[2,K]=X[2,I]
590 X[1,I]=T1
600 X[2,I]=T2
610 NEXT K
620 PRINT " STORING"
630 STORE  DATA #5,47,X
640 PRINT
650 PRINT "FFT COMPLETED"
660 PRINT
670 STOP
680 END
690 DEF FNI(J)
700 E=8
710 J1=J
720 I8=0
730 FOR I4=1 TO E
740 J2=INT(J1/2)
750 I8=I8*2+(J1-2*J2)
760 J1=J2
770 NEXT I4
780 RETURN I8
790 END
```

PROGRAM NO. 6: CONTINUED

```
10 PRINT "THIS PROGRAM PLOTS THE DATA OUTPUT BY THE FFT"
20 PRINT
30 DIM Z[2,256],A[2,256]
40 DEG
50 LOAD  DATA #5,47,Z
60 Y1=33000
70 Y2=0
80 FOR M=1 TO 256
90 A[1,M]=SQR(Z[1,M]*Z[1,M]+Z[2,M]*Z[2,M])
100 A[2,M]=ATN(Z[2,M]/Z[1,M])
110 Y=A[1,M]
120 IF M=1 OR M=2 OR M=256 THEN 170
130 IF Y>Y1 THEN 150
140 Y1=Y
150 IF Y<Y2 THEN 170
160 Y2=Y
170 NEXT M
180 PRINT "THE -Y- IS FROM";Y1;"TO";Y2;
190 PRINT "ENTER SCALE UNIT FOR THE -Y- AXIS "
200 PRINT "NOTE THAT WHEN THE AMPLITUDE IS SMALLER THAN 1/2 OF A DIVISION"
210 PRINT "THE PHASE WILL BE CONSIDERED EQUAL TO 0"
220 INPUT T2
230 Y3=T2*INT(Y1/T2-2)
240 Y4=T2*INT(Y2/T2+1)
250 PRINT "-Y- AXIS FROM";Y3;"TO ";Y4;"IN UNITS OF";T2;
260 FOR M=1 TO 256
270 IF A[1,M] >= T2/2 THEN 290
280 A[2,M]=0
290 NEXT M
300 PRINT "PREPARE PAPER, PEN AND GRAPH LIMITS THEN PRESS -CONT-EXEC-"
310 STOP
320 SCALE 1,256,(2*Y3-Y4),Y4
330 XAXIS Y3,16
340 XAXIS Y4,16
350 XAXIS (Y3-(Y4-Y3)/2),16
360 XAXIS (2*Y3-Y4),16
370 YAXIS 1,T2,Y3,Y4
380 YAXIS 256,T2,Y3,Y4
390 YAXIS 1,(Y4-Y3)/20,2*Y3-Y4,Y3
400 YAXIS 256,(Y4-Y3)/20,2*Y3-Y4,Y3
410 FOR I=1 TO 256
420 I6=I
430 IF I <= 128 THEN 450
440 I6=I6-256
450 I6=I6+128
460 Y=A[1,I6]
470 X1=I
480 PLOT X1,Y
490 NEXT I
500 PEN
510 FOR I=1 TO 256
520 I6=I
530 IF I <= 128 THEN 550
540 I6=I6-256
550 I6=I6+128
560 Y=(A[2,I6]*(Y4-Y3)/200)+Y3-(Y4-Y3)/2
570 X1=I
580 PLOT X1,Y
590 NEXT I
600 PEN
610 PLOT 256/20,(Y3+(Y4-Y3)/20),1
620 LABEL (*,1.4,2,0,1)
630 LABEL (*)"VERTICAL SCALE:";Y3;"TO";Y4;"IN UNITS OF";T2;
640 PRINT "PLOT  COMPLETED"
650 PRINT
660 END
```

PROGRAM NO. 7: PLOTTING THE OUTPUT DATA OF THE FFT COMPUTATION